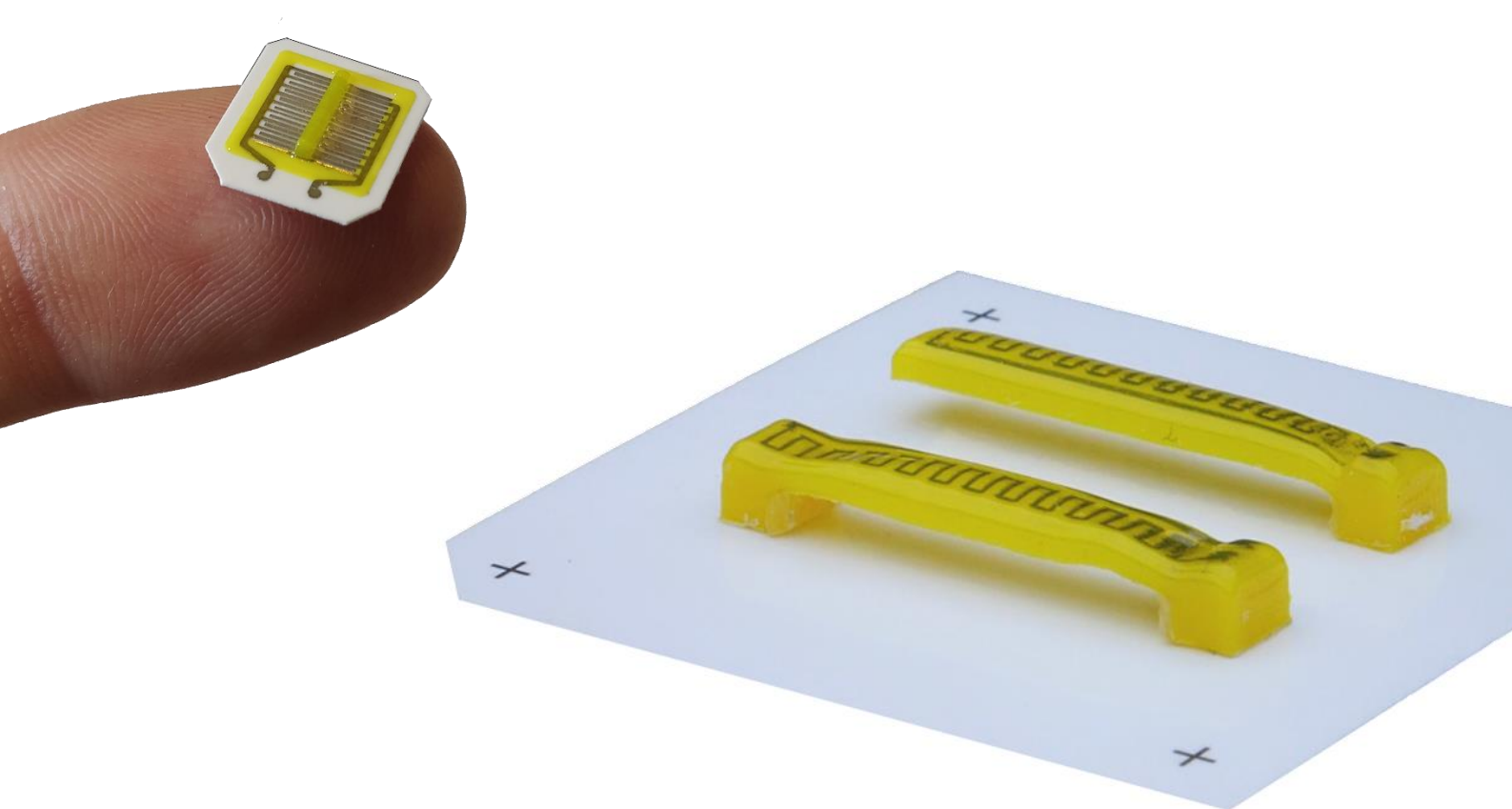


Department of Precision and Microsystems Engineering

Multi-material 3D inkjet printing for functional structures using UV sintering and photopolymerisation

C.T. Davenne

Report no : 2021.035
Supervisor : Dr. ir. J.F.L. Goosen
Specialisation : Mechatronic System Design
Type of report : Master Thesis
Date : 11 June 2021



Multi-material 3D inkjet printing for functional structures

using UV sintering and photopolymerisation

by

C.T. Davenne

to obtain the degree of Master of Science
at the Delft University of Technology,
to be defended publicly on Friday June 25th, 2021 at 10:00 AM local time.

Student number: 4369912
Project duration: March 1, 2020 – June 25, 2021
Thesis committee: Dr. ir. J.F.L. Goosen, TU Delft, supervisor
Dr. A. Hunt, TU Delft
Dr. ir. M. Tichem, TU Delft

An electronic version of this thesis is available at <http://repository.tudelft.nl/>.

Preface

I present before you the results of my master thesis I've been working on for the past year. The topic of 3D printing has fascinated me ever since the patent by mister S. Scott Crump (co-founder of Stratasys) expired in 2009. The FDM technology suddenly opened up to commercial, DIY, and open-source (RepRap) applications. Of course, I too started building a 3D printer which I still own today. This thesis dives deeper in the realm of 3D printing; combining even older techniques (inkjet) with state-of-the art materials and machines to printer smaller, more detailed, functional multi-material parts.

I would like to thank Hans Goosen for supervising my thesis and providing feedback on bi-weekly updates. Lab support for their lab training and willingness to help. Tessa Essers for several meetings about the Stratasys Polyjet printer, supply of Stratasys ink and printing of a sample on the F735 for comparison. Thim Zuidwijk for his kind assistance with the spectrometry analysis experiments, flexible availability and purchases of dedicated tools to aid in my experiments. Andres Hunt for his advice about printing with DMC cartridges and repairing the Dimatix HPB quickly to minimize delay for all relying on the DMC cartridges for their research. Last but not least, I want to thank friends, roommates and family for their feedback on my report and support during my studies in general!

*Niels Davenne
Delft, June 2021*

Abstract

Multi-material 3D inkjet printing has great potential for rapid prototyping and manufacturing of functional mesoscale structures when novel inks are combined into a fully integrated AM process. This process can be faster and cheaper than conventional methods to produce functional structures. Research is conducted on a large range of potentially inkjet-printable materials to extend current possibilities with 3D inkjet printing. Material incompatibility together with strict fluid properties limit the range of multi-functional inks available for an integrated print process. This raises challenges such as printing with three or more materials simultaneously, and finding inkjet printable materials that can be cured simultaneously using the same curing method. The aim of this research is to print functional structures using at least three materials consisting of a structural, support, and conductive material, requiring only one curing technique involving UV light exposure. An experimental setup of PiXDRO LP50 inkjet printers and various printhead assemblies are used to conduct experiments. Suitable off the shelf available inks are selected after a state of the art literature review. Stratasys Vero-series and Stratasys SUP706B are industry standard, compatible materials and cure using UV induced photopolymerisation. They are chosen as structural and support material, respectively. Novacentrix Metalon JS-B25P and Mitsubishi NBSIJ-MU01 silver nanoparticle inks are chosen as conductive inks. First, multi-material printing is set up and extended to 3D printing using the structural and support material inks only. Afterwards, conductive inks are tested for resistivity and behaviour on different substrates before integrating with the structural and support material ink into a multi-material 3D print. Conductive nanoparticle inks show good conductivity on photopaper substrate, but not when printed on top of structural material. Several experiments are performed to document ink behaviour and optimise performance. A workflow is designed allowing the conversion of complex CAD models to inkjet-printable files. Custom support material density for stronger supports can be generated using an in-house developed conversion application. Proof-of-concept multi-material functional structures are printed showcasing success of the proposed methodology.

Contents

Preface	i
Abstract	ii
Abbreviations	v
1 Introduction	1
1.1 Background	1
1.2 Motivation	1
1.3 Research question	2
1.4 Report outline	2
2 State of the art	3
2.1 Additive micro-manufacturing techniques	3
2.2 Inkjet printing	4
2.2.1 Inkjet printing process	4
2.2.2 Inkjet printing inks	7
2.2.3 Ink and process combinations	11
3 Approach	13
3.1 Selection of inks	13
3.2 Multi-material printing	13
4 Sintering and polymerisation using UV light	14
4.1 Working principles	14
4.1.1 Sintering	14
4.1.2 Photopolymerisation	15
4.2 Selection of inks	16
4.2.1 Selection of conductive inks	16
4.2.2 Selection of photopolymer inks	16
4.3 Spectrum analysis experiments	18
4.3.1 Method	18
4.3.2 Results	18
4.3.3 Discussion	19
5 Multi-Material inkjet printing	20
5.1 PiXDRO LP50 printers	20
5.1.1 Printheads	21
5.1.2 Jetting options	21
5.1.3 Printing options	22
5.2 Multi-material prints	24
5.2.1 Printhead settings	24
5.2.2 Substrates	24
5.2.3 Alignment	25
5.2.4 Recipe settings	25
5.2.5 Results	26
6 Printing 3D functional structures	27
6.1 Requirements for functional structures	27
6.2 Printing 3D structures	27
6.3 Printing overhanging structures	32
6.3.1 Support structure modification	32
6.3.2 Support removal	33

6.3.3	Results	35
6.4	Printing conductive traces	36
6.4.1	Printing on photopaper substrate	36
6.4.2	Printing on structural material	38
6.4.3	UV and thermal sintering	42
6.4.4	Overprinting AgNP ink	43
6.4.5	Results	43
6.5	Process workflow	44
6.5.1	Computer aided design	44
6.5.2	Slicing	44
6.5.3	Support modification	44
6.5.4	Printer and recipe settings	44
6.5.5	Post-processing	45
6.5.6	Results	45
6.6	Proof of concept	46
6.6.1	Resistivity moisture sensor	46
6.6.2	Multi-material moisture sensor	47
6.6.3	Downscaling the sensor	48
6.6.4	Conclusion	49
7	Discussion	50
8	Recommendations	52
9	Conclusion	54
	Bibliography	55
A	Spectrometry experiments	60
A.1	Design	60
A.2	Setup and components	60
A.3	Results	61
A.4	Honle UV source intensity output	61
B	AgNP channels in structural material	62
C	Technical drawings	63
C.1	50x50 substrate	63
C.2	Multi-material-bridge	64
C.3	AgNP moisture sensor	64
D	Support removal solution preparation	65
E	Preparing a CAD model for 3D printing	67
E.1	CAD model and support generation	67
E.2	Model exporting and slicing	70
E.3	Organising images and colour inversion	70
E.4	Support material modification	71
E.5	Organising images (2)	72
E.6	Printing on PiXDRO LP50	72

Abbreviations

Abbreviations can be found throughout the text. A summary in alphabetical order is given here below.

AM	Additive manufacturing
AgNP	Silver nanoparticle
CIJ	Continuous Inkjet printing
DoD	Drop-on-demand (inkjet printing)
DPI	Drops per inch
DPL	Digital light processing
FDM	Fused deposition modelling
FFF	Fused filament fabrication
HMI	Human-machine interface
HPB	Head personality board (PiXDRO LP50 interface to printheads)
IPA	Isopropyl alcohol
IPL	Intense Pulsed Light
MNE	Micro and Nanosystems Engineering
PHA	Print head assembly
PME	Precision and Microsystems Engineering
QF	Quality factor
SEM	Scanning electron microscope
SZ	Stepsize
ToF	Time of flight (ink droplets)
UV	Ultraviolet

Introduction

1.1. Background

Inkjet printing has been an indispensable technique since its invention. Although mainly used to print text on plain paper, inkjet technology is also used extensively in the industry to print labels, serial codes and expiration dates on products. Different kinds of deposition techniques exist, yet all relying on the same principle of jetting tiny droplets of ink from a nozzle. A major advantage of inkjet printing for the consumer market is the use of disposable print heads, making personal printing affordable. Modern inkjet printers are capable of printing high resolutions, rich colours, and with high speeds, be it on a flat surface only. In the recent decade, researchers have started to investigate the potential of inkjet printing for three-dimensional (3D) structures and with different kinds of inks.

1.2. Motivation

Rapid prototyping (RP) has become a popular term in the manufacturing industry, educational institutions and consumer markets alike. Especially fused-deposition-modelling (FDM) also known as fused-filament-fabrication (FFF) made a popularity surge due to the introduction of affordable machines capable of quickly manufacturing plastic parts for consumer markets. However, in the industry, additive manufacturing (AM) techniques have been around for decades and consist of more than FDM alone. Inkjet printing is also part of AM techniques though it is still limited to fabricating plastic parts mainly, be it with colours and even support material [49]. Research is conducted on a large range of potentially inkjet-printable materials to extend to current possibilities with 3D inkjet printing. Printing novel materials such as conductive and biodegradable materials on 2D substrates has already been shown to work by many researchers, but this has only just recently found its way to 3D inkjet printing combined with conventional materials. Many challenges need to be faced in order to make multi-material 3D inkjet printing truly work. Material compatibility together with strict fluid properties limit the range of multi-functional inks available for an integrated print process [24]. However, multi-material 3D inkjet printing has great potential for rapid prototyping of functional structures when novel inks are combined into a fully integrated AM process. This process can be faster and cheaper than conventional methods to produce small (mesoscale) structures.

Current technologies to manufacture mesoscale 3D functional structures such as etching- and lithography-based methods offer good results but are relatively expensive for low-quantity products and require production of expensive lithography masks. Manufacturing of mesoscale 3D functional structures can be viable but still has culprits when using 3D inkjet printing alone. 3D inkjet printing is not new and novel technologies and materials have been increasingly researched the last decade. To print complex structures, at least a structural and support material is required. To make the product capable of actuation or sensing, also electrically conductive materials are needed. Multi-material 3D printing using inkjet technology has not been used to print structures with three or more materials at the same time and requiring only one curing method. This raises challenges such as printing with 3 or more materials simultaneously, and finding inkjet printable materials that can be cured simultaneously using the same curing method.

1.3. Research question

In the past couple of years, researchers have shown to be able to manufacture multi-material parts with structural and conductive inks or structural and support inks. However, to manufacture microscale functional structures with complex structures, having a multi-material 3D inkjet printing process with ability to deposit structural, conductive, and support material simultaneously opens up many more possibilities. At the same time, photonic curing is used more often to cure materials. Photopolymerisation of polymers has been used quite some time, and is characterised as having the best resolution and feature size [31]. Sintering nanoparticles using light has only been explored the last decade and has a lot of potential to replace conventional heating sintering techniques.

Therefore, the proposed research is to combine multiple materials, of which at least structural, conductive and support materials, into a compatible printing process. The goal is to manufacture 3D functional micro-structures with complex geometries not possible in the past due to the lack of support material. Combined with the use of photonic curing, each layer can be printed with a combination of these materials and cured simultaneously and faster than with conventional heating techniques. This yields the following research question:

How to combine structural, conductive, and support material ink into a 3D inkjet printing process to print functional structures using only UV light curing?

1.4. Report outline

In this master thesis report, the goal of manufacturing functional multi-material 3D prints as mentioned in the motivation section is challenged by systematic research and experiments in the field of interest. In chapter 2 general theory of well-established but also state-of-the-art literature is discussed which is used in this thesis. In chapter 3, the approach and methods used in this thesis are presented. Next, chapter 4 provides in-depth information needed to understand the process behind sintering of nanoparticle inks and the polymerisation effect of certain resin inks used in experiments. Experimental methodology and results are given in chapter 5. More advanced experiments and process strategies towards prototyping and actual manufacturing of functional multi-material 3D prints is presented in chapter 6. Discussion points are given in chapter 7 which precedes the recommendations for further research in chapter 8. The conclusion of this master thesis is given in chapter 9. Appendices contain additional information and can be found at the end of the report together with all references.

2

State of the art

In this chapter the state of the art is presented. It includes a brief overview of micro-manufacturing methods used nowadays, and is then extended with an in-depth section about inkjet printing and inks.

2.1. Additive micro-manufacturing techniques

A broad range of additive manufacturing techniques exist, which can be classified in various ways depending on their applications, capabilities, or fundamental working principles. An internationally accepted classification is described by the American Society for Testing and Materials; They present seven distinct classes: material extrusion, material jetting, vat photo-polymerisation, powder bed fusion, reactive binder jetting, directed energy deposition, and stacked sheet lamination [3]. An overview showing each class with some of the more popular technologies and advantages and drawbacks is presented in fig. 2.1.

Some of these techniques are restricted to small or large scales with limited production capacity, but others can be used from micro- to macroscale and have the potential to manufacture many products simultaneously, so-called scalable AM techniques. Inkjet printing (material jetting) is one of them. Since most AM techniques are originally developed to manufacture macroscale products, it is generally non-trivial to use the same technology and scale it down to manufacture microscale products.

When focusing on additive manufacturing using deposition of a material by a nozzle, there are still multiple classes that use this principle. Material jetting ejects small droplets of liquid ink which solidify to form a structure. Note that this is different from the binder jetting process, in which the structural material is already in place and is only fused by the binder being deposited by jetting each layer. Also direct write, which deposits material via a nozzle, is fundamentally different as the nozzle handles fluids with much higher viscosity and deposits the material directly in place, whereas inkjet is a non-contact printing technique. This minimises damage from the nozzles touching the preprinted patterns or substrate during printing [15].

Manufacturing micro functional structures

The manufacturing of microscale functional structures and MEMS originate from the process technology in semiconductor devices. Basic techniques are material deposition, patterning by photolithography and etching to form structural shapes [20]. The combination of material deposition and subtraction has advantages and disadvantages. The main advantage is that complex shapes can be manufactured in this way, altering between addition and subtraction of material in different process steps and combined with patterning steps by photolithography to only target specific parts of the product to manipulate. This also has drawbacks; altering between additive and subtractive manufacturing takes time and usually multiple expensive masks need to be made for the lithography steps.

To overcome these drawbacks, additive manufacturing techniques can be used. Combined with appropriate post-processing steps such as removing support material, similar results are possible. Multiple examples of MEMS devices manufactured using AM techniques only are already available. A comparison between MEMS components made using conventional techniques and 3D-micro AM techniques is shown by Vaezi [50]. Another publication presents a micro lens system, several sensors and actuators

	Categories	Technologies	Advantages/Drawbacks
	Vat-Photopolymerization	<ul style="list-style-type: none"> ▪ SLA ▪ DLP ▪ CLIP 	<ul style="list-style-type: none"> • High Building Speed • Good part resolution • Overcuring, scanned line shape • High cost for supplies and materials
	Material Jetting	<ul style="list-style-type: none"> ▪ Polyjet ▪ MJP 	<ul style="list-style-type: none"> • Multi-material 3d printing • High surface finish • Low-strength material
	Material Extrusion	<ul style="list-style-type: none"> ▪ FDM ▪ FFF ▪ ADAM 	<ul style="list-style-type: none"> • Inexpensive extrusion machine • Multi-material printing • Limited part resolution • Poor surface finish
	Binder Jetting	<ul style="list-style-type: none"> ▪ MJF ▪ SPJ 	<ul style="list-style-type: none"> • Full-color objects printing • Require infiltration during post-processing • Wide material selection • High porosities on finished parts
	Powder Bed Fusion (PBF)	<ul style="list-style-type: none"> ▪ SLS ▪ SLM ▪ DMLS ▪ EBM 	<ul style="list-style-type: none"> • High accuracy and details • Fully dense parts • High specific strength • Powder recycling • Support and anchor structure
	Directed Energy Deposition (DED)	<ul style="list-style-type: none"> ▪ LENS ▪ EBAM ▪ LMD-w ▪ WAAM 	<ul style="list-style-type: none"> • High deposition rate compared to PBF process • Repair of damaged/worn parts • Functionally graded material printing • Require post-processing
	Sheet Lamination (SL)	<ul style="list-style-type: none"> ▪ LOM ▪ UAM 	<ul style="list-style-type: none"> • High surface finish • Low material, machine, process cost • Decubing issues

Figure 2.1: ASTM classification of 3D AM processes. Adopted from [40]

that are all manufactured using inkjet technology [30].

From these comparisons and publications, it is clear that scalable AM techniques have a lot of potential and further research should be conducted to make them feasible. Inkjet printing is a well-established technique with the rapid development of printheads and ink production techniques creating new opportunities.

2.2. Inkjet printing

2.2.1. Inkjet printing process

An inkjet printing process can be divided into three main steps, occurring in listed order. A distinction can be made between ink deposition, substrate interaction, and curing processes. The deposition process defines the way an ink droplet is ejected and formed from the nozzle. After successful deposition and on the substrate or another layer, the ink droplet forms to its final shape and dries. This is referred to as the curing process, and can be influenced in multiple ways to accelerate ink drying.

Deposition

Several common techniques exist to deposit ink. A distinction is made between drop-on-demand (DOD), and continuous inkjet dispensing (CIJ). Some authors [54] also regard aerosol printing as a third technique for inkjet printing, others regard this as a direct-write technique. [50].

In Continuous inkjet printing, a continuous stream of ink is fed through the nozzle. The stream of ink breaks up into small droplets by means of Rayleigh instability. To properly locate each droplet, charged deflection electrodes alter their direction. This poses a fundamental restriction on CIJ printing; inks are

required to be electrically conductive [16]. If no ink should be deposited on an instance, all droplets can be directed to a collector for recycling. It is one of the oldest inkjet printing techniques, and still used nowadays in the textile and labelling industry for its high-speed characteristic. However, the possibility of contamination during recirculation and the need to use an electrically conducting fluid are limitations for many applications, especially in 3D inkjet printing. For this reason, drop-on-demand (DoD) is the method of choice when manufacturing small structures, also due to its higher placement accuracy and smaller drop size potential [14]. DoD handles higher viscosity fluids which is also an advantage for printing structures; these higher viscosity inks typically require less solvent evaporation and hence dry quicker.

As the name suggests, a drop-on-demand printhead only fires a droplet when demanded. Usually, this technique relies on creating temporary overpressure in the nozzle to eject a small volume of ink, that after ejection again rapidly forms a droplet. A thermal DOD inkjet printer, also referred to as bubble-jet, dispenses ink after rapidly expanding a vapour bubble by locally heating the ink. Thermal DOD may impose restrictions on the inks used, as generally water is used as a solvent, although non-aqueous inks are available. Inks need to be rather volatile since the mechanism of ejection relies on evaporation of inks to create gas. Also, some inks might not be compatible with a thermal DOD printer as they are heat sensitive or degrade in response to heat. [14]

A piezoelectric DOD printer on the other hand uses a small piezoelectric transducer to rapidly compress the volume in the ink reservoir and eject an ink droplet through the nozzle orifice. They provide significant advantages over thermal inkjet printing, such as better drop formation control, easier operational principle, and inks do not suffer from rapid heating. However, they are more complex and expensive to fabricate. A schematic representation of CIJ and the two types of DOD is given in fig. 2.2

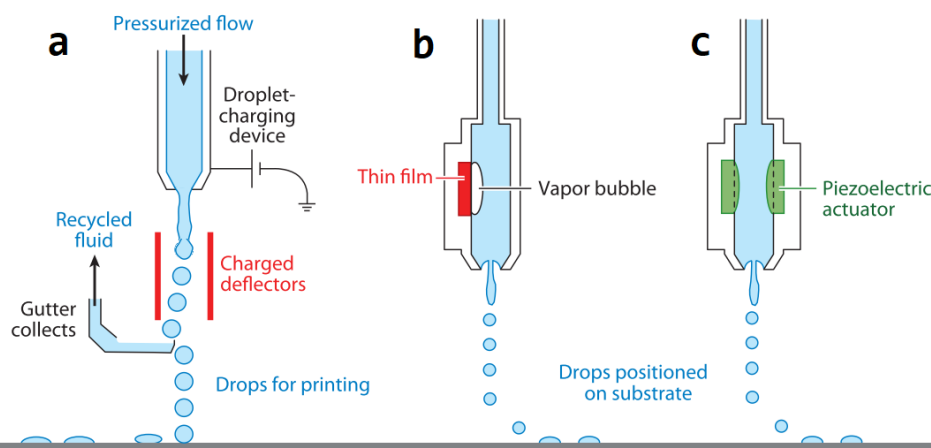


Figure 2.2: A schematic representation of Continuous inkjet (CIJ) printing (a) and two common types of drop-on-demand (DOD) printing; thermal DOD (b) and piezoelectric DOD (c). Adopted from [15, 54]

Other DOD-techniques that are less often used are electrostatic and electro(hydro)dynamic inkjet printing. Similar to CIJ, they require an electrically conductive ink to work. Electrostatic inkjet printing has a merit that the formation and location of the droplet can be controlled by using an electric field and the possibility to use highly viscous liquids with minimal solvent volumes [26]. With electrohydrodynamic inkjet printing, it was shown that vertical structures could be built due to the rapid solidification of the ink droplets [2]. Sometimes additional features can improve the capability of DOD printers, like heated printheads to lower viscosity of the ink. This also enables the possibility to print wax-like inks with a low melting temperature, which have an otherwise too high viscosity.

Substrate interaction

Fluid and substrate interaction is an important characteristic for all printable materials, and largely determines the effectiveness of printing a first layer of ink. Though important for the first layer, subsequent layers show other behaviour as they are not printed on the substrate, but on previously printed layers of dried ink. A careful selection of the substrate should be made based on the desired properties of the final product. In some cases the substrate remains part of the product, hence its properties are important to consider. For example, when printing electronics, usually glass, silicon-based or polymer

substrates are used [33]. If flexible electronics are desired, only the latter can be used. Also, flexible polymer substrates are chemically incompatible with resists, etchants and developers used in conventional integrated circuit processing [27].

Figure 2.3 shows progression of an ink droplet forming on the substrate after impact. This process depends largely on ink properties and to a lesser extent on substrate properties. The first phase of final drop settling is impact driven. The droplet impacts the substrate at a relatively high velocity and spreads out. Spreading is resisted by surface tension and viscosity of the fluid and reaches a maximum, dissipating all kinetic energy before retracting to a smaller drop. In the capillary phase, capillary action can slowly spread out the droplet over the substrate. With inks loaded with particles, this can lead to the well known 'coffee-ring' effect [15].

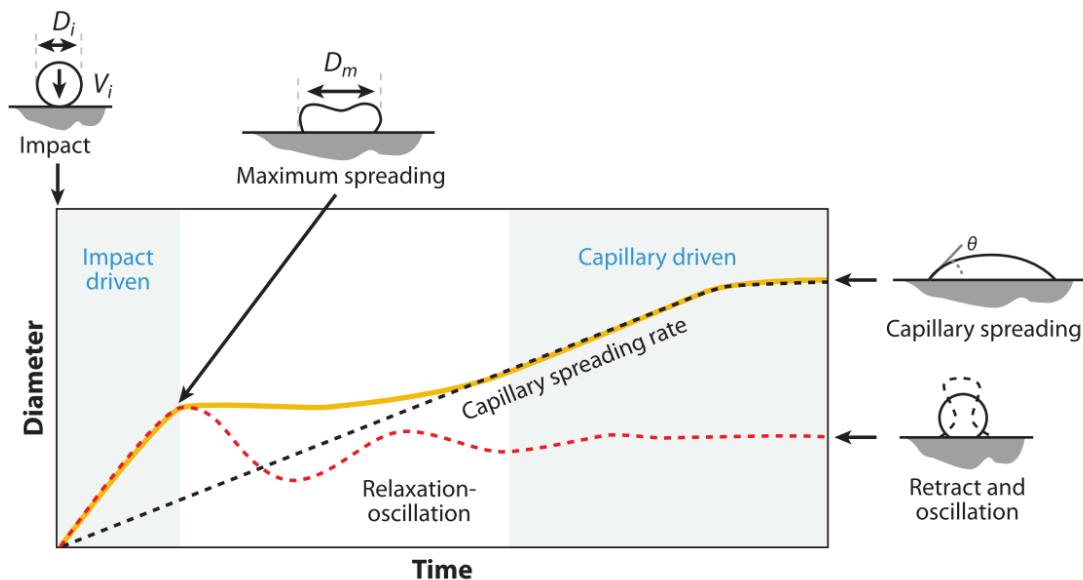


Figure 2.3: Drop spreading upon impact on a substrate. A distinction can be made between the impact driven phase and capillary driven phase. Amount of maximum spreading D_m and final contact angle θ depend on ink and substrate physical properties. Adopted from [15]

Solidification

After deposition on either the substrate or printed material, ink droplets form to their final shape and solidify. For example, inks used in office inkjet printers dry by evaporating their solvents in ambient air, leaving only the adhered pigments on the paper. The rate of evaporation naturally depends on the fluid properties of the ink and substrate it is deposited on. In some applications, this phase change will generate the desired final product, whereas in other cases a separate process step is required, called curing. The liquid to solid phase change can occur by a number of methods, which are discussed in this section. Their effect largely depends on the type of ink that is being deposited. With special inks such as nanoparticle conductive inks, it is desirable to obtain a high conductivity. This often requires a sintering of the particles. Techniques from an indispensable publication about sintering techniques for conductive tracks [44] will also be treated here.

Cooling

When heated inks are deposited, they usually don't require any other form of curing. The ink drops that are still hot are exposed to cooler ambient air and cool down past their melting temperature transition point to solidify. Examples of inks that use this method are waxes and gels [14, 51]

Substrate heating

In most applications when impacting the substrate, the liquid drop will rapidly transform into a solid after a phase change. Heating the whole substrate can be an effective way to indirectly heat up the ink droplets and accelerate their rate of solvent evaporation. This technique is easy to implement by placing a heater under the substrate table and hence heating the substrate and subsequent ink drops. This effective method is mainly used in older works and for all kinds of inks [10, 27, 32].

Photonic curing

A modern technique is photonic curing, which uses photons to locally heat and transfer energy to the material. Photons are irradiated onto the material from a powerful light source, usually placed close to the printed layer. Polymer pre-cursors can be cross-linked to form polymer chains, known as photopolymerisation [31]. Nanoparticles can be sintered, known as photonic sintering, or other chemical reactions can take place under the influence of high energy light.

Several techniques exist which all rely on the principle of energy transfer using photons to cure the material. The most well known technique is probably laser, extensively used in other industries as well. A coherent light source bundles photons in a high energy concentration beam that is aimed at specific parts of the print area to locally heat up material. The laser quickly moves over desired locations, similar to how 3D metal sintering works [50].

Using relatively low-frequency microwaves or infrared light, the print surface can be warmed up all at once. Infrared generally has too little energy to crosslink polymers or sinter nanoparticles, but can evenly warm up the material. Infrared does not penetrate deeply into the material. This has an advantage over substrate heating and microwave as only the printed layers that need heating are warmed up and not all subsequent layers up to the substrate itself [44].

Using higher energy light passing the visible spectrum, UV is a commonly used type of light to cure inks. Several works even show how to sinter inks with a UV light source that were designed to be sintered using a laser [46]. UV light is also able to photopolymerise polymer precursors, creating strong structures from UV-sensitive inks.

A similar technique to UV light exposure is Intense pulsed light (IPL). Short intense pulses are flashed on to the printed ink using high power xenon lamps. Again, this rapidly heats up the material through photonic absorption. Although effective, if it is not well controlled IPL can lead to a destruction of the printed tracks owing to extreme rapid heating and cooling. This is in contrast to IR and UV, where generally a constant exposure for several seconds to minutes is applied. IPL instantaneous energy transfer is magnitudes higher than IR and UV, hence the pulsed application of light in stead of constant exposure [17, 46]. A commercially available setup for IPL is the PulseForge by Novacentrix, used in most works using IPL to cure their inks [47, 48].

All aforementioned techniques are applied to the whole print surface, with exception of laser which is applied very locally. However, only the materials with sufficient photonic absorption of the specific emitted frequency will heat up, others will reflect the electromagnetic waves and not heat up as much.

2.2.2. Inkjet printing inks

Four main classifications of the inks can be made. First of all, structural inks are used to build a mechanically stable structure that is not removed at the end of the manufacturing, but is part of the product. Secondly, conductive inks are used as a conductive trace for electricity or heat. Addition of these inks to the product usually makes it an active device rather than passive, being able to transfer energy or information using conductive traces. Third, support or sacrificial inks which provide structural rigidity during printing, but can later be removed. Normally this is done using solvents or heat. Lastly, other inks are listed such as piezoelectric and magnetic inks and derivations of aforementioned materials. Note: the terms 'material' and 'ink' are sometimes used interchangeably by authors. Material refers to the main substance of interest, while ink refers to the material mixed with a carrier fluid to make it suitable for inkjet printing.

Physical properties

When designing inks for inkjet printing, the properties of interest are primarily viscosity and surface tension. The viscosity should be suitably low, typically below $20 \text{ mPa} \cdot \text{s}$ to allow droplets of ink to flow through the small nozzle and surface tension should be suitable to form drops quickly after firing from the nozzle [14, 36].

In fact, the behaviour of inks can be characterised by several dimensionless groups depending on these physical parameters, the most important ones being Reynolds (Re), Weber (We) and Ohnesorge (Oh):

$$Re = \frac{v\rho a}{\mu} \quad (2.1)$$

$$We = \frac{v^2\rho a}{\gamma} \quad (2.2)$$

$$Oh = \frac{\sqrt{We}}{Re} = \frac{\mu}{\sqrt{\gamma\rho a}} \quad (2.3)$$

where v, ρ, μ and γ are velocity, density, dynamic viscosity, and surface tension of the fluid respectively, and a is a characteristic length [15]. Figure 2.4 shows the relation between the relevant dimensionless numbers for inkjet print-able inks. Low values of Reynolds numbers cannot be printed as the ink is too viscous and cannot be jetted. High values means too many individual drops will form which is not desired. When the Weber number is low, no drops can form due to insufficient surface energy. A combination of high Reynolds and Weber numbers poses a risk of splashing when impacting the substrate. The printable region is a combination of proper parameters and is framed by red dashed lines in fig. 2.4.

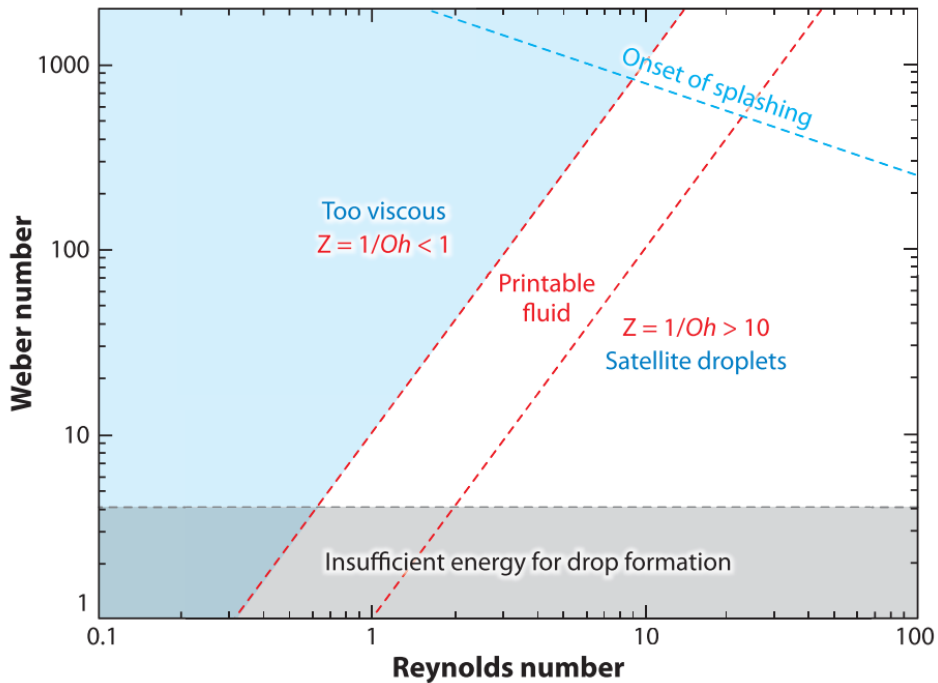


Figure 2.4: Relations and requirements for Weber, Reynolds, and Ohnesorge number for printable inks. Only a small region is suitable for printing, framed by red dashed lines. Adopted from [15]

Another way to classify printable inks is the printability assessment number Z , found in one of the earliest works on the mechanisms of drop generation in fluids. The Z number is basically the reciprocal of the Ohnesorge number [15, 16].

$$Z = \frac{1}{Oh} = \frac{\sqrt{\gamma\rho a}}{\mu} \quad (2.4)$$

where $1 \leq Z \leq 10$ to have an ink suitable for inkjet printing.

These dimensionless numbers provide a way to quantify the value of fundamental fluid properties of most inks. For non-Newtonian fluids, other dimensionless numbers also play a role such as the Weissenberg Number (Wi), which compares the elastic forces to the viscous forces in such fluids [50]. When working with particle-loaded solutions, the zeta-potential and pH of the fluid is also of importance to keep the particles from agglomerating [53, 54].

Structural inks

A lot of structural inks exist, since they have been explored in early works in the field of inkjet printing. After inks for labelling applications, usually consisting of only one or several layers, the focus was gradually shifted towards printing higher numbers of layers to print 3D structures. A structural material is part of the final product and should have the right material properties to be compatible with conductive traces, sacrificial material and the corresponding curing and post-processing steps. Polymer solutions were the main type of ink used for printing multi-layered structures, and are still used today [14]. Polyimide and polyketone are examples of this and are good insulators [55]. Sometimes, other materials are added to create a hybrid solution with beneficial properties, like adding ceramic particles for more strength of the final structure [21, 31]. Newer polymer based inks consist of a polymer precursor that is crosslinked by the application of heat or light irradiation. UV-curable resins usually consist out of oligomers and acrylate monomers. Upon photopolymerisation, they harden but have a low glass transition temperature. Their low heat distortion temperature makes these materials less suitable for purposes requiring elevated temperatures, or if combined with materials that require an elevated temperature for curing [31]. For that reason, it is a challenge to combine the right structural inks with other inks like conductive or support inks.

Conductive inks

Printing of conductors is based on either conductive ink or molten solders [30]. Conductive ink contains conductive polymers or nanometer-sized conductive particles that are later sintered in a curing step. However, graphene and carbon-based printable inks can use particle sizes magnitudes greater, since they rely on another curing method to improve their conductivity [54].

Molten solders

An effective way to print conductive traces is based on solder tracks. Molten solder is jetted from a heated printhead and solder drops are deposited on the substrate. Drops are still molten when an adjacent drop is deposited, melting them together to form a trace. A disadvantage of this method is the use of high temperatures needed to melt the solder, and potentially damaging the substrate. On the other hand, when the solder is solidified after cooling down, it has low resistance compared to other conductive inks and requires no further post processing [30].

Polymer based conductive inks

Before nanoparticle-based conductive inks were common, (semi-)conducting polymers were used to print conductive tracks. These polymers print in a similar way as structural polymers, usually dispersed in a solvent which evaporates after heating. In some cases a polymer precursor is printed which transitions to a fully conducting polymer after curing.

Nanoparticle based conductive inks

In a lot of works, the use of nanoparticles (NP) is described. Nanoparticles are usually dispersed in a carrier fluid to lower the viscosity and make the ink printable. Normally, around 20-50 wt% of the ink consists of nanoparticles. The majority of NP-inks contain metal nanoparticles; their sizes ranging from tens to hundreds of nanometers. Smaller nanoparticles are hard to consistently manufacture and bigger particles have a potential of nozzle clogging and require significantly more energy to sinter, which is important when applying photonic curing or laser sintering. The vast majority of all nanoparticle inks are silver-based. Silver (*Ag*) has excellent electrical and thermal conductivity, even better than the commercially most used conductor, copper. However, silver is almost ten times as expensive as copper on average, making it a less interesting material for large scale products requiring a lot of the metal. In small scale applications like inkjet 3d printing however, small volumes of metal are used. The price of metal NP ink is mainly determined by the processing costs to make the nanoparticles and ink dispersion [38]. Other NP inks include gold (*Au*), cobalt (*Co*), copper (*Cu*) and iron-oxide (Fe_xO_y) based. Ferrous and copper NP inks show increased risks of corrosion and pose health risks, making them less attractive. Gold inks are expensive compared to silver-based inks, even for small volumes of the metal [2, 10, 45]. Graphene and carbon-based inks are both subject of an increasing number of publications last decade because of their promising mechanical and electrical properties [22]. Jabari et al. showed how inkjet printed graphene oxide traces compare with silver nanoparticle traces. They also report a performance increase of an ink which combines graphene and silver nanoparticle, leading to less print failures and a stronger, crack free trace [23]. All of these nanoparticle inks need to be sintered by a heat source for effective conduction. It ranges from low temperature sintering (up to 80 °C) to high temperatures (260 °C and above), depending on particle size. Figure 2.5 shows silver nanoparticles before and

after heating to different temperatures. Alternatively, other sintering techniques using electromagnetic waves or Ohmic heating can be used and has been demonstrated to work [28, 32].

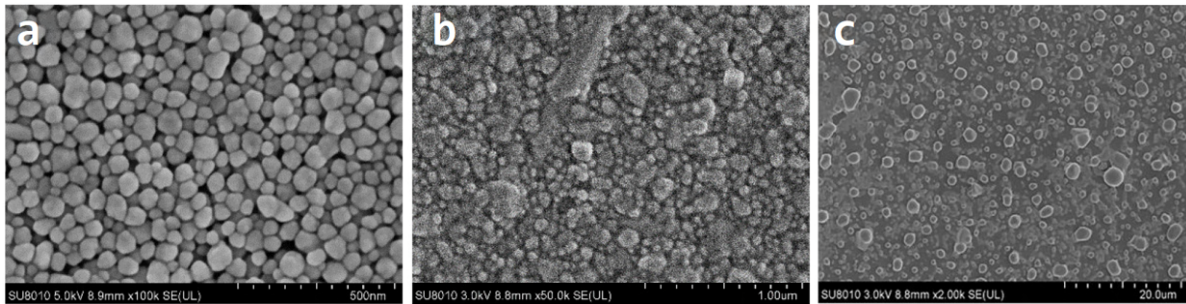


Figure 2.5: Scanning electron microscope (SEM) images of silver nanoparticle inks at a) uncured state, b) heated to 300 °C, c) heated to 400 °C. The nanoparticles are sintered at sufficiently high temperature, providing a better conductivity. Adopted from [7]

Support inks

Support materials or sacrificial materials are commonly used in the additive manufacturing industry to temporarily support a structure while the product is manufactured. In lithography, sacrificial materials are also used to shield another materials from destructive light sources. For 3D inkjet printing applications, its purpose is to provide a solid base for a next layer to print upon. Similar to FDM printing, an inkjet printer cannot print features mid-air. In FDM sometimes a 'bridge' can be formed by exploiting the stringing behaviour of hot molten plastic to span a line of filament over a gap. With inkjet printing, this is not possible since each jetted drop has a high downwards velocity and the drops are naturally separated. A typical approach to print a bridge-like structure in 3D inkjet applications is shown in fig. 2.6.

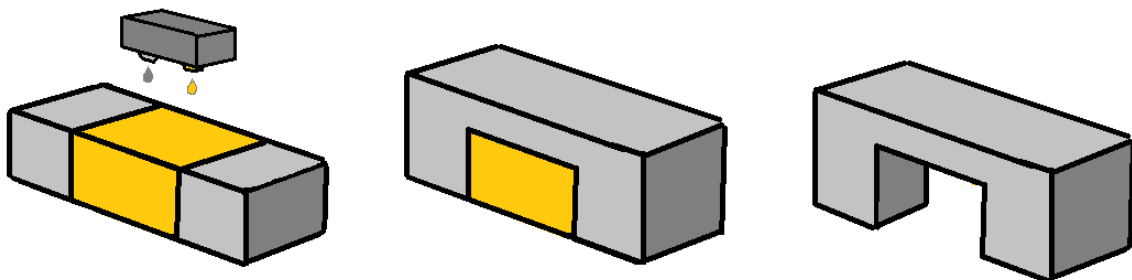


Figure 2.6: Support materials deposition and removal process. Manufacturing steps from left to right. Support material (orange) is deposited simultaneously each layer with structural material (grey). To form a bridge, structural material is deposited on top of the support material. After the structure is completed, support material is removed, leaving only the desired structure.

In industry-grade prototype machine such as Polyjet, Objet and Projet printers, support structures can be removed by hand and water jetting. Gel-like materials are using in Polyjet and Objet printers, whereas the support structure in Projet machines is wax [49, 50]. Waxes like kemamide have a low melting point, usually less than 100 °C. By melting them in a heated nozzle, the hot drops can be jetted and solidify again upon impact on the substrate due to rapid cooling. They can later be removed by heating the product to the melting point of the wax. Gels behave similarly, though not requiring a heated nozzle to be dispensed. They can be washed away with water or a solvent.

Newer research tries to find alternative materials to support structures, for example with cellulose-based support material. The cellulose is water soluble and can be easily washed away with water. Waxes in contrast are traditionally petroleum-based and therefore non-soluble in water, unsustainable, and non-recyclable. Bio-degradable support materials have potential to replace waxes if their printability improves [34].

Other inks

Other materials that are modified to be jettable include piezoelectric, magnetic substances and many others. Piezoelectric materials are the active part in a sensor or actuator. They are generally either ceramic or polymer. [30]. Ceramic elements show a greater piezoelectric effect than polymers. However, these ceramic particles are dispensed in a carrier fluid to make the mixture printable. The particles then need to be sintered at high temperatures.

Inkjet printing in the medical industry has seen an increase the last couple of years. Drug tablet printing for medical applications is described in several newer works as it has the potential to customise the dosage for each patient. Inks contain the drug which is printed in tablets [6, 11]. Live tissue cells can also be printed; Cell-laden hydrogel structures are printed by Negro et al. [42].

2.2.3. Ink and process combinations

Only in recent years researchers started actively combining inks to create multi-material structures with 3D inkjet printers. Before, the focus was more on individual ink performance and not so much multi-functional and multi-material performance. Now the potential of 3D inkjet printing is recognised, more and more publications focus on finding appropriate ink combinations to make multi-material prints.

A lot of focus is on combining structural and conductive inks. A broad range of structural inks is used, be it all polymer-based. Most of them can be crosslinked using UV or IPL. Only in a few cases heating cured the inks. For almost all conductive tracks, silver nanoparticle inks are used. Mostly substrate heating or oven heating is required, though newest works use IPL and UV to sinter the nanoparticles.

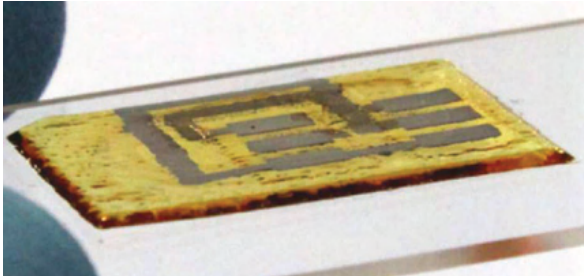
Table 2.1: Number of works using specific process and material combination out of around 65 scientific publications.

		Materials						
		Structural		Conductive		Support	Piezoelectric	Others
		Polymers	ceramic	Nano particles	others			
Curing process	None	1	0	1	3	2	2	2
	UV / photonic exposure	9	2	4	0	0	1	2
	(Laser) sintering / Substrate heating / IR	5	2	16	6	0	2	1
	Other	1	0	1	0	2	0	1

Potentially, a lot more combinations are possible if one takes all inks into account and identify the processes used to print and cure them. When deposition and curing processes are similar, the inks might be able to be combined into one print process, depositing and curing both inks simultaneously each layer. The feasibility of actually combining inks depends on more parameters than deposition and curing methods, though identifying these fundamental dependencies in an early stage provides a good starting point for further research. An overview of a number of works using specific process and material combination out of around 65 scientific publications is shown in table 2.1.

Combining materials from different material groups based on similarity in curing process can yield feasible combinations for a multi-material inkjet printing process. For example, five works describe structural polymer inks that use a heat-induced curing mechanism. Also, sixteen works describe conductive nanoparticle using heat-induced curing as well. Inks from both these categories might be taken and combined into one printing process. Numerous researchers have already attempted to combine inks, but not many have combined different types of inks having a similar post-processing process. Saleh et al. [46] showed some promising results combining a photopolymer ink as structural material with silver nanoparticle ink for conducting traces in working functional structures. Both inks were post-processed using a single 395nm UV-LED light source. The photopolymer ink with polymer precursors crosslinked

at this wavelength and the silver nanoparticles sintered due to plasmon resonance quickly heating the particles. In other cases, the inks may require a different post-processing step. Walczak et al. were able to print micro fluidic valves and a lab-on-a-chip for capillary gel electrophoresis using a combination of a structural material and support material ink [51, 52]. The structural ink is a photopolymer based ink which cures under UV-light exposure. The support material is a wax-like ink that solidifies when cooling down after jetting at an elevated temperature. These fundamentally different inks also have different solidification processes yet are compatible.



(a) Conductive and dielectric inks printed and UV irradiated forming security chip with specific conductive layout. Adopted from [46]



(b) Lab-on-a-chip for capillary gel electrophoresis made using a structural and support material ink. Adopted from [52]

Figure 2.7: Examples of multi-material inkjet printed structures

All post-processing techniques for solidification of inks mentioned earlier have their own applications and strengths. However, when it comes to speed and ease of use, some techniques have a clear advantage. Photonic curing using can be integrated on the printhead and applied directly when printing, greatly speeding up the production of parts. Contrarily, heating as a post-process with low temperatures of around 100 °C might be feasible using substrate heating, but higher temperatures require a dedicated enclosure or an oven and is harder or impossible to apply during the print process. Ambient air drying for wax-like inks are simple and require no extra post-processing but waiting for layer to dry and cool can be slow. It is for this reason that photonic curing was already popular for structural and support material inks, and is gaining more interest for curing conductive inks. A process allowing rapid manufacturing of structures with structural, conductive, and support material ink requiring only photonic curing using UV light will therefore be the main goal of this thesis.

3

Approach

To make multi-material functional 3D structures using inkjet technology, it is first required to choose the inks to print the structures with, and a proper selection of an experimental setup to actually use these inks in inkjet printheads. In the following sections, a high level overview of the methods used in this thesis is given. More details can be found in the chapters involving the subject of interest.

3.1. Selection of inks

In chapter 4, the phenomena of sintering and photopolymerisation using high frequency UV light is explained. Combined with the knowledge gained from state of the art literature, several types of ink are proposed for multi-material print experiments using one common curing technique. Technical datasheets from ink manufacturers provide a good basis for the most important physical properties of the inks such as viscosity, and usually contain instructions on how to print their inks best. Inks specifically designed for photopolymerisation also include information about their composition and wavelength sensitivity to use for curing. Nanoparticle-based generally do not, since they are required to be post-processed using heat according to their datasheets. As shown in chapter 2, researchers have proven to be able to post-process inks in other ways as intentioned by the manufacturer. To investigate the possibility of using only UV light as the primary curing technique for some of the proposed inks, experiments are performed to assess the spectral sensitivity of the inks.

3.2. Multi-material printing

After careful consideration of inks to use, a suitable experimental setup is selected to actually use the inks. In this thesis, a PiXDRO LP50 inkjet printer [39] is used. The PiXDRO LP50 is a state of the art research and development device capable of printing with multiple printheads. The selected inks are matched with specific printheads based on the capabilities and performance of the printheads and the PiXDRO LP50. An HMI allows for advanced customisation of print settings of the PiXDRO LP50 and printheads. Before attempting to print with multiple inks at once, each printhead and ink combination is first thoroughly tuned to produce reliable jetting. A substrate is chosen that is versatile and suitable for the tests. To ensure proper alignment between printheads and substrates, a calibration method is developed. Basic multi-material prints with two inks are made and analysed before moving on to more complex structures involving more inks and layer-dependent process settings. Using these results, printing functional 3D structures is attempted in chapter 6. A process workflow is presented used to successfully print structures, of which a proof-of-concept is given at the end of the chapter.

4

Sintering and polymerisation using UV light

In the following section, a brief overview of the principles behind sintering and photopolymerisation is given. Then, appropriate inks are selected for further experiments.

4.1. Working principles

4.1.1. Sintering

Sintering is the process of forming and compacting a solid conductive mass of material by heat and/or pressure without melting it to the point of liquefaction. In the scope of this thesis, only sintering of nanoparticles will be treated. Sintering of nanoparticles in particular can be achieved at way lower temperatures than the bulk materials melting point, due to the large surface area compared to volume for tiny nanoparticles. The particles locally fuse together, creating a structure with interconnected particles while not having melted. This effect was already discovered by Buffat *et al.* in 1976 [5] but only found its way into nanoparticle ink sintering about a decade ago. Commercially available nanoparticle inks nowadays exploit this phenomenon by requiring heating to only a fraction of the bulk material melting point to create a conductive structure. Using a lower temperature has many benefits such as a smaller chance of damaging substrate and printed materials. More recently, researchers started to exploit plasmon resonance of nanoparticles to sinter nanoparticle inks. High intensity light is used to irradiate the ink including the nanoparticles. Plasmonic nanoparticles can interact with light in several different ways. The particles can scatter or absorb the light which excite nanoparticles and generate heat or strong electric fields [41]. Plasmon resonance strongly depends on particle size and geometry, explained in detail by Amendola, Bakr and Stellacci [1]. Ag, Au and Cu nanoparticles, as used in many conductive inks, have an absorption maximum in the range of $420nm$, $520nm$ and $600nm$, respectively. These wavelengths lie in the UV-Visible spectrum of light.

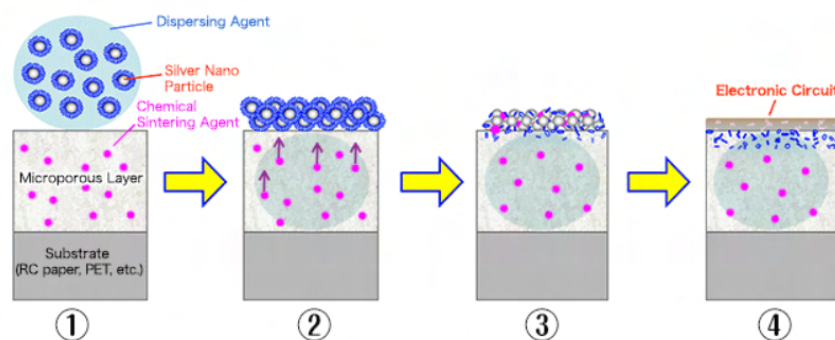


Figure 4.1: Printing of self-sintering nanoparticle inks. Adopted from [35]

Chemical sintering, where a chemical agent binds particles together in a similar way as sintering by heat, is also possible. Nanoparticles are dispersed in a solution and encapsulated by a dispersing agent to prevent them from accumulating. After deposition, the nanoparticles accumulate on the surface of special media selectively. Chemical sintering agents diffuse from the microporous layer of special media. Dispersing agents react with chemical sintering agents and come off from nanoparticles. The nanoparticles fuse together and transform into a porous foil. A schematic overview of such sintering process is depicted in fig. 4.1 for Mitsubishi NBSIJ-MU01 silver nanoparticle ink.

4.1.2. Photopolymerisation

A process known as photopolymerisation (or: photocuring, photo-cross-linking) occurs when a polymer changes its properties when exposed to light, often in the ultraviolet or visible region of the electromagnetic spectrum. Such polymers are also called light-activated resins. The change of property is often permanent, for example solidification of a resin. A mixture of dispersed chemicals with photoinitiators, monomers and oligomers transforms into a solidified structure after exposure to light with a certain wavelength. Mechanisms causing photopolymerisation differ depending on the type of photoinitiator present in the mixture. A distinction can be made between radical systems and cationic systems which are described in detail by Bagheri et al.[4]. An example of a photopolymerisation process is shown in fig. 4.2 depicting a mixture of monomers, oligomers, and photoinitiators that conform into a cured polymeric material.

Due to the versatile polymer chemistry-related innovations, photopolymerisation-based 3D printing techniques have attracted special attention from polymer chemists, material scientists, and engineers. Photopolymerisation techniques have found their way to many fields, including 3D printing. Digital Light Processing (DLP) 3D printers are perhaps the best-known example. These machines use UV lights to cure, or photopolymerise, a liquid polymer to create 3D printed objects. The liquid polymer is exposed to UV light which transposes the sliced image of a 3D design onto the liquid, which solidifies. The cured layers are slowly retracted from the liquid container, or vat, allowing liquid uncured polymer to flow into position for the next exposure. This process is repeated until a 3D part is created. A similar strategy can be employed when using photopolymers in 3D inkjet printing. Light-sensitive liquid polymers can be made suitable for inkjet printing by altering viscosity and surface tension to create a substance with appropriate Z-number, see chapter 2. As a bottom-up manufacturing technique, each layer can be printed and cured with light separately. Overprinting a solid layer with new ink and curing again creates a 3D structure.

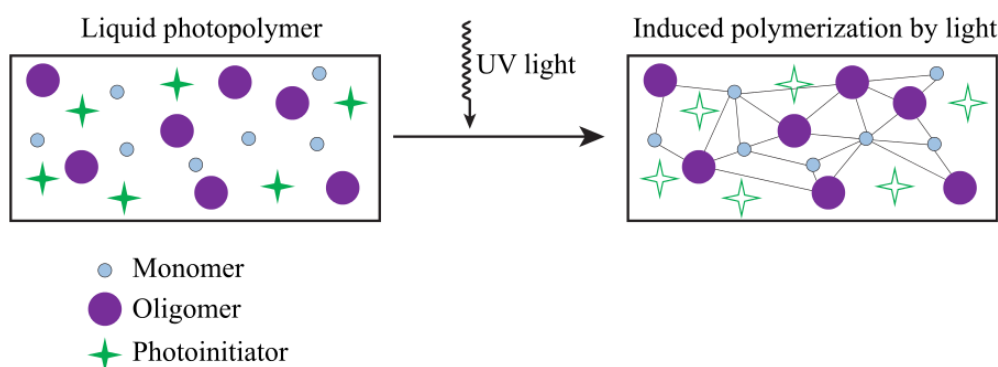


Figure 4.2: Photopolymerisation process. Freely dispersed monomers, oligomers, and photoinitiators are irradiated by UV light which induces photopolymerisation. Free radicals react and create a network of connected monomers and oligomers. Adopted from [56]

4.2. Selection of inks

Based on the results found in the literature survey, a selection of inks can be made for further experiments. The inks ideally need to have well defined absorption spectra for sintering and photopolymerisation while also meeting all other criteria. Moreover, these inks all have to be compatible with inkjet printheads to be viable. This means physical properties need to be as such that the ink's Z-number is in the printable region. All inks considered below meet this fundamental criterion.

4.2.1. Selection of conductive inks

Conductive inks suitable for curing with light are generally nanoparticle inks, as discussed in chapter 2. Silver nanoparticle inks are widely available, and generally provide best conductivity. Other nanoparticle inks have disadvantages such as being more prone to corrosion or can be more dangerous for humans and organisms compared to silver nanoparticles [8]. For these reasons, only silver nanoparticle inks are considered for this research. It is important to select the right type of nanoparticle ink to be able to exploit the plasmon resonance phenomena to sinter the particles and create a conductive track. Unfortunately, due to the novelty of this technique combined with the difficulty of properly assessing nanoparticle dimensions and geometry in inks, not many ink manufacturers provide this data with their inks since most inks are meant to be thermally treated. However, manufacturers do provide data about the composition of the ink and particle sizes. Candidate silver nanoparticle inks have been arranged based on their composition and particle size in table 4.1.

From these inks, NovaCentrix JS-B25P and Mitsubishi NBSIJ-MU01 were chosen to further analyse based on their differences in size of nanoparticles and readily availability in the lab. Novacentrix JS-B25P is normally sintered using IPL. Mitsubishi NBSIJ-MU01 is a 'self-sintering' ink which produces conductive traces when printed on coated photopaper or special substrate provided by the manufacturer and does not require any additional post-processing, fig. 4.1.

Table 4.1: Overview of nanoparticle inks considered

	Brand	Name	Silver content	NP size	Properties
Conductive	NovaCentrix	JS-A1xxx series	40 wt %	30-50 nm	5-12 cPs
		JS-B25xx series	25 wt %	60-80 nm	3-10 cPs
		JS-B40xx series	40 wt %	60-80 nm	2-12 cPs
	Mitsubishi	NBSIJ-MU01	15 wt %	20 nm	
		NBSIJ-FD02	15 wt %	20 nm	
		NBSIJ-KC01	17wt %	20 nm	
	ANP	DGP-40LT-15C	38.85 wt %	30-40 nm	
	NanoDimension	AgCite		80 nm	
	SunChemical	Nanosilver EMD5730	40 wt %		10-13 cPs
Harima chemical	NPS-J	62-67 wt %	12 nm	7-11 cPs	

4.2.2. Selection of photopolymer inks

At least two types of ink are required next to the conductive ink to create complex multi-material 3D structures. First, structural or building material ink is used as the primary ink to create mechanically strong and solid structures. Second, support material ink or sacrificial ink is used to temporarily support structures to create overhanging geometry by preventing printing 'in air'. From the state of the art review in chapter 2, candidate inks are identified. Structural inks range from inkjettable photoresists to specifically made inks for dielectric structures. Support material inks are not used in a lot of previous works and neither are they abundantly available. The listed materials are used in some industrial prototyping printers (Stratasys Objet, ProJet) or are spin-coat photoresists suitable for inkjet printing. It is important that inks are chosen that are compatible; the inks should not contain chemicals that interfere

with working principle of the other ink and impeding its function. For the same reason, they should also be compatible with the conductive inks. This property is hard to assess and will be experimentally validation. From the listed inks, two already compatible and readily available inks were selected, Stratasys Vero-series structural and SUP-series support material (VeroBlack RGD875, VeroYellow RGD836, SUP706B). These inks are used in industrial inkjet printing machines in which multi-material and overhanging structures can be made. They inks have proven to be compatible and produce quality 3D structures [49].

Table 4.2: Overview of structural and support material inks considered

	Brand	Name	Type	UV sensitive wavelength	curing energy
Dielectric	Microresist	InkOrmo	transparent	300-410 nm	
		InkEpo	transparent	300-390 nm	
		mr-UVCur26SF	negative resist	365-405 nm	
	SunChemical	SolSys EMD6000		undoped mercury lamp	0.1 – 0.3 J/cm ²
		Solsys 6044			1 - 1.5 J/cm ²
		U6415 JET9525			0.1 – 0.3 J/cm ²
NanoDimension	dielectric ink				
Stratasys	Vero series	Opaque colored			
Sacrificial	Stratasys	SUP705	NaOH soluble		
		SUP706b	NaOH soluble		
		SUP707	water soluble		
	Kemlab	KL5315	spin coat positive resist, 15 cSt		
		KL6002	spin coat positive resist, 21 cSt		
		K-PRO 7	spin coat positive resist, 150-177 cPs		
		Custom K-Pro	spin coat positive resist, 12 cPs		
	SunChemical	EMD2000	etch resist	undoped mercury lamp	0.2 - 0.3 J/cm ²

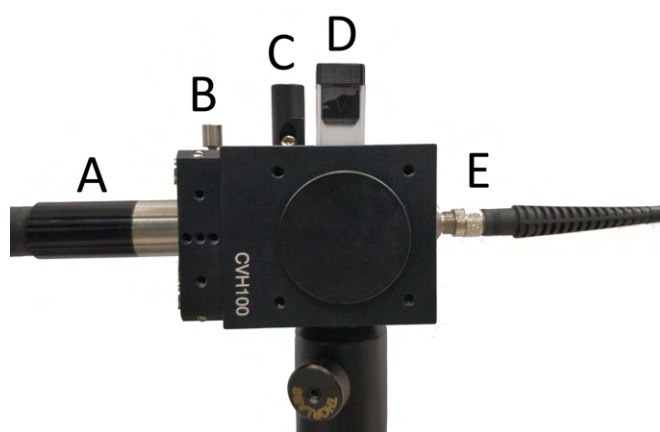
All chosen inks are available off-the-shelf which makes them a viable choice for a project with limited time. An advantage is that manufacturers provide details about the composition of the inks and others have successfully printed with the inks. The downside is that compromises need to be made, especially regarding the conductive ink. Inks are manufactured with a specific use case and post-processing requirement in mind, and the available inks for this research are no exception. The exact composition of the inks is not given which can result into incompatibilities with the proposed post-processing technique relying on photonic curing because of possibly added sintering agents, surfactants, solvents, or other chemicals. This will be verified in the experiments to follow.

4.3. Spectrum analysis experiments

Experiments were performed to verify the desired properties of the chosen inks for later experiments. The goal of these experiments is to find the sensitive wavelength for sintering or photo-polymerisation of the selected inks when this information is not given or to verify the information when it is provided.

4.3.1. Method

The setup consist of a light source, light spectrum analyser and ink cuvettes. A UV source [Honle Blue-point 4 ecocure] is connected to the setup via an optic fiber cable and provides the light for measurements. The UV source has a non-linear intensity output over a range of $300nm$ to $1000nm$, depicted in fig. A.4. Inks that need analysis are pipetted into small square plastic cuvettes [Ocean optics CVD-UV1S-SAM] and placed in a setup [Thorlabs CVH100] with custom aperture and filter options to control the intensity and wavelengths of light irradiating the sample cuvette with ink. No filters or apertures were used during the experiment. A spectrum analyser [Yokogawa, AQ6374] is used to plot the intensity of wavelengths of light transmitted through the ink cuvette. An illustration of the main components of the setup is given as fig. 4.3a. Multiple inks with respect to a control were analysed. The control is distilled water, $400\mu L$ dispensed in a cuvette. fig. 4.3b lists the number and composition of cuvettes used in the experiment.



(a) Spectrum Analyser setup. UV light enters the setup via a fiber optic cable (A) and is mounted via an adapter (B). A filter (C) can be inserted depending on desired wavelengths and light intensity. The sample cuvette (D) is loaded into the holder from the top for easy removal. Transmitted light exits the setup via another fiber optic cable (E) towards the spectrum analyser.

Cuvette number	Remark	Water content	SUP706b content	Ag NP content	
				Mitsubishi	Novacentrix
1	Control	400 uL			
2	UV ink		400 uL		
3			400 uL		
4	Ag Mitsui	399 uL		1 uL	
5		399 uL		1 uL	
6		399 uL		1 uL	
7		399 uL		0.5 uL	
8		398 uL		2 uL	
9		399 uL			1 uL
10		399 uL			0.5 uL
11		399 uL			0.2 uL
12	Ag Nova	399 uL			0.1 uL
13		399 uL			0.1 uL
14		600 uL			0.1 uL

(b) Overview of composition of cuvettes

Figure 4.3: Setup component overview and composition of cuvettes used in the experiment

4.3.2. Results

Plotted results from the control spectrometry analysis and SUP706B ink sample analysis are shown in fig. 4.4. The control is mostly transparent to all wavelengths and shows only a minor impedance of the light source spectrum which is due to the cuvette material and the water itself. A clear difference in absorption between water and SUP706b is visible in fig. 4.4a. However, in the normalised SUP706b spectrometry results in fig. 4.4b, it is easier to see that SUP706b has most of its light absorbance under $450nm$, peaking at the lowest value to be detected by the spectrometer, $350nm$. This is in accordance with the expected sensitive wavelengths of the ink in the UV-C spectrum.

In all samples loaded with nanoparticle ink, a noticeable coloration was visible after a few seconds of irradiation, depending on the percentage of nanoparticles. After some of time, this resulted in absorption of all light and no more transmission to the spectrometer. It was therefore important to make quick measurements and in that way recording the time-dependent absorption response of the nanoparticle ink samples. These results for a cuvette with $0.5\mu L$ Mitsubishi NBSIJ-MU01 and $399\mu L$ water are shown in fig. 4.4c. Results for other samples and inks are similar, as the composition remains almost the same. For increasing time, the ink sample gradually started to absorb more light as can be concluded from the shifting of the normalised graphs to unity, fig. 4.4d. This suggests that the nanoparticle inks are sensitive to the wavelengths output by the light source and this reaction might be exploited to sinter the nanoparticles after printing.

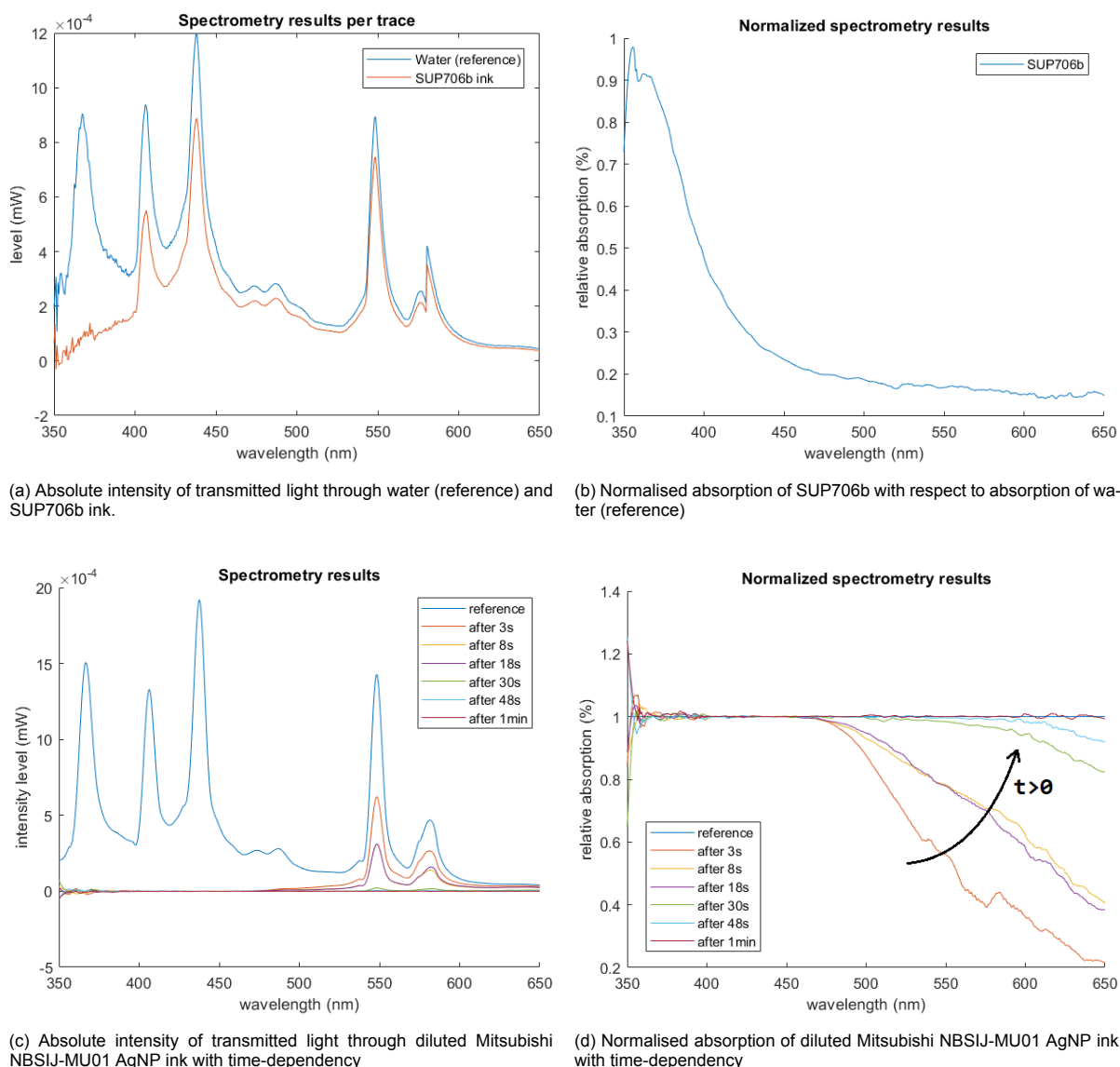


Figure 4.4: Absolute and normalised light absorption for SUP706B support material ink and diluted Mitsubishi NBSIJ-MU01 AgNP ink

4.3.3. Discussion

Due to the nature of the setup, only transparent inks could be tested. Results from the SUP706B test meet the expectations, as no dilution of this ink was necessary due to the transparent nature of the ink itself. Results of tests with diluted nanoparticle ink were mixed. A strong dilution of the inks was necessary before a measurement could be conducted. Undiluted or not sufficiently diluted nanoparticle inks transmitted too little light for the spectrometer to detect and make accurate measurements. However, this is also done by other authors to make valid measurements [18]. Dark coloration was observed only locally in the cuvette, possibly due to lens effects of the cuvette's non-square geometry. The reason for strong coloration effect is unknown, though a possibility is breakdown of the dispersing agents around the nanoparticles resulting in rapid oxidation of the particles in water. Heating from the irradiated light causes local currents in the fluid, spreading the coloration effect within the sample slowly. Manually shaking the cuvette caused immediate mixing and temporary homogeneous (dark) solution. After some time, the dark colour would gradually fade to the bottom of the cuvette only, suggesting agglomeration of heavier particles on the bottom due to gravity. See appendix A for photographs of this phenomenon.

5

Multi-Material inkjet printing

5.1. PiXDRO LP50 printers

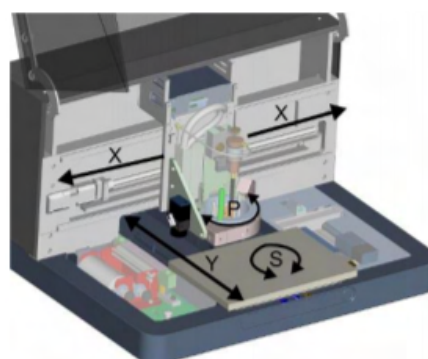
PiXDRO LP50 inkjet printers are desktop devices designed for research and development of inkjet processes and applications, as well as evaluation and development of inkjet materials [39]. A large substrate table supporting A4-paper with dimensions $227 \times 327 \text{mm}^2$ is installed with a vacuum pump to hold substrates in place without the need for adhesives. High precision motion systems are installed on all axis, being X,Y,Z for the linear translations of the substrate table (Y) and printhead (X,Z), and P,S for printhead rotation and substrate table rotation respectively. The machine has an accuracy of about $15 \mu\text{m}$ and a precision of around $5 \mu\text{m}$ in the X and Y axis. A software package named PiXDRO HMI is used to configure the printer and perform basic ink drop analysis and tune printer and printhead parameters. More advanced packages are offered by the manufacturer such as Advanced Drop Analysis, Automatic Print Optimization, and Advanced Gerber File Rasterizer, but are not used in this research. The printer is equipped with two cameras for analysis. One is directly mounted to the printhead and is aimed downwards to inspect or align the substrate and to calibrate printheads. A second camera is installed to analyse ink drops jetting from the printhead using an in-line strobe light. Standard maintenance functions are available to improve performance in case of nozzle clogging. Via the Pixdro HMI these maintenance functions are set for automated and reproducible execution, allowing optimization of printhead maintenance without an operator dependency.

Available maintenance functions are:

- Vacuum capping (applied to the nozzle plate to efficiently unclog a printhead)
- Purging (applying overpressure to the ink supply to 'push' ink out)
- Wiping (clean the nozzle plate over a lint-free cloth with a pre-set force and speed)
- Jetting (at set period and frequency)



(a) PiXDRO LP50 commercial research inkjet printer



(b) PiXDRO LP50 motion system

Figure 5.1: PiXDRO LP50 inkjet printer and motion system. Both images obtained from the PiXDRO LP50 user manual

5.1.1. Printheads

Several DoD printheads are available for use in the LP50, ranging from printheads using dispensable cartridges to multi-head setups with dedicated ink reservoirs. All compatible printheads are controlled by the LP50 via an electronics box, called the head personality box (HPB). The printhead itself is embedded in a printhead assembly (PHA), see fig. 5.2. Each type of printhead has its own PHA and consists of:

- Specific type of mount for the printhead
- Mounting ring with magnetic kinematic mount
- Electrical interface for heating and driving waveform
- Pneumatic interface (meniscus pressure)
- Ink supply interface and/or system

Also non-printhead modules can be installed. Currently available modules are for example a SPI G4 laser and Innophysics Plasma On Demand system. For this research, two PiXDRO LP50 printers are available, each having their own specific features. One offers support for Dual head PHA's and is equipped with a UV-light bridge (Phoseon FireEdge FE300). The other printer offers support for use of the Océ printhead. Other available PHAs are Dimatix DMC and Konica-Minolta KM512 PHA, which are supported by both printers.



Figure 5.2: PiXDRO LP50 PHA and HPB

5.1.2. Jetting options

Depending on the installed PHA, certain parameters for ink jetting can be set. Fundamental parameters that can be set for all printheads are piezoelectric waveform shape, printhead temperature, active nozzles and frequency. Waveform shape is defined setting timings and voltages for each step in the jetting process. Stable and reliable jetting is an optimization of at least these parameters which takes time when manually performed, which is why packages like Automatic Print Optimization exist. After tuning, it is usually not required to change these settings anymore. A typical waveform used by several printheads on the PiXDRO LP50 is shown in fig. 5.3. Notice the difference between rather simple waveforms on the left, compared to more complex waveforms with a specific nozzle filling operation on the right.

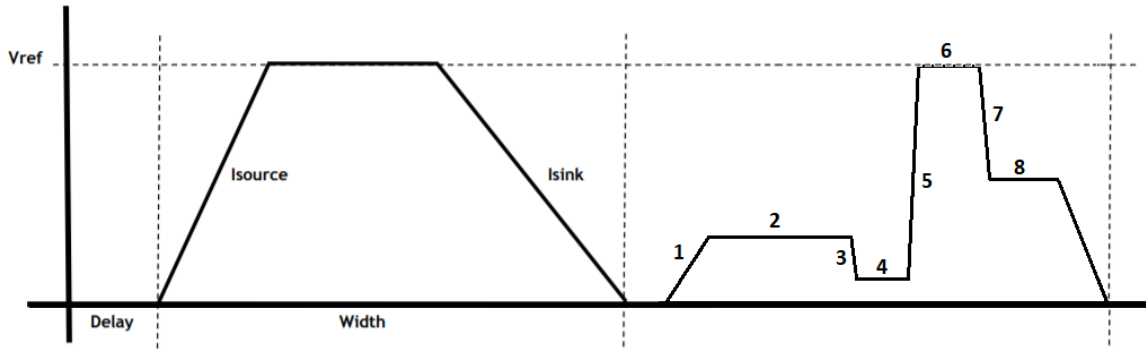


Figure 5.3: Typical waveform as used in KM512, Océ and Spectra heads (left) and more complex waveform with 8 different timing settings for DMC (right). Voltages and timings can be set to optimise jetting performance.

5.1.3. Printing options

Print parameters do not directly affect the printhead, but rather the printer and its motion systems and define a 'strategy' for printing. Print parameters are for example print speed, resolution, and size of the image. The majority of these parameters are constant between prints and are therefore saved in a file which is simply loaded during each print. Some parameters though, like the image to print and active nozzles, are often changed and can be stored in a separate file that overwrites the default parameters. These parameters are collected in a file which is referred to as 'recipe' and is easily modified by the operator per print job.

Resolution

Resolution determines the amount of droplets of ink per unit of length and is commonly expressed in dots per inch (DPI). A low resolution value results in drops printed further apart. A higher value results in drops closer together and coalescing. A proper resolution setting is influenced by jetted drop volume, capillary spreading upon ink-substrate interaction, and the user's desired outcome. The resolution can be set in X- and Y-direction.

Direction and speed

Direction of printing can be set to either bi-directional and uni-directional in both X and Y-directions. Bi-directional printing has the advantage of roughly halving print time but introduces the need for time-of-flight (ToF) compensation. This ToF setting aligns swaths in bidirectional prints, and will compensate the offset in unidirectional prints. It will compensate for the time the ink drop is travelling from the nozzle to the substrate. Print speed determines the speed at which the printhead is moved over the substrate (or substrate is moved under the printhead) and is constrained by the motion systems acceleration and jetting frequency of the printhead. Higher print speeds decrease print time but can introduce artefacts when pushing the limits and increase the need for proper ToF calibration when printing bidirectionally. The maximum scan speed is a function of the maximum drop ejection frequency and the in-scan resolution, eq. (5.1):

$$V_{max} = (25.4/DPI) * F_{max} \quad (5.1)$$

where V_{max} is maximum print speed (mm/s), DPI is resolution setting ($dots/inch$) and F_{max} is the maximum jetting frequency (Hz) of the printhead and printer. In practise, the print speed is never set above the maximum speed since the maximum frequency on the PiXDRO LP50 and printheads is quite high (up to $20kHz$) and resolutions are usually around 500 to 1000 DPI , yielding V_{max} of more than 500 mm/s .

Quality factor and stepsize

When printing with all nozzles enabled on a printhead, chances are that some nozzles might be failing or not jetting at expected performance. When a failing nozzle is supposed to print multiple adjacent lines this can cause visible artefacts in the printed results, see fig. 5.5. To mask these artefacts, a periodic change of nozzle printing adjacent lines can be introduced. This is called stepsize (SZ) and defines the number of pixels in cross-scan direction to skip for a nozzle before using that nozzle again. The stepsize is therefore an arrangement in cross-scan direction, compared to the quality factor (QF), which sets how many nozzles jet in one column in scan direction. The stepsize is not correlated with printing time, however the quality factor is. With a higher quality factor more nozzles are used to print one line in scan direction, which requires more time. With quality factor and stepsize the printer defines that an area of quality factor by stepsize in pixels should not be printed twice by the same nozzle. A schematic representation is given in fig. 5.4. This means that the printer needs at least the amount of $QF \times SZ$ available nozzles to print and takes at least $QF \times Printtime_{QF1}$ time to print. By varying the stepsize and quality factor, drying time between droplets can also be controlled. At stepsize 1, a droplet is printed adjacent to a droplet from the previous swath which might mean that the droplet has not yet dried and they coalesce. With other stepsizes, drops could land far away from each other and only after several swaths they start overlapping. This could give radically different drying behaviour.

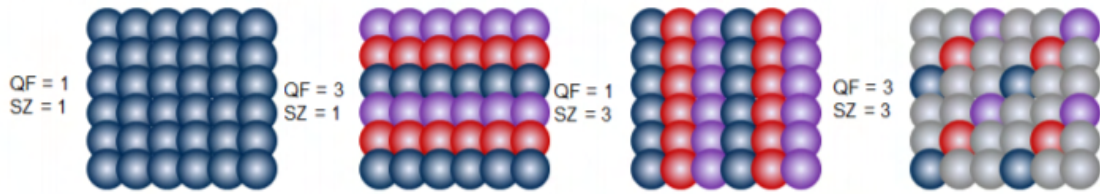


Figure 5.4: Stepsize and Quality factor differences illustrated.

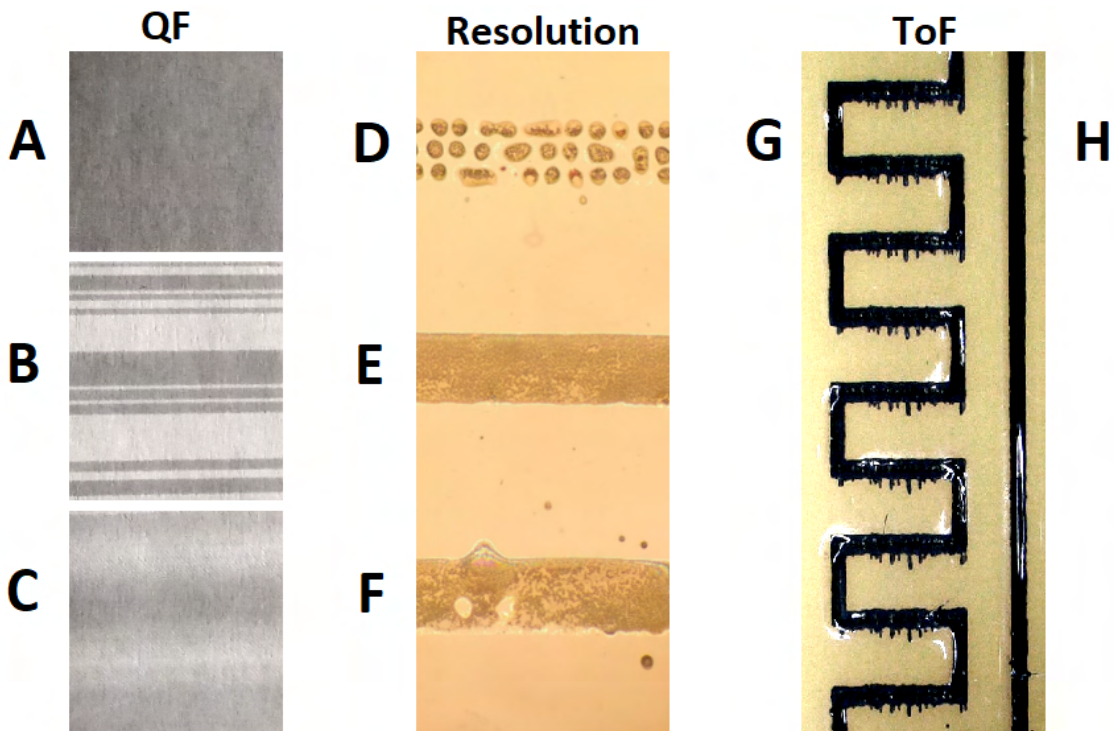


Figure 5.5: Print options and consequences for print quality. **QF:** Selected active nozzles (A) with QF1 yield a homogeneous print surface. All nozzles active with QF1 (B) show gaps due to failing nozzles. All nozzles active with QF16 (C) yields a better surface. **Resolution:** 500 DPI (D), 1000 DPI (E), 1500 DPI (F). **ToF:** Artefacts due to improper ToF settings with bi-directional printing in horizontal (cross-scan) lines (G). Vertical lines do not suffer from ToF setting (H).

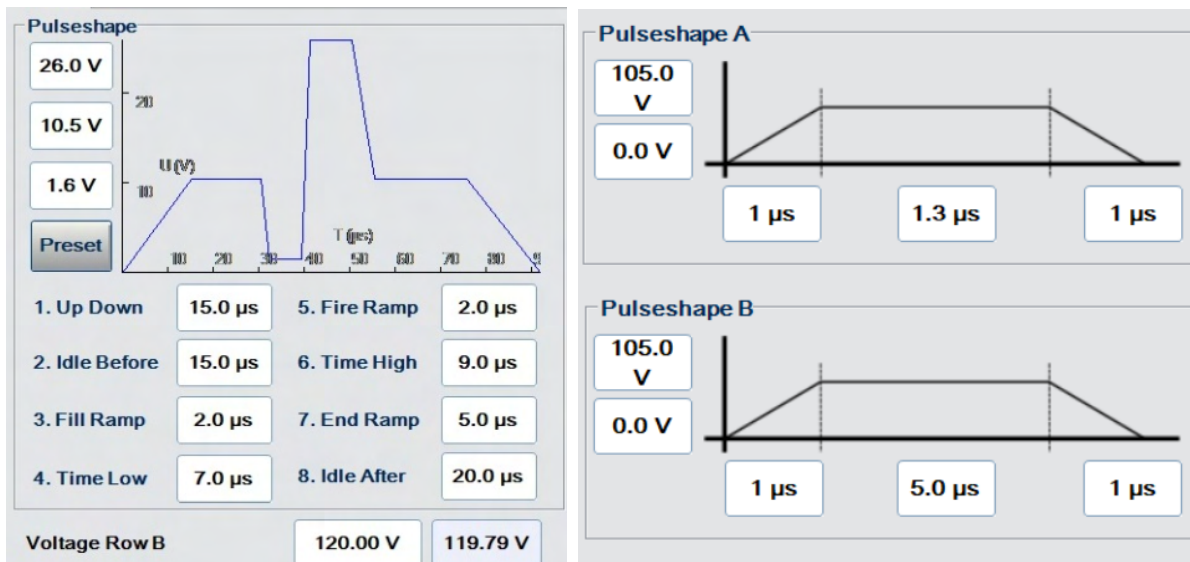
5.2. Multi-material prints

To make multi-material structures using three types of ink, it would be preferable to be able to use all inks simultaneously. However, the PiXDRO LP50 currently only supports two printheads at a time. This implies that only two types of material can be deposited at once and for the last material the operator has to either change inks, swap PHA, or switch the substrate to a printer with another printhead installed. The last option turned out to be most efficient. In the subsection following, more details are given regarding printing with the inks and substrate choice considering the aforementioned challenges.

5.2.1. Printhead settings

Nanoparticle inks have an increased risk of wearing and clogging nozzles and are therefore used in dispensable cartridges (DMC 11610, 10 pL) combined with the Dimatix DMC PHA. These relatively cheap cartridges are easily replaced in matter of seconds in case of failures. Only 16 nozzles are available in these printheads and only one DMC cartridge can be used simultaneously. Printhead settings to produce stable jetting with both Novacentrix JS-B25P and Mitsubishi NBSIJ-MU01 inks are given in fig. 5.6a.

The photopolymer inks are used to print the structural and sacrificial parts of the parts. Although these inks are alike and designed to be compatible, there are some differences in composition of the inks reflecting in different print settings for each ink. Printhead settings to produce stable jetting with both Stratasys inks are given in fig. 5.6b. These settings differ significantly from each other but produce a very similar droplet in terms of speed and volume, which is ultimately desired.



(a) Stable jetting waveform settings for Dimatix DMC disposable cartridge (b) Stable jetting waveform settings for Stratasys SUP706b (upper) and VeroYellow inks (lower) in Spectra Dual PHA

Figure 5.6: Jetting settings and waveforms for the primary inks used during experiments

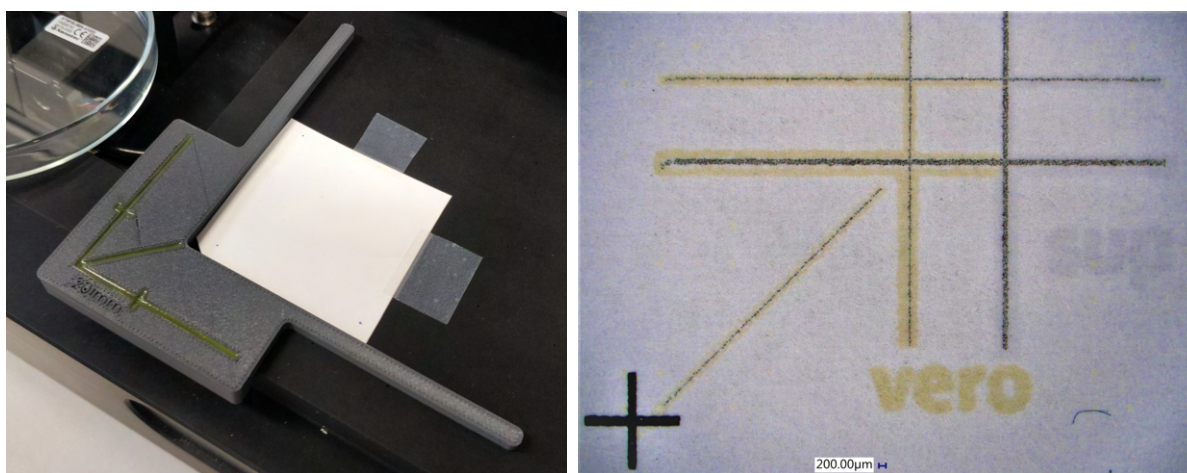
5.2.2. Substrates

A range of substrates can be used on the LP50 printers. The printer is equipped with a rotatable substrate table for $\pm 1^\circ$. The maximum size of 1 A4-paper (210 x 297 mm) is sufficient for most tests. In fact, most test structures are way smaller and do not need the full substrate table space. The substrate of choice should be easy to attach to the substrate table and be compatible with the inks. Additionally, the substrate should allow for easy alignment when swapping between printers. Plain photopaper (Epson Premium Glossy) was chosen as the main substrate because both nanoparticle inks and photopolymer inks printed well on this substrate. Other substrates such as glass and plain paper were unable to provide the same quality of the first layer. Another advantage is that markers could be accurately printed on these photopaper substrates with a standard desktop laser- or inkjet printer. The use of markers for alignment of the substrate between printers is important in this setup and explained next.

5.2.3. Alignment

Alignment of printheads is often a one-time operation and a persistent setting across print jobs. Hence, misalignment in the printheads is also persistent and should be prevented by carefully adjusting the settings in PiXDRO HMI.

Aligning the substrate is an important step in the print process and ensures that the images to be printed are printed at the right place. Printing a single small image on a large substrate might not need a precise alignment since enough space is left on the substrate to allow for alignment errors. However, when printing on small substrates that need to be able to consistently realign between printers, alignment errors should be minimised. Therefore, a custom alignment tool is developed to reliably place substrates on the printbed. By using the tool, the substrate can be accurately placed at the same location each time and easily adhered to the substrate table using tape. Misalignment by the operator and small dimensional differences between substrates can be compensated by the PiXDRO LP50's built-in marker detection and alignment system. This workflow has proven to work consistently across many prints between the two PiXDRO LP50's.



(a) Alignment tool placed in left-hand bottom corner of the PiXDRO LP50 substrate table with photopaper substrate

(b) Proper alignment of three inks. Structural ink (yellow, vero) and SUP706B support ink (transparent, sup) surround traces of AgNP ink (grey)

Figure 5.7: Alignment of substrates

5.2.4. Recipe settings

Careful tweaking and experimenting with different settings combined with knowledge obtained from state of the art industrial printers, a working set of parameters was found and used throughout the remainder of the research to print multi-material structures, of which the most relevant are summarized in table 5.1.

Table 5.1: Recipe settings for different inks

Ink	(Printhead)	Speed	Scan-direction	QF	SZ	ToF	Resolution
Stratasys VeroBlack and VeroYellow, SUP706B	Spectra SM-128	400	Y-normal, bi-directional	2	>2	0.25	400
Mitsubishi NBSIJ-MU01 and Novacentrix Metalon JS-B25P	DMC-11610	400	Y-normal, uni-directional	1	1	0.2	1000

A print speed of 400 mm/s was found to be a practical value while still producing quality prints at high speeds. Occasionally, for even higher print quality, the speed is lowered to 200 mm/s. Quality factor and stepsize for AgNP inks are always set at 1, because no more than 1 nozzle is used at a time. Even when selecting more than one active nozzle and increasing QF and SZ, the results are way worse. This is due to jetting inconsistency of the DMC cartridges. For spectra dual heads, selecting as much working nozzles as possible produced best results, combined with a quality factor of 2 and stepsize

setting of 2 or more, depending on allowed values¹. Also, uni-directional printing is used for AgNP inks in contrary to bi-directional printing for Stratasys inks to ensure printed conductive tracks have as few misalignments as possible. When printing rough shapes or whenever else possible, bi-directional printing is used as it is way faster. As the produced droplets of the DMC cartridges are way smaller, a high resolution of 1000DPI has to be used to make coalescing lines. For Spectra heads with Stratasys inks, a resolution of 400DPI sufficed and produced good quality lines.

5.2.5. Results

Printhead and recipe settings as presented produce good quality results. Lines have an overall good definition, connecting droplets and leaving no voids. table 5.2 lists values regarding drop and line properties on photopaper substrate.

Table 5.2: Jetted drop properties and photopaper substrate interaction behaviour

Ink	<i>(Printhead)</i>	jetted drop		substrate interaction	
		volume	speed	drop diameter	line width
Stratasys VeroBlack and VeroYellow, SUP706B	Spectra SM-128	20 pL	4 m/s	80 um	80 um
Mitsubishi NBSIJ-MU01 and Novacentrix Metalon JS-B25P	DMC-11610	9 pL	4.5 m/s	20-30 um	30 um

¹As explained in section 5.1, quality factor and stepsize have an influence on print quality and require a specific number of selected nozzles to work. As recommended per user manual's instructions, trail-and-error approach is used to determine exact setting of stepsize each time active nozzles are changed.

6

Printing 3D functional structures

6.1. Requirements for functional structures

An functional structure is defined as a structure that is capable of actively moving or transmitting electricity or heat, depending on the situation. To print an functional structure, at least two materials are needed. A conductive ink able to produce conductive traces and a structural material to provide a mechanical structure. Strictly speaking, active parts have been made using only conductive ink on substrate. However in that case, the substrate is part of the active part and basically replaces the role of structural ink. In this research, the substrate is a (temporary) means to support the print and is not regarded as part of the final product, although strategy might be desirable in some situations as is explained in chapter 2. Active parts made out of structural and conductive inks are generally static and used for data transmission, comparable to a printed circuit board (PCB). Examples are inkjet printed multi-layered transformers [12], There are some exceptions, such as planar sensors or actuators that are released from the substrate after printing. However, to print 3D functional structures with the possibility to actuate or sense, the structure requires more complex geometry. This introduces the need for overhanging features and thus support material. In total, three types of ink are selected in chapter 4.

6.2. Printing 3D structures

Printing simple 3D structures on the PiXDRO LP50s has in fact already been demonstrated in the previous chapter, where a print job is repeated a few times to improve ink visibility on the paper substrate. Naturally, when ink is at some point only partially absorbed by the substrate, a natural elevation will arise due to ink accumulation. When actual 3D structures are to be printed, the approach is similar; repeat a print job multiple times until the ink accumulates and forms a 3D structure. Since 3D inkjet printing is a bottom-up process, a change in shape is possible by selecting another image to print after each layer. For simple structures with repeating images every layer, this can be done manually by the operator.

Custom recipe code

Complex parts require different images and print settings each layer. Manually setting a new image each layer quickly becomes a troublesome and time consuming task. Automating this process is key for fast and successful prints. The PiXDRO LP50s recipe code which natively only supports flat, 2D prints is modified to aid in this process. The following modifications are implemented to enable autonomous printing of 3D structures:

1. Custom print settings:
 - (a) processStart
 - (b) Number of printRepeats
 - (c) Number of ImageRepeats
 - (d) Number of processRepeats
2. Automatic procedures:

- (a) Printhead height adjustment after each layer
 - (b) Loading new images to print after set amount of layers
 - (c) Curing with predefined settings after set amount of layers
 - (d) Wiping printhead with cloth after set amount of layers
3. Print job remaining time estimator

Starting with the custom print settings, these settings show up in a recipe file and hence are easily manipulated in PiXDRO HMI. The *processStart* defines the image to start printing with. By default, this is set to 1. Number of *printRepeats* defines the amount of images that need to be reprinted without intermediate UV curing. Number of *imageRepeats* defines the amount of images that need to be reprinted with UV curing. Number of *processRepeats* basically sets the amount of unique layers to be printed (excluding *printRepeats* and *processRepeats*).

Besides the custom print settings, a few automatic procedures have been added to improve print performance. Naturally, for all additive manufacturing techniques, a height adjustment needs to be made after deposition of a layer to prevent a collision between printhead and printed material. After each layer, the PHA height is automatically increased to ensure distance between printhead and printed material remains constant. A deviation in this distance leads to ToF changes and can lead to quality issues, especially when printing bi-directional at high speeds. Also after a set amount of layers, a new image is loaded for each printhead and if desired, the newly deposited layer of ink is cured using the UV light bridge. Additionally, the nozzle plate of the printheads are cleaned on the cloth wiping station to ensure no nozzles are prevented from jetting by a film of old ink, dust or other dirt.

At the start of the print job, a timer is set to keep track of the elapsed time since starting. Based on the number of layers completed and number of layers still to print relative to the elapsed time, a prediction of remaining print time can be made. This is particularly useful for long print jobs, running overnight. Print settings can be tweaked to optimise quality and at the same time ensure a completed print the next morning. An application flow diagram is depicted in fig. 6.1.

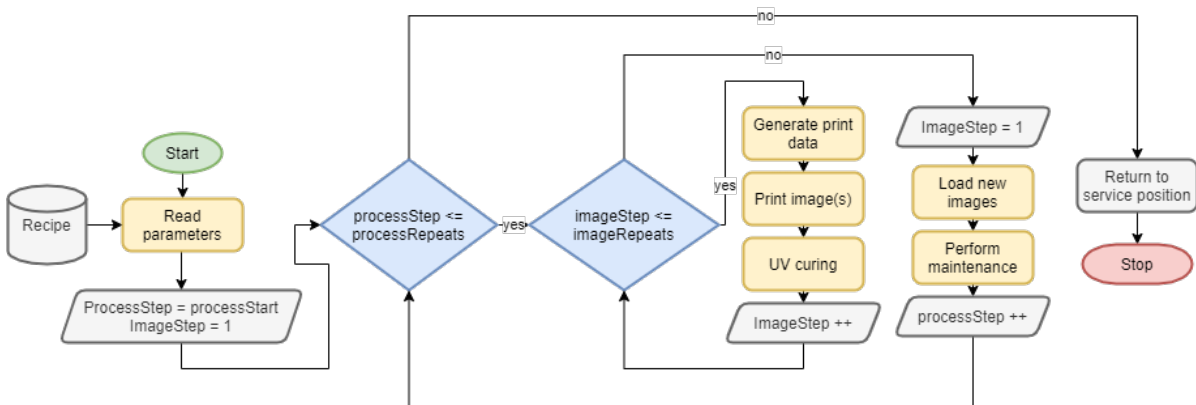


Figure 6.1: Application flow diagram of custom recipe code for autonomous 3D printing with PiXDRO LP50

In the application flow diagram, two main loops (marked by blue diamonds) can be identified. First, whenever an image should be printed multiple times, the printer will do so and UV cure afterwards. If a new image is required when *imageStep* equals *imageRepeats*, the loop is reset and new images will be loaded. Maintenance functions can be performed if desired to clean the printhead. The program then continues until *processStep* matches *processRepeats*, exiting both loops and halting the program. All rectangular boxes marked yellow are individual processes, either custom or left as-is. For all further experiments throughout this thesis, the custom recipe code was used unless otherwise noted.

UV curing

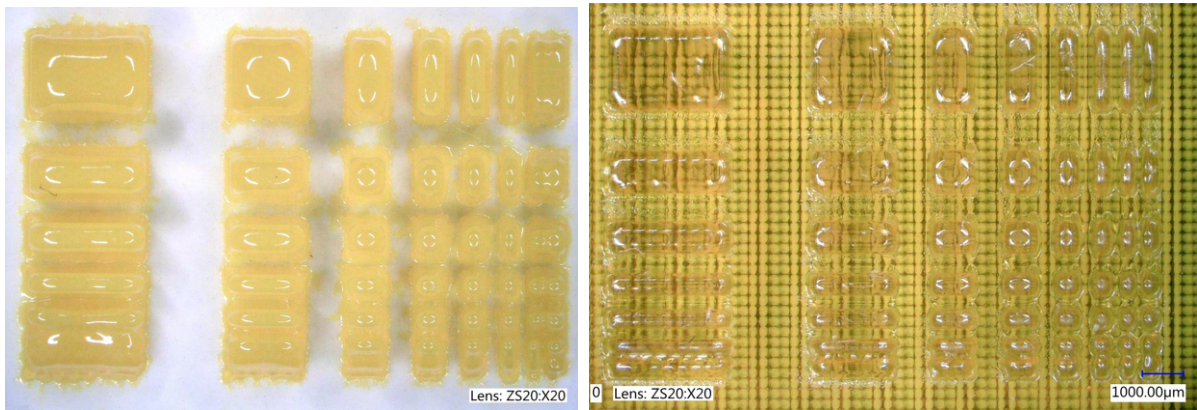
To cure each printed layer of material, the PiXDRO LP50 is equipped with a $3W/cm^2$ UV light (Phoseon FireEdge FE300). The light bridge spans over the whole substrate table and has an approximate illuminated area width of $1cm$, which varies only slightly by lifting or lowering the unit.

$$D = P * I_{const} * w_{const} / v \quad (6.1)$$

Where dose D is the amount of irradiated energy per area (J/cm^2) as a function of the variable light source power setting P (%), constant intensity of the light source I_{const} ($3W/cm^2$), constant width of the illuminated area w_{const} ($1cm$) and variable speed of scanning v (cm/s). By varying the power setting and scanning speed linearly, the applied dose remains constant. E.g., a high scanning speed at a high intensity yields the same dose as with a low scanning speed at a low intensity. Knowing this can greatly improve overall print speed by choosing high scanning speeds at high intensity when printing multi-layered parts.

Comparison with Stratasys Polyjet

To compare print quality of industrial printers with the experimental setup used in this thesis, a model is printed on both a Stratasys Polyjet J735 and the PiXDRO LP50 with custom recipe code. A top view of a part of the print for both machines is shown in fig. 6.2.



(a) Structure containing small features printed on PiXDRO LP50 with custom recipe code, VeroYellow ink

(b) Structure containing small features printed on Stratasys Polyjet F735, VeroYellow ink

Figure 6.2: Comparison between small structures printed on PiXDRO LP50 and an industrial-grade Stratasys Polyjet F735

On the PiXDRO LP50, the test structures are printed directly on photopaper substrate, hence a good contrast between ink and substrate is visible (fig. 6.2a). On the Stratasys F735, printing on substrate directly is not possible as these machine have no interchangeable substrate - the substrate is a fixed table capable of moving in height only. As a workaround, a few layers of support material is printed with a structural layer on top, acting as a substrate itself that can easily be removed after printing. The small structures are therefore harder to distinguish (fig. 6.2b).

The structures seem to be of similar size for both prints, though with a slightly better shape definition on the Stratasys prints for the smallest structures. Also, closely inspecting the images reveals a subtle, but important difference between the prints which can be analysed from glare. Glare indicates rounding of a corner where light is able to reflect into the camera lens. Round corners are a side effect of printing with liquid ink and are undesirable in most cases. Even when trying to print perfectly square geometry, rounded corners are inevitable. Glare from light reflecting of the structures appears closer to the centre for the LP50 prints, compared to glare on the Stratasys prints. This indicates a difference in geometry; since the rounded corners are close to the edges, the top surface is expected to be relatively flat on the Stratasys prints, which is desired. On the other hand, glare close to the centre indicate large rounded edges and thus a non-flat top surface.

One of the reasons for this difference is that Stratasys Polyjet printers use a heated roller attached to the printhead at a precise height to flatten each layer after UV-curing. This so-called planeriser moves over the printed part just after the UV-light has irradiated the layer. Because the roller is hot, cured ink

can locally warm up and deform more easily and be flattened. Excess material that sticks to the roller is removed using a scraper blade and discarded by a suction system. As an integral part of the process each layer, level layers are ensured.

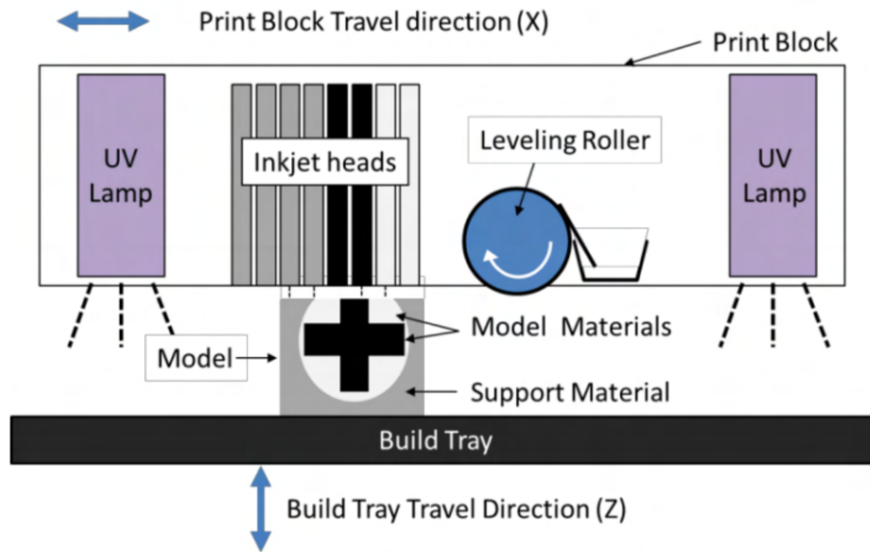
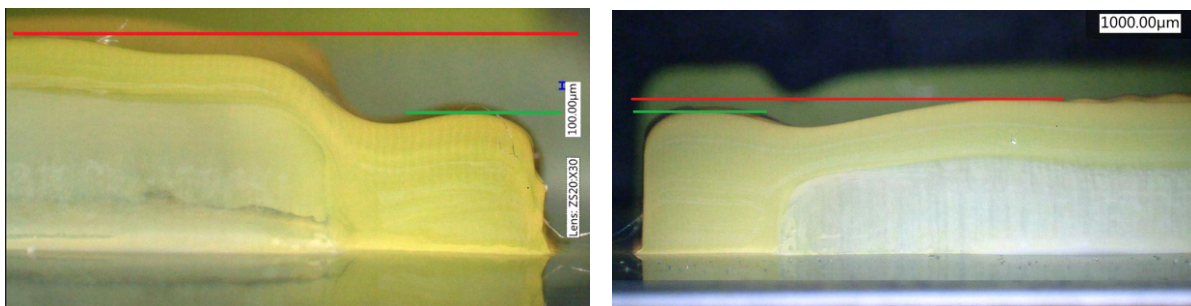


Figure 6.3: Industrial inkjet printhead with multiple printheads, integrated Ultraviolet curing lights and a layer planeriser system to flatten layers after deposition and curing. Adopted from [37]]

When no planeriser is used, fluid interactions cause each subsequent layer to become less even, resulting in large dimensional deviations the more layers are printed. This effect is most pronounced near edges or corners and is illustrated in fig. 6.4a and previously observed as glare in fig. 6.2a.

In this research, no planeriser is used as the PiXDRO PHAs do not natively support it. This greatly limits the dimensional accuracy when parts are printed with high layer counts. In addition, a well-tuned printhead for each ink is necessary to ensure the right amount of ink is deposited each layer. A difference in volume of deposited inks can result in increased overlaps, hence bulging of material since no planeriser is used to counter these inconsistencies. Printhead settings for the structural and support material inks as presented in chapter 5 are used and found to give satisfactory results for 3D printing, which is shown in fig. 6.4b



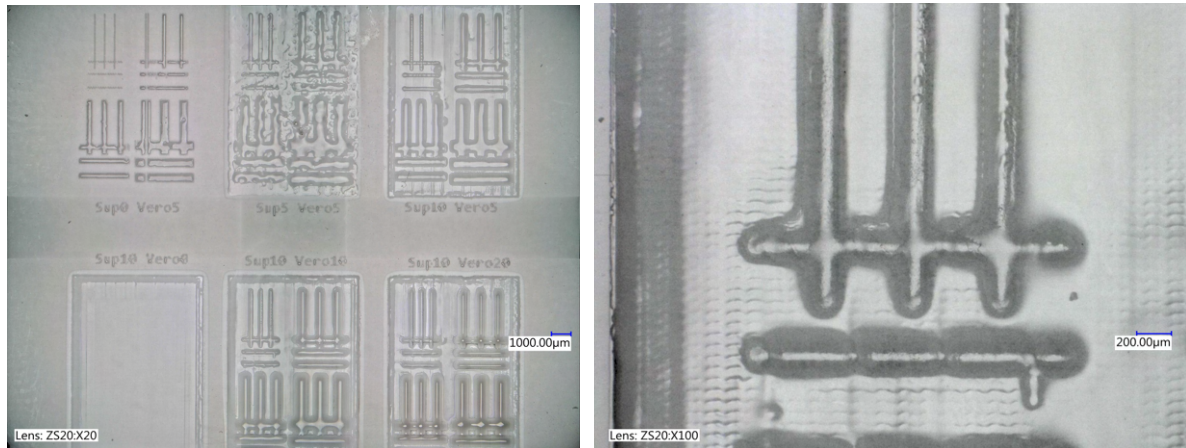
(a) Large dimensional and volumetric errors in prints with high number of layers without the use of a planeriser and poor tuning of the printheads.

(b) Well-tuned printheads yield acceptable results when no planeriser is used

Figure 6.4: Side view of high layer count 3D inkjet printed structures. Coloured lines indicate height difference between features were ideally this difference should be zero.

Small features test on SUP706B

To assess minimal achievable line widths and resolutions, several tests were performed with Veroblack and SUP706B inks on photopaper substrate. A template shown in appendix C is printed in different configurations and layer heights to observe the effect of multi-layered printing on resolution, line width and definition. A top-view of the results after printing is shown in fig. 6.5a. One of the results, with 10 layers of SUP706B ink supporting 10 layers of Veroblack structural material is shown in fig. 6.5b. Each printed test figure contains multiple crossing and non-crossing lines in various widths. All of the printed figures were examined under a microscope to assess the overall quality and measure line widths. The obtained information can be used to predict ink behaviour for similar multi-material prints.



(a) Top view with 20x magnification of printed results.

(b) 10 layers of SUP706b ink supporting 10 layers of Veroblack lines

Figure 6.5: Small feature test top view and detailed view of one of the results

All dimensions in X and Y were measured at different locations at least three times to exclude the effect of local inaccuracies. Results of the measurements are listed in table 6.1. From these results, a clear increase of line width can be concluded when printing on support material compared to photopaper substrate. With a constant number of Veroblack layers, no significant difference is observed in the line width when changing the number of support material layers. Contrarily, increasing the number of Veroblack layers with a constant number of support material layers does change the line width. An increase is observed up to around $270\mu m$ for both X and Y directions.

Table 6.1: Line widths at different layer heights of support material and structural material

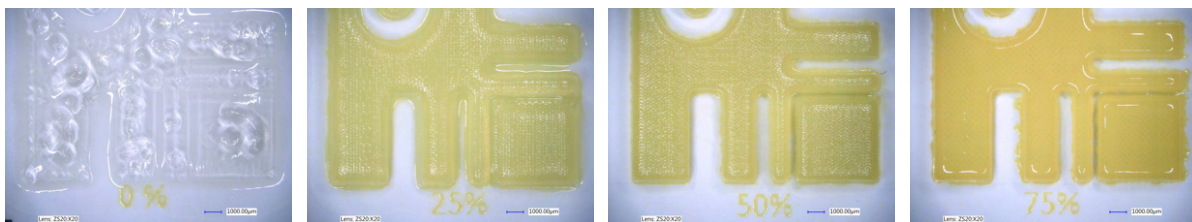
test	layers		line width (μm)			
	SUP706B	Veroblack	mean X	std. dev X	mean Y	std. dev Y
1	0	5	86.89	0.95	84.01	2.80
2	5	5	184.19	10.92	197.65	3.64
3	10	5	196.23	6.33	196.25	4.13
4	10	0	-	-	-	-
5	10	10	265.62	12.33	273.59	17.32
6	10	20	246.44	27.06	227.33	13.20

6.3. Printing overhanging structures

Printing overhanging structures is similar to printing 3D structures with one ink as described in the preceding section. However, one big difference is the use of support material ink in addition to structural ink. An object requiring support material is built from repeatedly printing layers comprised of support material ink and structural material ink. On the PiXDRO LP50's, such layer is defined by the use of two bitmaps containing the images for printing both inks respectively. Each image is sent to the corresponding printhead. An empty image for either one of the inks results in no ink being deposited by the affected printhead in that layer. The images can be changed after each layer, changing the shape of the part as the height increases. For small and simple prints, this can be done manually by the operator. An automated process is discussed in section 6.5. In this way, complex overhanging structures can be fabricated.

6.3.1. Support structure modification

Use of SUP706B support material alone to support overhanging structures of VeroYellow was observed to be insufficient. The support structure is unable to remain its shape and provide enough support to hold the structural material in place, resulting in sagging and failed overhangs. This is not due to insufficient curing or improper printhead settings, rather a property of the support material ink itself. The main feature of the support material, to be easily removable, causes it to have a gel-like composition. Compared to the structural material, its mechanical properties and print quality are cumbersome, which is clearly observed in test prints. In Object and Polyjet industrial printers where this ink is originally meant to be used, a strategy is used to improve the quality of the support material [49]. When setting parameters in the slicing software, the operator can select different strengths of support material. This setting determines the mechanical properties of the support material, its ability to be removed, and the ease thereof. Hence the support structure is a composite of structural material and support material. The amount of structural material compared to support material depends on the settings and can be adjusted based on the desired results. If a strong support structure is desired, more structural material can be mixed with the support material. For weaker but easy to remove support structures, less structural material is used. The exact composition of structural and support materials in these grids is proprietary. To recreate this ability of stronger composite support structures on the PiXDRO LP50 printers, several tests were performed to assess the influence on print quality of different support structure compositions. First, support compositions with 0%, 25%, 50% and 75% structural material added were assessed. These compositions were made by creating a test image and masking it with appropriate pixel-perfect masks in different black-white pixel densities. For example, a mask containing 50% black pixels is a raster of alternating black and white pixels in every direction. For a 25% black pixel mask, this raster reduces to one with only a black pixel for every 3 white pixels. After masking the support material image, the corresponding image for structural material is obtained by inverting the colours, effectively swapping the black and white pixels. The same result is obtained by applying an inverted mask to the original image. More on the applications of masks for increased support material strength is discussed in section 6.5. Results of the test with different compositions of support material are depicted in fig. 6.6. Only using support material without addition of structural material results in an almost transparent structure with very poor line definitions, fig. 6.6a. With 25% structural material added, substantially better quality prints are achieved, fig. 6.6b. Addition of even more structural material slightly improves the quality, but the difference between 50% and 75% is negligible, fig. 6.6c and fig. 6.6d. More tests involving composites with 10%, 20% and 25% were performed to address performance for lower amounts of added structural material.



(a) 0% structural material added (b) 25% structural material added (c) 50% structural material added (d) 75% structural material added

Figure 6.6: Support material composites with different amounts of structural material added

Support modification application

In simple test prints comprising only a few images, manual masking of images can already be troublesome. For large prints with hundreds of sliced images, manually masking each image would take a very long time; to modify the support material for one layer, both structural and support material images need to be modified. A custom application has been developed to aid in this time-consuming process and automate the process. The application logic flow has been depicted in fig. 6.7. The application applies changes to the images per layer using logic operations per pixel. As inputs, it takes a user selected mask with specific pixel density and the structural and support material images for that layer. The support material image is combined with the inverted mask through an AND-operation; only where both images have black pixels, the resulting image will also have a black pixel. Secondly, the support material image is combined with the normal mask through an AND-operation. The resulting (temporary) image is combined with the structural material image through an OR-operation; where either one of the two images or both have a black pixel, the resulting image will also have a black pixel. The resulting images are the outputs of the application and are ready to be imported into PiXDRO HMI for printing.

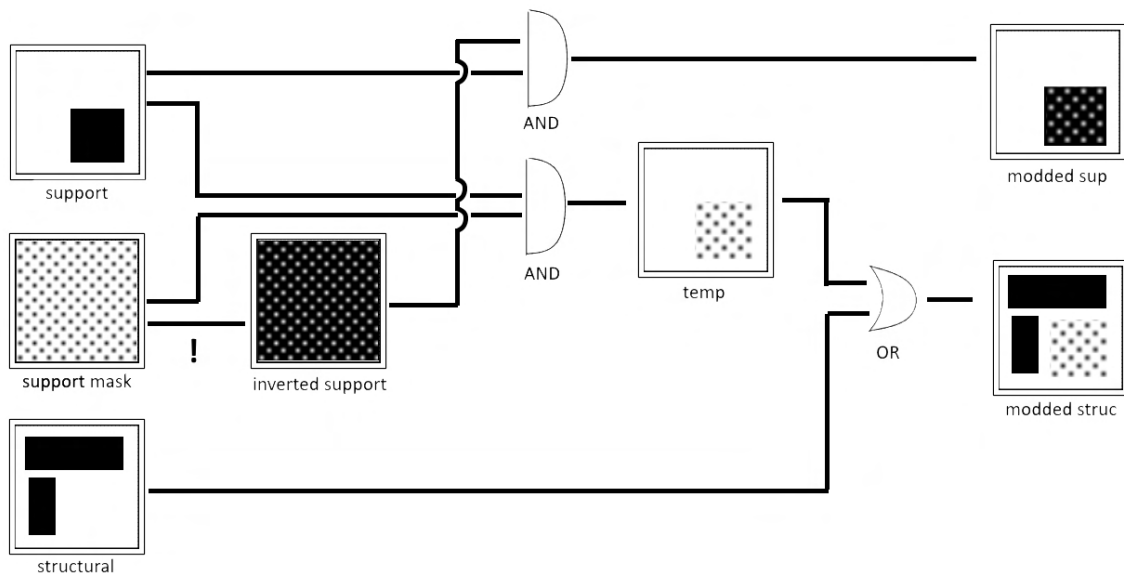


Figure 6.7: Custom image modification application flow overview to generate stronger support structures. Original support structure and building material structure bitmaps (left) are combined with a mask in logic operations to produce modified support and structure bitmaps (right)

6.3.2. Support removal

Several methods exist to remove support material after a print job is succeeded. Appropriate methods differ from material to material, but are generally very similar. Methods suitable for the selected support material ink are considered here. According to the support material SUP706B user manual, three methods are recommended:

- Method 1: Dissolve support material:
Prepare a base solution of 2% sodium hydroxide ($NaOH$) (caustic soda) and 1% Sodium Metasilicate (Na_2SiO_3)
- Method 2: Break-away support material
Mechanically remove most of the support material by hand or using tools
- Method 3: Removing with water pressure
Using a water jet to partially weaken and dissolve the support material and simultaneously washing it off the part

Generally, you can use any of the above support removal methods that best suits to situation. However, in some cases, to ensure optimum results, a specific method is preferred. For delicate prints, mechanically removing most of the support material and dissolving the remaining material is the strategy of choice. In this way, the delicate parts are exposed to the support removal solution no longer than necessary, since prolonged exposure can weaken the structure or cause deformations. Additionally, to improve surface quality and part strength, the printed model can be dipped in a 15% glycerol solution for 30 seconds and then left to dry for a few hours. Additional information on the preparation of the support material removal solution is given in appendix D.

Ease of support removal depends on the amount of added structural material to the support structure. Several composite support structures with different compositions are printed and tested for ease of removal in the recommended caustic soda and metasilicate solution. No material was removed manually. For example, the composite tests with 0%, 25%, 50% and 75% structural material are left to dissolve in an actively stirred support removal solution and inspected several times. The results are shown in fig. 6.8. After 1 hour of dispersion, the pure support material is already dissolved and most of the 25% composite is dissolved. After one night, both pure support material and 25% composite are completely dissolved. Clearly, the 50% and 75% composites did not dissolve. The 50% composite was weakened and absorbed a lot of water, drastically increasing its size. The 75% composite was nearly unaffected. A similar study was performed for the 10%, 20% and 25% composite structures with comparable results regarding the time required to dissolve a composite structure.

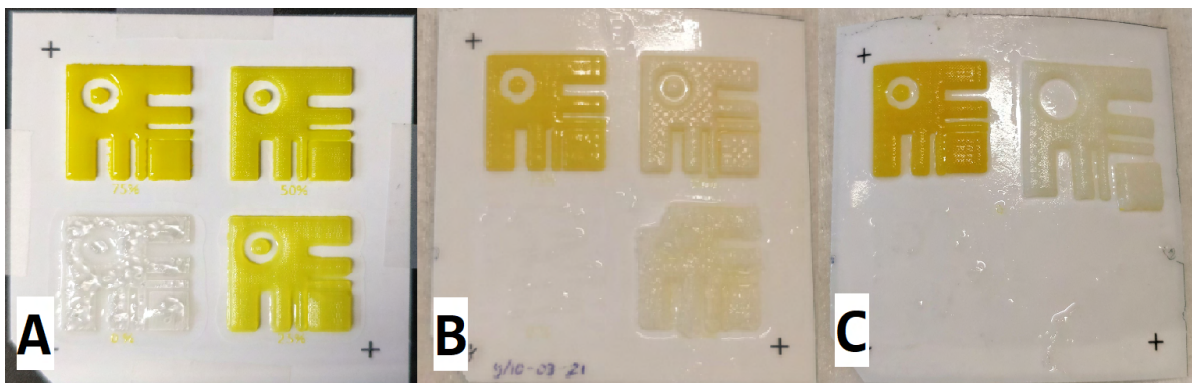


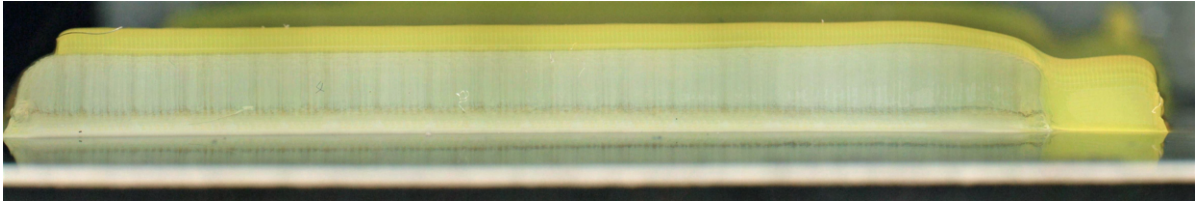
Figure 6.8: Removal of support material structures with different compositions in a stirred solution of 2% $NaOH$ and 1% Na_2SiO_3 . (A) printed support structures prior to dispersion in removal solution. (B) results after approx. 1 hr of soaking. (C) results after one night of soaking.

If large objects are to be printed requiring a lot of support material with a large contact area, it might be difficult to remove the support material from the part. In that case, a thin interface layer of pure or reduced-concentration structural composite support material can be printed between the overall support structure and the structural part. When removing the structural material, this weak interface layer will quickly release, easing support removal.

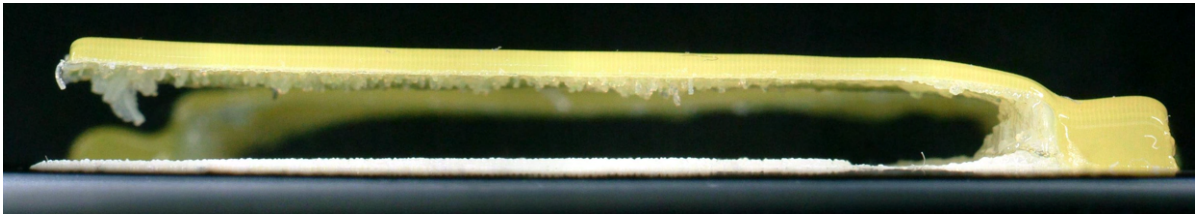
Improvement of print quality with composite support structures comes at a cost; All composite support material prints took substantially longer to dissolve in the support removal solution compared to 'pure' support material. A good compromise between sufficient support strength and ease of removal has been found with compositions of 80% support material mixed with 20% structural material. This composition assures quality prints of the support structure with good line definitions and supported overhanging parts fine in subsequent tests. Mechanically removing most of the support material structure followed by a relatively short dissolving step successfully removed the support material leaving the structural parts undamaged. No weakened layers were used for the interface between support structure and structural material since this was not found to be necessary for the small parts printed during this research.

6.3.3. Results

Using support structures comprised of 20% structural material, overhanging structures were printed successfully. One of the structures is shown in fig. 6.9a. After printing, mechanically removing most support material and soaking the part into a base solution removes most of the support material. The released structure as depicted in fig. 6.9b is obtained. Upon close inspection, some residual support material is left and the structure is slightly bend upwards. The leftover support material can be removed by soaking the part in the removal solution longer or mechanically removing it. However, longer exposure to the base solution causes more pronounced material deformations, especially for delicate parts. Alternatively, a weakened interface layer could be used. Nonetheless, the obtained results provide a solid base to move onto printing more complex multi-material prints.



(a) Overhanging structure printed using a composite support material containing 20% structural material



(b) Overhanging structure released after having removed support material

Figure 6.9: Support material composites with different amounts of structural material added

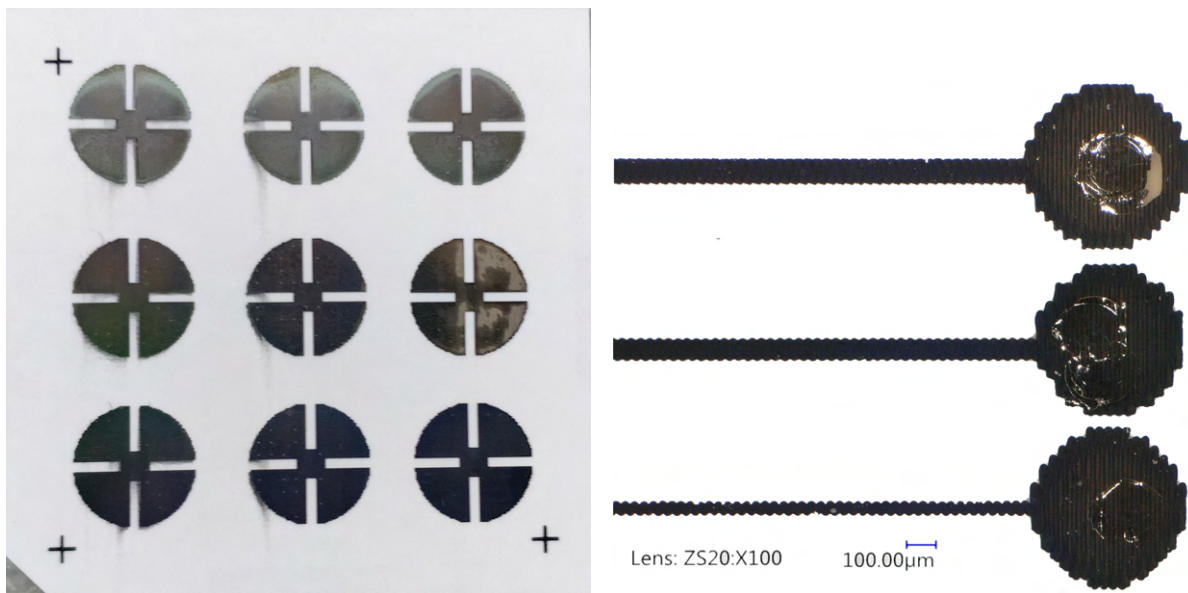
6.4. Printing conductive traces

To print conductive inks on the PiXDRO LP50s, the Dimatix DMC disposable cartridges are used. Even after careful tuning of the printheads, consistent results are rare due to the quality of the printheads. Still, good results were obtained by selecting only stable nozzles and keeping them from clogging by continuous jetting in the service position when not printing. Printing conductive traces and patches is quite similar to printing structures with other inks. An image defining the geometry and dimensions of the lines to print is loaded, converted and send to the printhead. This method is the same for both Novacentrix and Mitsubishi silver nanoparticle inks. In the subsequent subsections, more details are provided regarding the print settings in different scenarios.

6.4.1. Printing on photopaper substrate

Most nanoparticle inks are manufactured to be printed directly on a suitable substrate. Resin coated paper and PET films suitable for inkjet printing of chemically sintered silver nanoparticle ink are commercially available. However, printing on photopaper works fine, as has also been confirmed by other authors [25], albeit with a slightly higher resistance. The resistance achieved directly after printing is already acceptable for most applications, though the sheet resistance value of an instant inkjet pattern is still around 4 times higher than that of a pure copper trace with the same width and thickness.

To verify these findings, Mitsubishi NBSIJ-MU01 (chemical sintering ink) is printed on photopaper (Epson Premium Glossy photo paper) to test conductivity. A cloverleaf figure suitable for van der Pauw conductivity measurements is printed multiple times with varying layer heights, fig. 6.10a. Additionally, thin lines of only a few droplets wide are printed in scan- and cross-scan direction to analyse conductivity for small features. Cross-scan lines are shown in fig. 6.10b.



(a) AgNP ink cloverleaf figures for conductivity tests

(b) Cross-scan printed thin AgNP lines with different widths

Figure 6.10: AgNP conductive figures printed on photopaper substrate

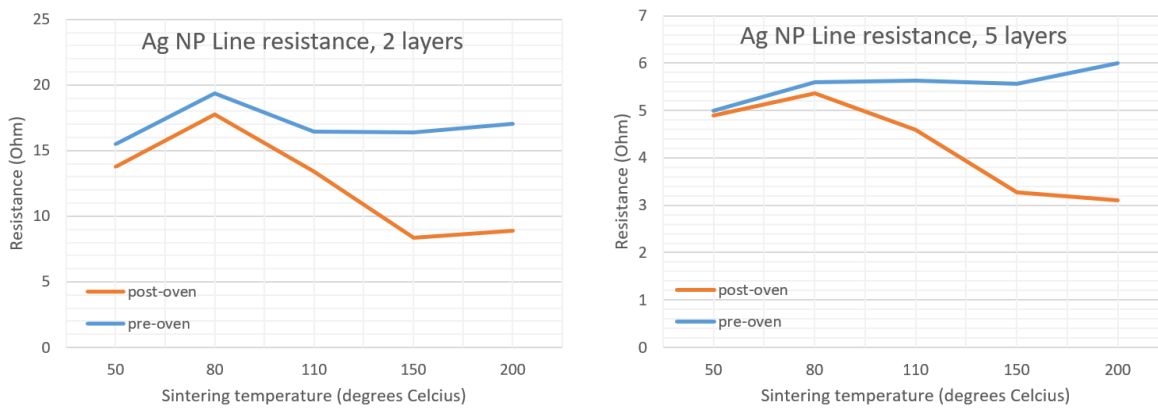
Cloverleaves are printed three times with 5, 10 and 15 layers, starting from the bottom row to the top row respectively. The distinct cloverleaf shape is preferred when performing van der Pauw measurements to determine (anisotropic) sheet resistivity and the Hall coefficient of a sample [29]. Scan- and cross-scan directed lines are printed bi-directional with 4 layers and have widths of 2, 4 and 5 drops. Line length is 38mm terminated by a connection pad with a diameter of 1mm. Results of the cloverleaf and small feature line conductivity tests are shown in table 6.2.

Table 6.2: Cloverleaf and small feature lines measurement results

Cloverleaves		Thin lines			
layers	resistivity (Ω)	drops	width (μm)	scan resistivity (Ω)	cross-scan resistivity (Ω)
5	0.5 ± 0.2	2	40	54 ± 0.2	∞
10	0.3 ± 0.1	4	70	26 ± 0.5	30 ± 1.2
15	0.2 ± 0.1	5	90	18 ± 0.2	20 ± 0.5

Van der Pauw measurements yield results indicating an isotropic conductive sheet of silver. Results are therefore summarized as one value, independent of measured direction. Thin lines show best conductivity in scan direction since bi-directional printing causes slight misalignments between drops in cross-scan direction, visible in fig. 6.10b, bottom line. Uni-directional printing resolves this difference, as ToF setting no longer influences alignment between droplets. Conductivity increases as line width increases, which is as expected. Similarly, conductivity increases as layer height increases. Both options yield a larger surface of material to conduct electricity, lowering resistivity.

To test performance of ink requiring heat to sinter, Novacentrix JS-B25P silver nanoparticle ink is printed on photopaper substrate and sintered at different temperatures for approximately 5 minutes in an oven. The samples are printed lines of 1mm wide by 5mm long and separately sintered. The results are given in fig. 6.11a and fig. 6.11b.



(a) 2 layers printed, 5 minutes sintering in hot-air oven at different temperatures (b) 5 layers printed, 5 minutes sintering in hot-air oven at different temperatures

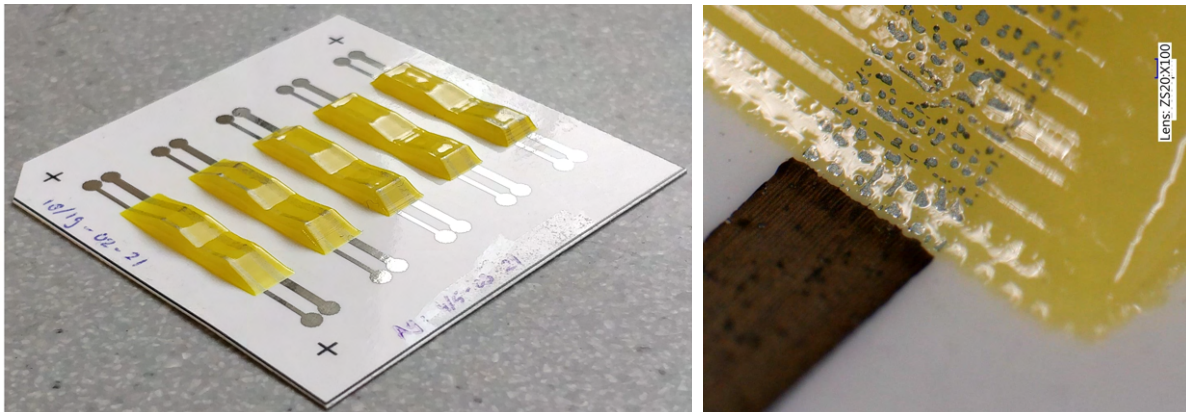
Figure 6.11: Oven sintering results for conducting lines of Novacentrix Metalon JS-B25P

Resistance is measured three times with a 95% confidence interval before and after the samples have been sintered, as indicated by the different colours of the graphs. A clear drop in resistance starts to be obvious around 110°C and settles around 200°C for both 2 layer and 5 layer printed samples. Indeed, both AgNP inks perform as expected on the photopaper substrate with their appropriate post-processing requirement.

6.4.2. Printing on structural material

Printing conductive traces on structural material can be achieved in a similar way to printing with any other ink. First, the desired layers of structural material are printed (supported or not), followed by the desired shape and amount of layers of conductive ink.

As explained in the preceding subsection, printing of AgNP ink on photopaper substrate gave satisfactory results. Printing conductive traces with AgNP ink on structural material instead of merely substrate greatly expands possibilities. To test behaviour of AgNP ink on structural material and the transition from substrate to structural material, a test involving structures with varying angles is performed. On these sloped surfaces, a silver ink trace is printed, connecting probe pads from either side of the structure to test conductivity, fig. 6.12. The completed result is given in fig. 6.12a.



(a) Completed print with AgNP traces on sloped structural material

(b) Substrate to structural material transition

Figure 6.12: AgNP traces on substrate and sloped structural material

These results were obtained by first carefully aligning the substrate, printing the structural material, followed by printing the conductive AgNP ink on top. Recipe settings as listed in section 5.2.4 are used.

The AgNP ink again printed fine on the substrate, but as can be observed on the zoomed image of the transition location, fig. 6.12b, AgNP ink on the structural material did not coalesce and remained as separate droplets. Obviously, these unconnected silver 'tracks' do not conduct electricity. To further analyse this behaviour and propose solutions, additional tests are performed.

Several key factors are identified that influence the behaviour of the ink on the structural material. The are itemised here below.

- Print speed
- Layer count
- Channel constraint
- Surface treatment
- Choice of inks

Other factors that are not listed may be considered, such as substrate or ambient temperature, but these are expected not to influence the behaviour too much, base on state of the art knowledge, chapter 2.

Layer count

An obvious attempt to increase conductivity performance of a AgNP track is by printing a trace with more layers. However, this is not as obvious as it seems. Of course, more AgNP ink will certainly be useful to fill any voids left in the first layers, but there's no guarantee that these next layers won't show gaps at the same location as the previous layer due to bad nozzle performance or due to another cause. Additionally, more layers can locally increase height deviations due to uneven spreading of the ink. Finally, more ink means a thicker trace. UV light might not penetrate through all of the ink and only sinter particles on the upper surface of the trace if it is too thick. In the case of chemical sintering, not all sintering agents may be able to reach all parts of the trace for the same reason. Generally, a

compromise has to be made between layer thickness for sufficient reliability of the trace's conductivity and the ability to sinter the trace.

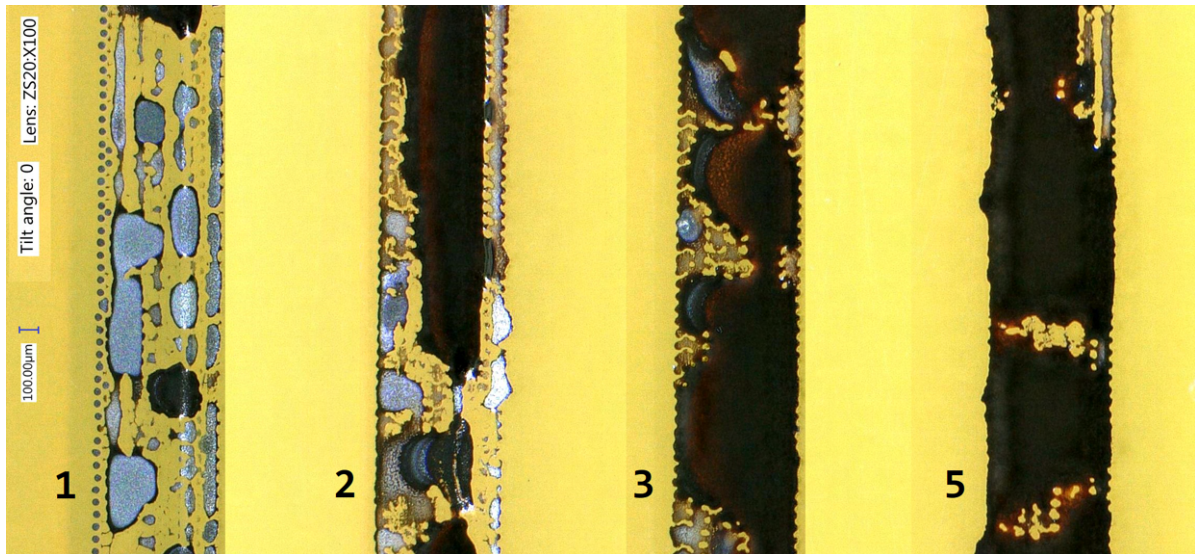
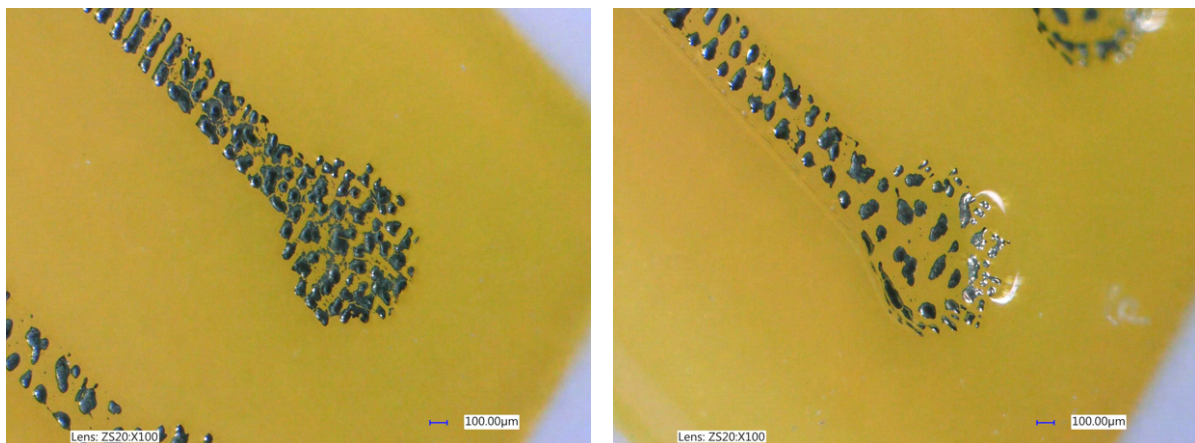


Figure 6.13: Different number of printed layers of Mitsubishi NBSIJ-MU01 AgNP ink on cured Stratasys VeroYellow structural material ink. From left to right; increasing number of printed layers (1,2,3,5)

In fig. 6.13 differences in layer count can be observed. Without additional measures, a minimum of 3 to 5 layers of silver ink needs to be printed in order to obtain a somewhat continuous trace, though having lots of voids. Those amounts of layers can already be too much to sinter effectively, so additional measures are needed.

Channel constraint

To force drops to coalesce, tests involving pre-defined channels are performed. Recessed channels are printed in the structural material where conductive traces are desired. Ink is subsequently deposited in these channels. Depending on drop size and channel geometry, drops are forced to spread out in the channel direction and excess ink is only able to flow in direction of the channel, improving coalescence. Different sizes of channels with different depths are evaluated.



(a) A 1mm deep and 0.5mm wide AgNP trace as printed on flat VeroYellow structural material (b) A 1mm deep and 0.5mm wide AgNP trace as printed in recessed channel

Figure 6.14: Channel recession compared to flat structural material

As can be seen in fig. 6.14, a clear difference is visible between a AgNP trace printed on flat structural material compared to a trace printed in a recessed channel. Channels are designed to have a square

corners, but are not exactly printed that way due to the fluidic nature of the ink. This effect also aids in AgNP ink causing to stick to the side of the channel, which is visible in fig. 6.14b. Drop spacing seems to increase when printing in channels, which is no surprise since the same amount of AgNP ink has to spread out over a larger surface.

The effect of channel widths has been investigated. Multiple prints have been made with varying channel widths from 0.05mm to 0.40mm wide with a fixed depth of 0.20mm . Mitsubishi NBSIJ-MU01 AgNP lines with according widths have been printed on top. Images have been taken after 1, 5, 10 and 20 layers for each channel width. In total 8 unique channel widths have been analysed (increments of 0.05mm between each sample). Best lines were formed at widths from 0.25mm with 10 or more layers. All images for elaborate inspection can be found in appendix B. Most noticeable results are shown in figure XXX. To compare behaviour of AgNP inks, similar prints have been made with Novacentrix Metalon JS-B25P ink on increasingly wider channels. This ink performed better in terms of drop coalescence; forming continuous lines with only 3 layers at channel widths as small as 0.15mm .

Sloped channels with several different angles have been printed to compare with square channels. No significant improvements were observed.

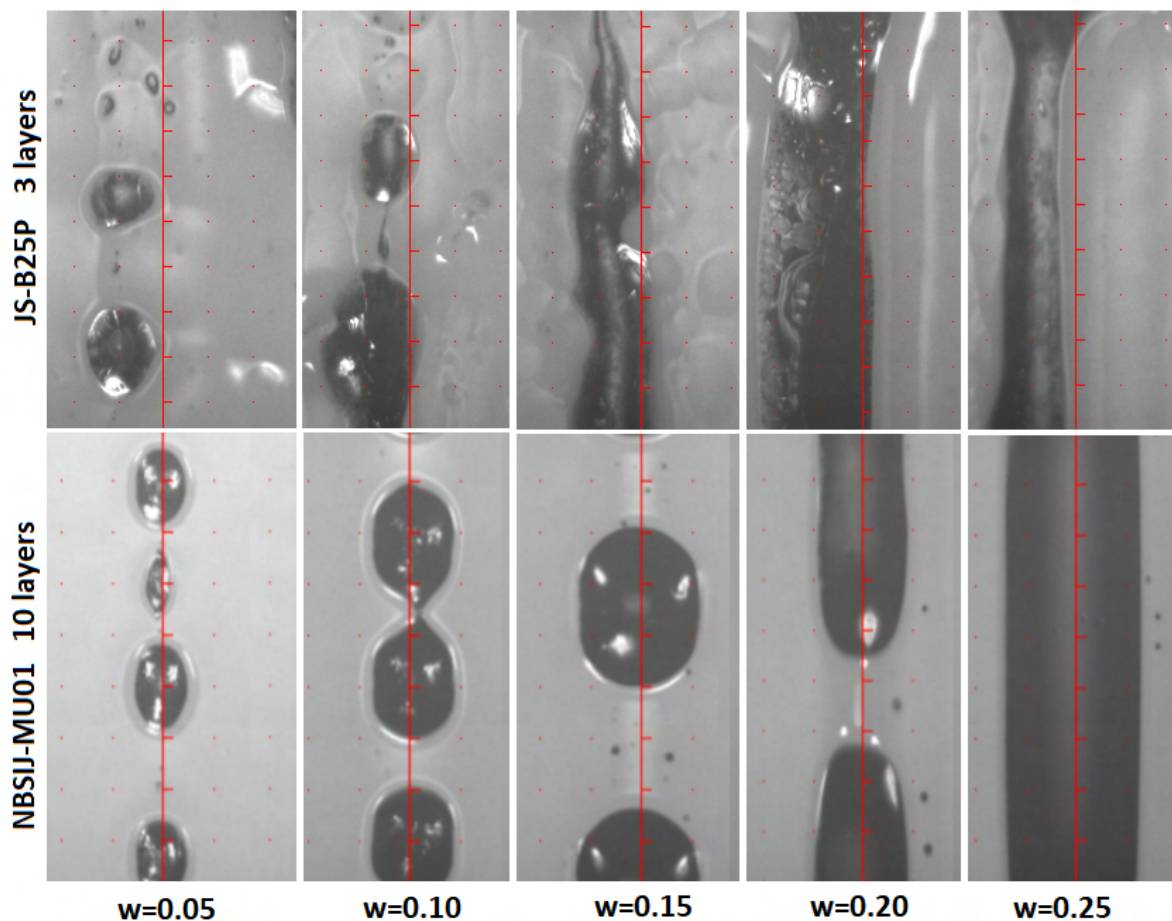


Figure 6.15: Channel width comparisons. Upper images: Novacentrix Metalon JS-B25P, 1000DPI , 3 layers. Lower images: Mitsubishi NBSIJ-MU01, 1000DPI , 10 layers. Left to right: Channel width of 0.05mm increasing to 0.25mm with 0.05mm increments. Dot matrix spacing 0.1mm

In general, when an excessive amount of layers is printed (>20 layers), almost all channels are eventually filled with ink and form continuous lines. As stated earlier, this is not a viable approach in many cases, especially when trying to sinter the lines with UV light. The lines are too thick to penetrate and uneven sintering is likely to occur.

Surface treatment

As discussed in chapter 2 and chapter 5, substrate-ink interaction plays a key role in obtaining quality first layers. It is observed that AgNP inks performed better on cleaned structural material surfaces rather than uncleaned surfaces.

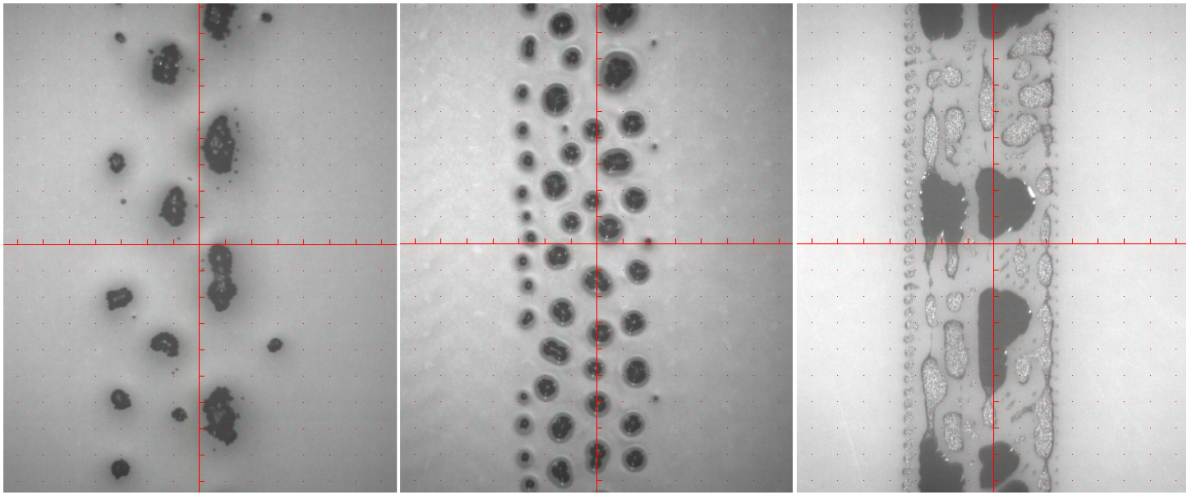


Figure 6.16: Surface treatments on 10 layers of VeroYellow structural material. Left to right: 1 uncured VeroYellow layer, untreated, and actively ethanol wiped surface, respectively.

As can be seen in fig. 6.16, no cleaning of the structural layer leaves AgNP ink droplets unconnected. This is likely due to a thin layer of uncured structural material always being present on top of the last printed layer. It is unknown why this thin layer won't solidify like the rest of the underlying material. To verify adhesion problems are caused by this thin uncured layer, a printed layer of structural material is deliberately left uncured and AgNP ink is printed on top of it. With this 'wet' interface layer, even less drops appear to remain close together. When removing the uncured layer from the top of the structural material using IPA or ethanol, leaving only solidified resin, a drastic improvement in adhesion of ink to the substrate is observed. Drops remain at their location and coalesce with adjacent drops in most of the time, defining a conductive line in stead of separate droplets. Plasma-treated surfaces and IPA cleaned surfaces have also been tested, with no significant differences compared to ethanol cleaned surface.

DPI setting

When changing the resolution of the printed AgNP lines, the amount of droplets used to fill one layer is effectively changed. Resolution has been lowered to $500DPI$ and increased to $1500DPI$ and printed on wet, untreated and cleaned structural material as well. Results are similar to images in fig. 6.16, with as only difference a larger or smaller drop spacing depending on resolution.

Print speed

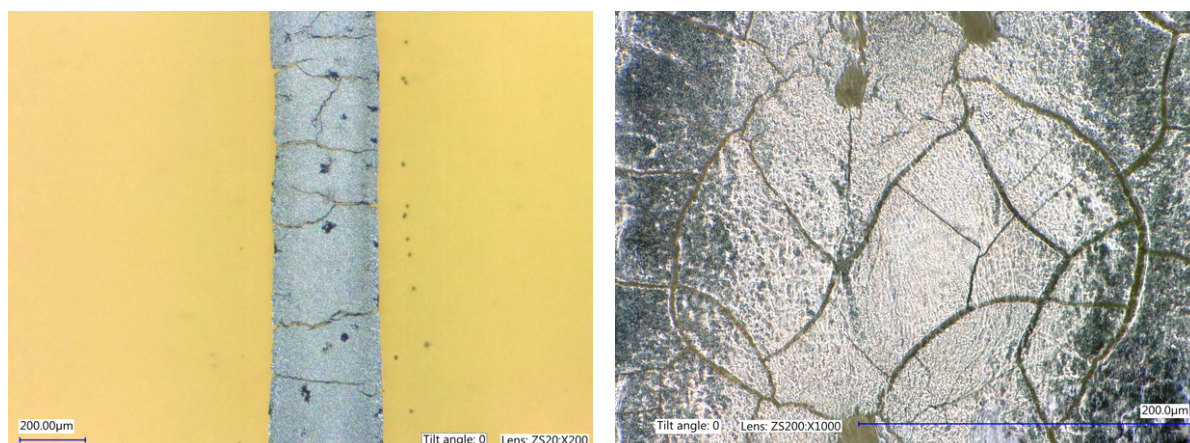
Print speed mainly influences the positional accuracy of the droplets and the time they have to dry before a next droplet is deposited. Positional accuracy can be important to ensure no gaps appear that impede conductivity. More important is the time a droplet gets to dry. When printing with one nozzle only and low print speed, drops mostly dried before an adjacent drop is deposited in the next swath. This prevented the drops from coalescing and forming an homogeneous structure. In contrary, when printing with more nozzles simultaneously and at higher print speed, the drops did not have time to fully dry and showed better coalescing. Printing at higher speeds and with more nozzles has the advantage of creating a continuous trace rather than separate drops.

6.4.3. UV and thermal sintering

Suitable settings have been found to print well defined coalescing AgNP lines on structural material. To make the AgNP tracks conduct, they should be sintered either chemically or thermally. Alternatively, UV irradiation can be used to exploit plasmon resonance as explained in chapter 4. To access the success of this approach, a test patch of structural material with recessed 35mm long and 1mm wide channels is printed on photopaper substrate which can be used to overprint with AgNP inks. The Phoseon FireEdge FE300 (wavelength: 365nm) is used to irradiate the samples with different intensities from 15% to 100%, corresponding to $0.45W/cm^2$ to $3W/cm^2$.

First, Mitsubishi NBSIJ-MU01 AgNP ink is used for its small nanoparticle size which should be susceptible to UV radiation in the 365nm range. It is printed with 5 layers without intermediate UV curing. Afterwards, the 5 layers are irradiated with UV light with different intensities in multiple samples. In all cases, the track changes from a dark (wet) colour to a more shiny metallic colour, suggesting a proper solidification of the ink. Another approach is to apply intermediate UV curing between printing the layers. Irradiating the AgNP printed trace every time one layer is deposited rapidly dries the layer, causing again a noticeable colour change from black (wet) to a shiny metallic colour. Printing a new layer on top shows poor adherence between the layers. A dried droplet is seen to repel a newly jetted droplet instead of coalescing. In both ways, 5 layers of Mitsubishi NBSIJ-MU01 AgNP ink have been printed without conducting results. Similar tests were performed with Novacentrix Metalon JS-B25P. However, also no conducting results were obtained. More samples of both AgNP inks were subsequently exposed to a UV spot source (Honle Bluepoint 4 ecocure) which has a broader range of transmitted wavelengths. Intensity settings to a maximum of $10W/cm^2$ are used. Neither of the AgNP inks were able to sinter and form a conducting track. At high intensity levels, substrate and structural material started to degrade by discoloration and warping due to heat.

To test if sintering of Novacentrix Metalon JS-B25P using heat is possible on structural material in a similar way as one photopaper, Novacentrix Metalon JS-B25P is printed on the same test patches of structural material and put in an oven for 5 and 15 minutes at $150^{\circ}C$, as this temperature is found to be a good compromise between conductivity and required time in the oven (see section 6.4.1). Although the heat-treated samples look good, the traces do not conduct. Damage in the form of warping of the structural material due to the high temperature was visible at 5 minutes and worsened at 15 minutes. In all samples, regardless of drying and sintering method, no conductive traces were able to be reproduced. Upon finer inspection, micro cracks were visible in most samples after completely drying, independent of the curing method. Even in perfectly defined and seemingly perfectly conducting lines, no conducting path was found. These micro cracks are not visible with the naked eye and can only be observed with a microscope, revealing the reason why the lines do not conduct; the cracks separate the line into many individual areas that are not or only partly interconnected with high resistance contact points. Cracks are formed during drying of the AgNP ink, caused by evaporation of the carrier fluid (water) and effectively lowering the volume of the substance. A decrease in volume causes a decrease in surface area, assuming the density of the substance changes only slightly. Although adhesion to the structural material is improved by cleaning the top layer, it is apparently not sufficient to keep the AgNP line from locally detaching and forming micro cracks. Sometimes when this effect is pronounced, also larger cracks are visible with the naked eye.



(a) Cracked AgNP printed line after one night of ambient air drying

(b) Microcracks visible across a printed AgNP line

Figure 6.17: Cracks and micro cracks in printed AgNP lines after drying

6.4.4. Overprinting AgNP ink

After printing AgNP tracks on substrate or structural material, it is exposed to the environment. Moist air, temperature changes, and other factors can negatively influence the conductive properties of the tracks over time. Researchers have found an increase of resistance of up to 15% in a period of 7 months, possibly due to oxidation of the silver tracks [25]. To tackle degradation, a film coating can be applied to prevent air interacting with the AgNP tracks. This coating is inkjet printed with structural material on top of the AgNP. In theory, 1 layer of structural material should be sufficient to shield all tracks. Other than air, the conductive tracks should also be shielded from the aggressive alkaline solution to remove support material. For this reason, more layers are printed to account for uneven surfaces or voids to ensure a proper coating. 20 layers of structural material ($10\mu\text{m}$ thick) provided a solid protective layer in all tested circumstances. No negative effects on conductivity were noted when overprinting AgNP tracks on photopaper substrate.

6.4.5. Results

Best results using the selected AgNP inks in combination with the selected structural and support material inks are achieved using a minimum of 5 layers of AgNP ink, deposited in a pre-printed channel in the structural material defining the desired shape of the AgNP tracks. Exact geometry of the channel is found to be not important, and a minimum width of 0.15mm gave best results. Structural material is manually cleaned with a cloth with ethanol or IPA to wipe off any uncured material and provide a clean surface for the AgNP ink to adhere to. The AgNP ink is best jetted using only one or a few nozzles at a time due to reliability issues of the DMC printheads. All layers should be printed subsequently without intermediate curing or drying to ensure best coalescence of the drops both in plane and between layers. Despite non-conducting traces when printing AgNP on structural material, the obtained results and insights are valuable for further research. When other NP inks are selected and show similar behaviour, appropriate measures can be taken according to the information obtained so far to improve performance. The physical phenomena defining ink behaviour are similar across NP inks, due to their analogous composition.

6.5. Process workflow

To demonstrate the success of the proposed methods for printing multi-material 3D functional structures, a process workflow is described in the following subsections. A design with two parts consisting of overhanging structures and a strain-gauge like conductive pattern printed on top will be used throughout this section as an example for the process from start to end. A detailed explanation on how to export a 3D CAD model for 3D printing on the PiXDRO LP50 is given in appendix E.

6.5.1. Computer aided design

As with any additive manufactured part, an idea or hand drawing is converted to a computer aided design which can be easily manipulated and used by other software as required. In this example, Solidworks [13] is used to model a bridge structure and single overhanging structure. Support material is designed to support the structure only where needed. A zig-zag pattern to mimic a strain-gauge or sensor are imprinted as channels on top of the structures to enhance AgNP ink adhesion performance. The model is saved as two separate 3D parts - one with the structural material geometry, the other with the support material geometry. These parts are in turn exported as simple 3D triangle geometry files in an STL container which is supported by most slicer software. AgNP tracks which don't require a 3D model are exported to a bitmap in a similar way.

6.5.2. Slicing

The 3D structural and support material parts are individually sliced by Chitubox slicer software [9] for SLA 3D printers, producing separate monotone images with a user-set layer height of the whole part. Additional settings such as resolution, infill and wall thickness can also be set. The images are stored in a .zip compressed archive which can be opened to see the individual images. Depending on the slicer software, the definition of black and white pixels can be reversed. E.g. black pixels mean material to be deposited, white means no material to be deposited. For this reason, a custom application has been developed to quickly revert the colours of all images. This application is then used for both structural material sliced images and support material sliced images to invert the bitmaps colours and make the images compatible with PiXDRO HMI software.

For this demonstration, 600 images for the structural material are created, 400 for the support material at a set layer height of $5\mu\text{m}$ at a resolution of $800\times 800\text{px}$.

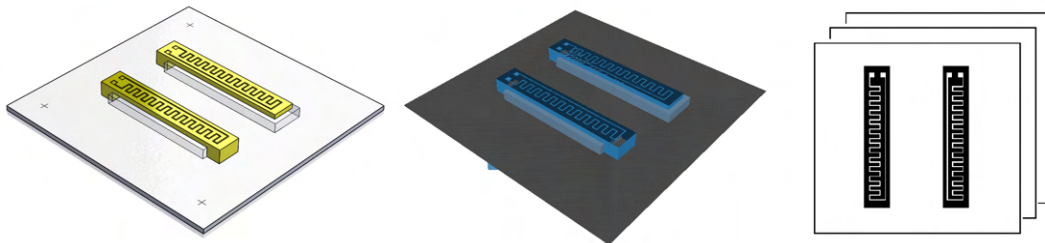


Figure 6.18: Workflow from CAD model to sliced images ready to be inkjet printed. From left to right: CAD model, STL files, and sliced images.

6.5.3. Support modification

As discussed in section 6.3, it is advised to print with a composite support material structure when large overhanging parts need support. The custom support modification application is used for this task to generate a composite support material throughout the print job of 20% structural material and 80% support material.

6.5.4. Printer and recipe settings

First, the structural and composite support material parts of the model are printed using the Spectra Dual head. A $50\times 50\text{mm}$ photopaper substrate is used and aligned using the alignment tool as described in section 5.2. A test pattern identifying failing nozzles is printed on a separate plain paper next to the photopaper substrate. Failing nozzles are excluded from the list of active nozzles in the recipe settings. Custom recipe code to autonomously print 3D structures is used. Details of the custom recipe settings

and code is explained in section 6.2.

After completion, the substrate with printed model is transferred to the other PiXDRO LP50 printer and realigned using PiXDRO HMI's alignment wizard. This LP50 is equipped with the Dimatix DMC-11610 (10 pL) printhead. The cartridge with Novacentrix JS-B25P AgNP ink is used to print the conductive traces. An overview of all recipe settings is given in section 5.2.4.

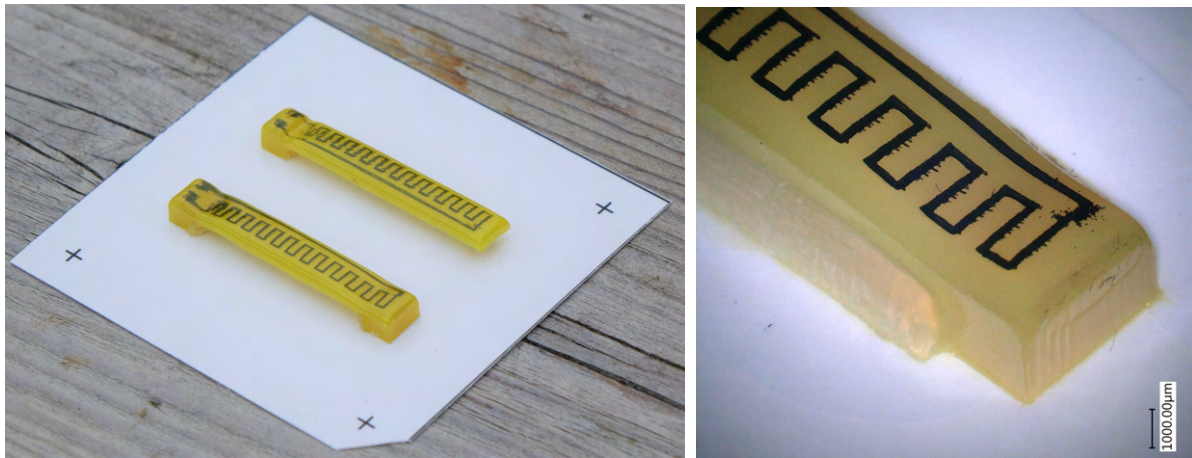
Lastly, the substrate with printed model and AgNP tracks is transferred back to the first PiXDRO LP50 printer and realigned. A few layers of structural material are printed on top of the AgNP ink and cured every layer to form a protective layer over the AgNP ink to prevent it from washing off during the post-processing step, as described in section 6.4.4

6.5.5. Post-processing

Finally, the substrate with printed model is removed. The majority of the support material is manually removed using a small spatula. Afterwards, the model is submerged in an actively stirred base solution to remove the support material for half an hour. The model is removed from the solution, rinsed with running tap water and left to dry.

6.5.6. Results

A model has been designed, converted to images, and inkjet printed using three inks on two PiXDRO LP50 printers and two PHAs. The result of these steps are two fully inkjet printed, multi-material 3d structures with AgNP tracks. The support material is successfully removed using the support removal solution, fig. 6.19a. Features are mostly according to specified dimensions though errors can be observed in the structure's geometry due to the lack of a planerizer levelling layers after each deposition step. Especially in interfacing areas where structural material meets support material, deformation is observed. The AgNP tracks are accurately printed in place with only minor random drop spreading, fig. 6.19b. AgNP tracks are undamaged by support material removal solution through the use of protective layers of structural material but were not sintered hence do not conduct.



(a) Multi-material print after support removal with released overhanging structures (b) Close up of AgNP tracks and overhanging structure.

Figure 6.19: Final results of multi-material prints with AgNP tracks and overhanging structures.

6.6. Proof of concept

An all-inkjet-printed moisture sensor with protective elements is printed as a proof of concept. First, a resistivity sensor is printed on photopaper substrate using Mitsubishi NBSIJ-MU01 self-sintering conductive AgNP ink. The sensor is then improved by adding structural elements protecting the conductive traces where no moisture should be detected. To shield the sensor from large objects and impacts, an overhanging structure is printed spanning the entire sensor.

6.6.1. Resistivity moisture sensor

In many fields, moisture sensors are used to gauge level of moisture content of air, soil and other substances. Many kinds of sensors exist, with various working principles ranging from simple resistivity measurements to more advanced Time or Frequency Domain Reflectometry [19, 43]. For this proof of concept, a resistivity sensor is used since its working principle is straightforward and only requires simple electronics.

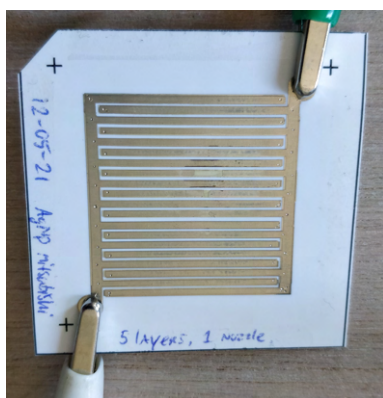
A resistivity moisture sensor consists of two electrodes with several long strands in near contact. Flow of electricity between the two electrode strands is possible when a medium connects (part of) the strands. The flow of electricity between the electrodes can be measured to gain an indication of the resistivity of the substance. The more strands a medium connects, the lower the measured resistance in the sensor.

Test setup

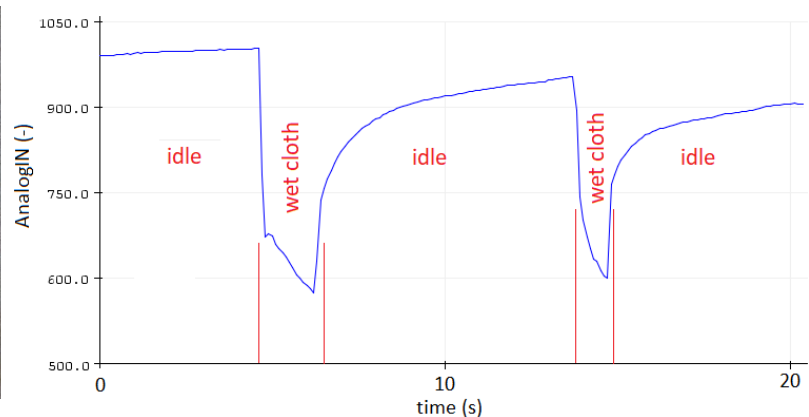
As reference, a cheap and commonly available resistive moisture sensor (YL-83) is connected to a comparator module (YL-38) and its output logged using an Arduino Nano microcontroller. The resistive moisture sensor module is disconnected and replaced by an inkjet-printed counterpart. The inkjet printed sensor, fig. 6.20a, is printed with five layers and has ten strands on each conductor with a width of 1.5mm and a length of 27.5mm . The Arduino Nano microcontroller is connected to a personal computer via USB on a serial port for communication. Comparator output is measured at a rate of 10Hz and displayed on the computer for monitoring. The comparator module has two outputs, a digital pin that switches state upon a set level of resistivity, and an analog output that produces a voltage between 0V and 5V depending on the measured resistivity. The analog output is logged on the Arduino Nano microcontroller.

Results

The inkjet printed moisture sensor performs similar to the reference sensor. When a damp cloth is placed over the conductive strands, a decrease in resistivity is logged. Similarly, droplets of water or a touch with a finger triggers a change in resistivity. A typical response to different materials is recorded and shown in fig. 6.20b.



(a) Printed moisture sensor connected to electronics via clamps



(b) Typical moisture sensor readouts in idle condition and when touched with a wet cloth.

Figure 6.20: AgNP printed moisture sensor and readouts

6.6.2. Multi-material moisture sensor

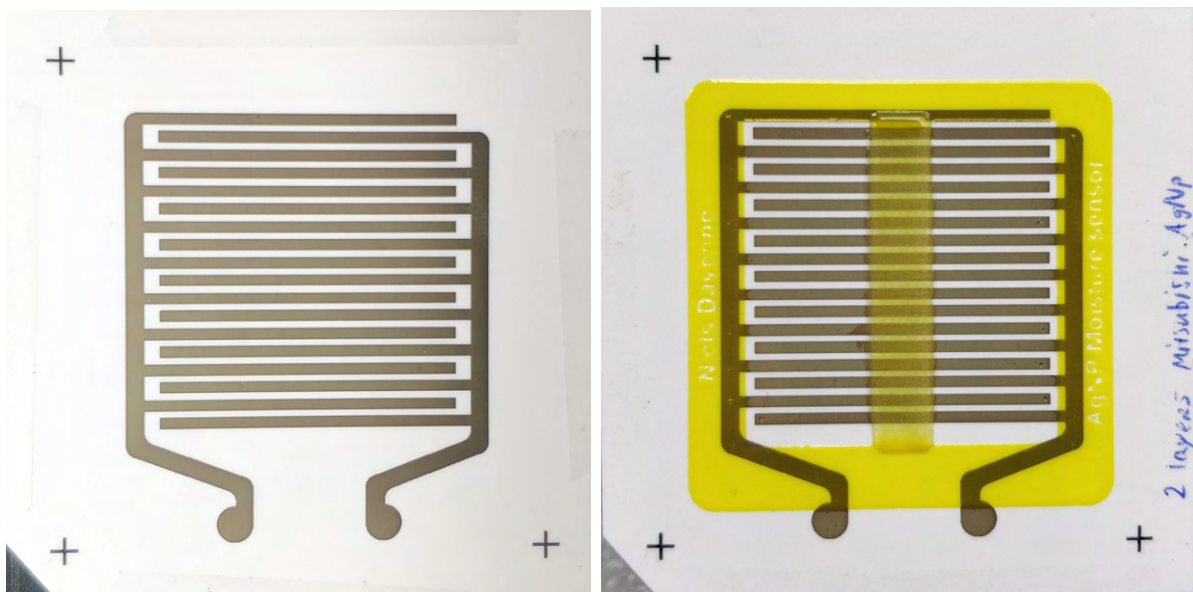
Next, a sensor is designed that has protective features and therefore requires the use of structural and support material ink in addition to conductive AgNP ink.

Design

A similar moisture sensor is designed as the preceding sensor. It is printed with 5 layers of Mitsubishi NBSIJ-MU01 AgNP ink and has 9 strands on each conductor with a width of 1mm and a length of 21mm , see fig. 6.21a. A technical drawing is provided in appendix C.

A conductive strand has a typical resistivity of a few ohms in vertical and horizontal direction.

The strands are surrounded by a 0.1mm thick enclosure of structural material, forming a dielectric layer between the environment and the conductors where no sensing should take place. Conductive pads are again exposed under the enclosure to allow for connection of probes. To shield part of the sensor strands, an overhanging part is placed spanning from one side of the protective layer to the other. This part is printed with a support material structure composite with 20% structural material which can later be removed, leaving only the overhanging structure. The finished multi-material sensor is shown in fig. 6.21b.



(a) Plain sensor without additional elements

(b) Sensor with protective elements and overhanging structure

Figure 6.21: Multi-material moisture sensor with and without protective elements

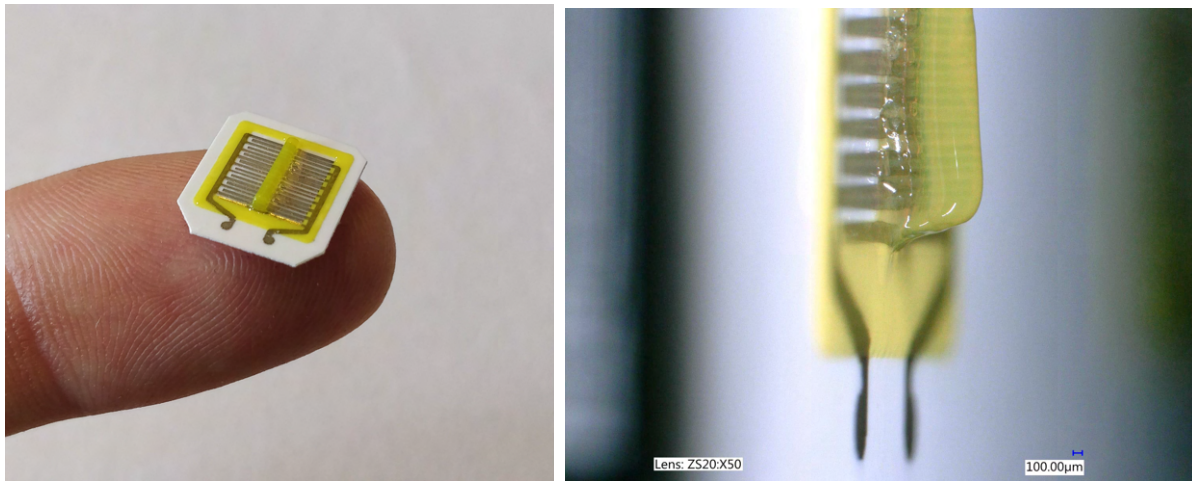
Support removal

The approach as described in section 6.5 is used to remove support material structures. First, as much of the support material is removed mechanically to minimize the required time in the removal solution. Next, the sensor is placed into the support material removal solution and actively stirred. It is observed that the AgNP strands tend to detach easily from the photopaper substrate under the influence of an aqueous solution, fig. 6.22a. After a few minutes, almost all strands detached leaving only a mark where the strands were printed. In return, all support material is dissolved and washed away. The overhanging structure is successfully released as is shown in fig. 6.22b.

be used which basically compromises available print size for more resolution. This limits the number of sensors that can be printed simultaneously. In this proof of concept, the default image resolution is kept and four sensors are printed on a single substrate simultaneously.

Method and results

The AgNP sensor itself is printed using the DMC printhead with Mitsubishi NBSIJ-MU01 AgNP ink. Five layers are printed using one nozzle and default settings. The surrounding structure of VeroYellow structural ink and SUP706B support material ink is printed with the Spectra Dual printhead and default settings. A printed small sensor is cut out of the photopaper substrate and can be seen in fig. 6.23a. Connecting the small sensor to the test setup yields desired results; the sensor reacts to moist touches and damp air in a similar way as the previously printed sensors. fig. 6.23b shows a side view of the small sensor in which the overhanging structure with support material is clearly visible. Support removal was attempted manually (mechanically) and using the base $NaOH$ solution. Manual support removal using a thin precision knife or spatula showed good results, leaving the sensor intact if handled carefully. Submersion in the base solution to dissolve the support material also damaged the sensor conductors, similar to the results as shown before in fig. 6.22. Small features such as printed text previously visible on the large scale moisture sensor become too small and are no longer visible.



(a) Small moisture sensor with overhanging structure on a fingertip (b) Side view of small moisture sensor with overhanging structure

Figure 6.23: Small scale moisture sensor with an surface area of no more than 1cm^2

6.6.4. Conclusion

Using the knowledge gained in preceding chapters and following the process workflow, a proof-of-concept moisture sensor is designed from scratch in CAD-software and converted to suitable files ready for printing on PiXDRO LP50 inkjet printers. Three types of inks are used to print a multi-material functional structure with overhanging part, requiring only UV light to cure the inks. The sensor performs as expected in a test setup even when scaling down the surface area of the entire sensor under 1cm^2 . In addition, the sensor is semi-flexible since it is printed on a relatively thin photopaper substrate which does not compromise its functionality. Submersion in a base solution to dissolve support material causes the AgNP conductors to detach, damaging the sensor. Support material can be removed mechanically to release the overhanging structure without damaging the sensor.

7

Discussion

In this chapter, several points are highlighted and discussed that could influence the results and should be considered. The points are treated on a per-chapter basis.

4. UV polymerisation

Ink selection

The selected photopolymer inks combined with the nanoparticle inks might not be ideal, but are representative for future research. Since all chosen inks have a Z-number in the suitable range for printing, physical properties are expected not to vary much. Compositions and (chemical) compatibility can vary and makes a difference. Chemical sintering additives of Mitsubishi ink most likely prevented it from sintering, though its nanoparticle size was correct for plasmon resonance sintering using UV light. Nanoparticle content in both chosen inks is too low. These inks are meant to be used on special substrate media with porous structure allowing for chemical sintering or partial absorption of the carrier fluid.

Ink spectrometry analysis setup

Due to the nature of the setup, only transparent inks could be tested. Results from the SUP706B test meet the expectations, as no dilution of this ink was necessary due to the transparent nature of the ink itself. Results of tests with diluted nanoparticle ink were mixed. A strong dilution of the inks was necessary before a measurement could be conducted. Undiluted or not sufficiently diluted nanoparticle inks transmitted too little light for the spectrometer to detect and make accurate measurements. However, this is also done by other authors to make valid measurements [18]. Dark coloration was observed only locally in the cuvette, possibly due to optical effects of the cuvette's non-square geometry. The reason for strong coloration effect is unknown, though a possibility is breakdown of the protective layer around the nanoparticles resulting in rapid oxidation and/or agglomeration of the particles. Heating from the irradiated light causes local currents in the fluid, spreading the coloration effect within the sample slowly. Manually shaking the cuvette caused immediate mixing and temporary homogeneous (dark) solution. After some time, the dark colour would gradually fade to the bottom of the cuvette only, suggesting deposition of heavier particles on the bottom due to gravity. See appendix A for photographs of this phenomenon. For the conductive inks, a range of filters could have been used to test if the nanoparticles are sensitive to the tested frequencies. With additional tests, an aperture could have been used when measuring the nanoparticle inks to slow down the coloration.

5. Multi-material printing

No hardware modifications on the PiXDRO LP50 printers were performed. A UV light mounted on the printhead would significantly decrease print time as no more separate movement from the substrate table is necessary for ink curing. Additionally, it might improve print quality, being able to instantly cure the deposited ink before the capillary phase causes the drops to spread out.

To lower viscosity, only printhead heating was available to heat the ink. Values have been determined experimentally and by comparing with temperatures used on a Stratasys Polyjet J735 printer. However,

the printheads used likely differ (slightly) from those machines. Nonetheless, acceptable results were obtained printing the inks with head heating.

Spectra printheads worked consistent, but many nozzles are clogged. Despite purging and other maintenance, unclogging the printhead was unsuccessful. Completely unclogging might only work by draining the printhead and flushing with solvent. Partially clogged nozzles result in manual selection of active nozzles every time, greatly increasing print times because many nozzles are set inactive. Stratasys inks as used were filtered using a 5um filter before use. Inks are stored dry at a cool place but inks in the printhead might experience degradation over time due to minor light and temperature changes, which can worsen nozzle clogging.

6. Functional structures

Photopaper substrate is mainly used as the substrate of choice as Mitsubishi NBSIJ-MU01 and Novacentrix Metalon JS-B25P both print well and yield conductive tracks. Stratasys structural and support material inks also print well on photopaper substrate. Other substrates might be suitable as well such as PET, PEI, Kapton and glass.

Sintering Novacentrix Metalon JS-B25P on VeroYellow structural material in oven tests could be more elaborate, to exclude all possibilities why no conductive tracks were obtained. Different layer heights combined with a range of sintering temperatures and heating duration can result in a working set. However, sintering using heat was is not the main focus of this research and is left as a recommendation for future research in this field of interest.

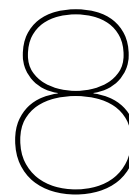
Support modification using the custom application yields a pixel-perfect raster with desired density of black and white pixels for optimal mixing of structural and support material. When loading these images in PiXDRO HMI, they are converted to printable bitmaps, which slightly changes parts of the raster to no longer be pixel-perfect. This has consequence for the strength of the support structure in certain parts where the raster is changed.

Ag Moisture sensor

Long exposure to damp cloth or drops oxidises the conductor strands. Effectively, electrolysis is performed. The anode will oxidise, limiting the conductivity of the strand over time.

For the small moisture sensor, the used resolution of the images is just barely high enough to keep appropriate spacing between strands.

A small alignment error between structural and conductive material due to manual placement in Chitubox slicer can be observed.



Recommendations

Several recommendations are proposed regarding interesting topics for future research.

4. UV polymerisation and sintering

- Selection of inks and experiments: Choose inks as used by other authors that have proven to work with UV sintering using plasmon resonance. Nanoparticle size, shape and way of production are important parameters that determine effectiveness of UV light sintering.
- For repeated measurements of the sensitive wavelengths of nanoparticles, use a spectrometer with accurate measurements lower than $350nm$, preferably a broad range centred around $400nm$, extending at least to under $300nm$ to capture all relevant data in the UV-Visible spectrum of light.

5. Multi-material printing

- Use multiple printheads next to each other to print with all required materials simultaneously. Preferably spectra heads for their ease of use and high reliability. Even better would be multiple Océ Crystalpoint printheads with self-diagnostic function, to detect and skip printing with failing nozzles (PAINT technology). This greatly improves print times and eliminates need of switching around substrates and/or PHAs and re-aligning between printers.
- Analyse the effect of different inks on each other when cross-printing in cured and uncured states. Printing hybrid or gradient structures with changing (mechanical) properties could be possible.

6. Functional structures

- A more comprehensive comparison of substrates, especially for semi-3D structures (2.5D) of only a few layers thick, or designs that incorporate the substrate as part of the structure. Substrates especially designed for conductive ink (Novacentrix Novele, Mitsubishi variants, PET/PVA coating etc.) could be beneficial for even better conductivity when printing directly on the substrate with conductive ink.
- Using UV lights with higher wavelengths such as $395nm$ or $405nm$ as found in literature, may have better results when sintering AgNP inks using UV.
- Research matching structural inks with AgNP inks; to make sure layers don't separate, no micro cracks are formed etc.
- Consider using other conductive inks which have inferior conductivity but might work better with the structural material in terms of adhesion and can also be sintered using light. Nanoparticle inks containing a higher number of weight percentage silver that are not specifically designed for porous media should yield better results. Alternatively, consider using another structural material that works better with the currently selected inks.
- Printing AgNP ink tracks with Spectra heads instead of Dimatix DMC disposable cartridges for better quality and higher speed.
- After printing, the model will stick to the substrate and cannot be removed without tearing parts of the structure or substrate. If this is undesired, a patch of 10 layers support material can be printed as is often done on industrial inkjet printers.

- Similarly, if support material is difficult to remove from structural material, an interface layer with less or weaker supports can be used. This should ease separation of the support from the structural material.
- Use a planerizer (or levelling roller) to flatten each printed layer as is done in Stratasys Polyjet machines. Substantial increase in print quality can be expected (refer to Polyjet comparison prints in section 6.2 for details). Additionally, a separate study on the topic of printing without a planeriser and assessment of quality can be viable.
- The printed AgNP Moisture sensor is just a proof of concept but has potential for improvements. A conductive sensor instead of resistive would not require exposed conductors, enabling safe support removal and total submersion of the sensor in water.
- To tackle oxidation of the conductive strands of the AgNP moisture sensor, solutions could be to only apply a voltage when reading the resistivity is required. Also AC operation of electrodes instead of DC eliminates oxidation on one electrode only.
- A study on fault tolerance for functional small scale structures. Printing at minimum line widths allows for small prints but a failing nozzle can quickly ruin a print if no redundant lines are printed, especially for conductive tracks.
- Improvement of the custom PiXDRO LP50 recipe code for multi-material 3D printing to support more options and printer faster. Code is maintained in an online repository (GitHub) and issues to fix are already filed.

9

Conclusion

The aim of this project is to combine multiple functional materials into a 3D inkjet printing process to print structures using only UV light curing. Structural, support and conductive inks are selected and thoroughly tested requiring only UV light to cure. PiXDRO LP50 research inkjet printers are used and its software is modified to allow printing of multi-material 3D structures. Functional parts were successfully printed including complex overhanging geometries and a resistivity sensing module as a proof of concept.

To come to these results, a systematic literature survey identified state of the art challenges and potential for improvements. From this, the problem statement is set and the experimental setup and inks were selected. Stratasys VeroBlack RGD875 and VeroYellow RGD836 are selected as structural (building) material together with Stratasys SUP706B as support (sacrificial) material. These photopolymer-based inks cure when exposed to ultraviolet light. Mitsubishi NBSIJ-MU01 and Novacentrix Metalon JS-B25P silver nanoparticle inks are selected as conductive materials, as silver nanoparticle inks provide a high conductivity and can be sintered using ultraviolet light by exploiting nanoparticle plasmon resonance. PiXDRO LP50 research inkjet printers, comprising a high resolution motion stage and interchangeable printheads are used for multi-material printing. By modification of recipe code, support to print 3D structures with structural and support material using two Spectra SE-128 AA printheads simultaneously was added. Due to the lack of a levelling roller (planeriser), tall structures suffer from bulging and errors in geometry that are caused by fluid interactions when the ink is deposited and still uncured. To minimize this effect, proper tuning of printhead jetting waveforms is performed resulting in reliable jetting with matching drop volume and velocity. Support material is released by submersion in a 2% $NaOH$ and 1% Na_2SiO_3 base solution. Mechanically removing most support material prior to submersion decreases required time to dissolve all support material and reduces damage to substrate. Conductive material is printed on a second PiXDRO LP50 using DMC-11610 disposable printheads. The substrate is easily aligned between printers using a custom tool and printed markers for software auto-alignment. Printing Mitsubishi NBSIJ-MU01 on photopaper substrate yields highly conductive lines without the need for sintering or post-processing. Novacentrix Metalon JS-B25P yields similar conductive lines after sintering at $150^{\circ}C$ for five minutes. Printing on structural material is successful with both nanoparticle inks, but requires cleaning of the surface. Better results are obtained when printing in recessed channels where silver ink is forced to flow and coalesce. Curing the structural and support material inks was successful using a UV LED source with a $365nm$ peak and an intensity of $0.45W/cm^2$. Sintering either one of the silver nanoparticle inks with UV light was unsuccessful even with higher intensities and other UV sources. This is due to the low weight percentage of silver (15-25wt%) and presence of dispersing agents for self-sintering ink. Using other inks containing higher weight percentages (40wt%) of silver nanoparticles with diameters under $50nm$ is recommended. A print process from CAD model to 3D printed part is developed, supporting composite support material to create stronger supports. A proof-of-concept functional silver nanoparticle moisture sensor is printed with overhanging geometry using three inks and only requiring UV light to cure the materials. To demonstrate the scalability of 3D inkjet printing, the sensor is decreased in size reducing the surface area to less than $1cm^2$.

Inkjet printing is a digital, quick, and low-cost manufacturing technique that is still evolving. Especially multi-material 3D inkjet printing has great potential for rapid prototyping and manufacturing of functional structures when novel inks are combined into an integrated process. The combination of three distinct inks in a process is shown, requiring merely UV light to cure the materials. The results provide a step towards efficient and quick manufacturing of all-inkjet printed functional structures.

Bibliography

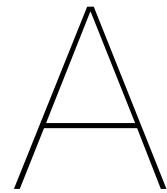
- [1] Vincenzo Amendola, Osman M. Bakr, and Francesco Stellacci. A study of the surface plasmon resonance of silver nanoparticles by the discrete dipole approximation method: Effect of shape, size, structure, and assembly. *Plasmonics*, 5(1):85–97, 2010. ISSN 15571955. doi: 10.1007/s11468-009-9120-4.
- [2] Byeong Wan An, Kukjoo Kim, Heejoo Lee, So-Yun Kim, Yulhui Shim, Dae-Young Lee, Jun Yeob Song, and Jang-Ung Park. High-Resolution Printing of 3D Structures Using an Electrohydrodynamic Inkjet with Multiple Functional Inks. *Advanced Materials*, 27(29):4322–4328, 2015. ISSN 0935-9648. doi: 10.1002/adma.201502092. URL <http://10.0.3.234/adma.201502092https://dx.doi.org/10.1002/adma.201502092>.
- [3] ASTM. ASTM 52900-2015-E-Standard Terminology for Additive Manufacturing Technologies-General Principles Terminology, 2016.
- [4] Ali Bagheri and Jianyong Jin. Photopolymerization in 3D Printing. *ACS Applied Polymer Materials*, 1(4):593–611, 2019. ISSN 2637-6105. doi: 10.1021/acsapm.8b00165.
- [5] Ph. Buffat and J-P. Borel. Size effect on the melting temperature of gold particles. *Physical Review A*, 13(6):2287–2298, 1976.
- [6] Hatim K. Cader, Graham A. Rance, Morgan R. Alexander, Andrea D. Gonçalves, Clive J. Roberts, Chris J. Tuck, and Ricky D. Wildman. Water-based 3D inkjet printing of an oral pharmaceutical dosage form. *International Journal of Pharmaceutics*, 564(April):359–368, 2019. ISSN 18733476. doi: 10.1016/j.ijpharm.2019.04.026. URL <https://doi.org/10.1016/j.ijpharm.2019.04.026>.
- [7] T. Chen. Facile preparation of high conductive silver electrodes by dip-coating followed by quick sintering, 2020.
- [8] Zhen Chen, Huan Meng, Gengmei Xing, Chunying Chen, Yuliang Zhao, Guang Jia, Tiancheng Wang, Hui Yuan, Chang Ye, Feng Zhao, Zhifang Chai, Chuanfeng Zhu, Xiaohong Fang, Baocheng Ma, and Lijun Wan. Acute toxicological effects of copper nanoparticles in vivo. *Toxicology Letters*, 163(2):109–120, 2006. ISSN 03784274. doi: 10.1016/j.toxlet.2005.10.003.
- [9] Ltd. CHUANGBIDE Technologies Co. Chitubox 1.0.0, 2021. URL <https://www.chitubox.com/>. URL: <https://www.chitubox.com/>, Last accessed: June 2021.
- [10] Jaewon Chung, Seunghwan Ko, Nicole R. Bieri, Costas P. Grigoropoulos, and Dimos Poulikakos. Conductor microstructures by laser curing of printed gold nanoparticle ink. *Applied Physics Letters*, 84(5):801–803, 2004. ISSN 00036951. doi: 10.1063/1.1644907.
- [11] Elizabeth A. Clark, Morgan R. Alexander, Derek J. Irvine, Clive J. Roberts, Martin J. Wallace, Sonja Sharpe, Jae Yoo, Richard J.M. Hague, Chris J. Tuck, and Ricky D. Wildman. 3D printing of tablets using inkjet with UV photoinitiation. *International Journal of Pharmaceutics*, 529(1-2): 523–530, 2017. ISSN 18733476. doi: 10.1016/j.ijpharm.2017.06.085. URL <http://dx.doi.org/10.1016/j.ijpharm.2017.06.085>.
- [12] B S Cook, C Mariotti, J R Cooper, D Revier, B K Tehrani, L Aluigi, L Roselli, and M M Tentzeris. Transformers on Flexible LCP Substrate. *Journal*, pages 6–9, 2014.
- [13] Dassault Systèmes SOLIDWORKS Corp. Solidworks 2019, 2019. URL <https://www.solidworks.com/>. URL: <https://www.solidworks.com/>, Last accessed: June 2021.

- [14] Berend Jan De Gans, Paul C. Duineveld, and Ulrich S. Schubert. Inkjet printing of polymers: State of the art and future developments. *Advanced Materials*, 16(3):203–213, 2004. ISSN 09359648. doi: 10.1002/adma.200300385.
- [15] Brian Derby. Inkjet Printing of Functional and Structural Materials: Fluid Property Requirements, Feature Stability, and Resolution. *Annual Review of Materials Research*, 40(1): 395–414, 2010. ISSN 1531-7331. doi: 10.1146/annurev-matsci-070909-104502. URL <http://10.0.4.122/annurev-matsci-070909-104502><https://dx.doi.org/10.1146/annurev-matsci-070909-104502>.
- [16] Brian Derby and Nuno Reis. Inkjet Printing of Highly Loaded Particulate Suspensions. *MRS Bulletin*, 28(11):815–818, 2003. ISSN 08837694. doi: 10.1557/mrs2003.230.
- [17] Lisa Marie Faller, Matic Krivec, Anze Abram, and Hubert Zangl. AM metal substrates for inkjet-printing of smart devices. *Materials Characterization*, 143:211–220, 2018. ISSN 10445803. doi: 10.1016/j.matchar.2018.02.009. URL <https://doi.org/10.1016/j.matchar.2018.02.009>.
- [18] Yulia Galagan, Erica W.C. Coenen, Robert Abbel, Tim J. Van Lammeren, Sami Sabik, Marco Barink, Erwin R. Meinders, Ronn Andriessen, and Paul W.M. Blom. Photonic sintering of inkjet printed current collecting grids for organic solar cell applications. *Organic Electronics*, 14(1):38–46, 2013. ISSN 15661199. doi: 10.1016/j.orgel.2012.10.012. URL <http://dx.doi.org/10.1016/j.orgel.2012.10.012>.
- [19] Miller J.D. Gaskin G.J. Measurement of soil water content using a simplified impedance measuring technique. *Journal of Agricultural Engineering Research* 63, 153-160, 1996.
- [20] Lin P. Ghodssi R. *MEMS Materials and Processes Handbook*. Springer, Berlin, 2011. ISBN 9780387473161.
- [21] Dennis Graf, Sven Burchard, Julian Crespo, Christof Megnin, Sebastian Gutsch, Margit Zacharias, and Thomas Hanemann. Influence of Al₂O₃ Nanoparticle Addition on a UV Cured Polyacrylate for 3D Inkjet Printing. *Polymers*, 11(4):633, 2019. ISSN 2073-4360. doi: 10.3390/polym11040633. URL <http://10.0.13.62/polym11040633><https://dx.doi.org/10.3390/polym11040633>.
- [22] Lu Huang, Yi Huang, Jiajie Liang, Xiangjian Wan, and Yongsheng Chen. Graphene-based conducting inks for direct inkjet printing of flexible conductive patterns and their applications in electric circuits and chemical sensors. *Nano Research*, 4(7):675–684, 2011. ISSN 19980124. doi: 10.1007/s12274-011-0123-z.
- [23] Elahe Jabari and Ehsan Toyserkani. Aerosol-Jet printing of highly flexible and conductive graphene/silver patterns. *Materials Letters*, 174:40–43, 2016. ISSN 18734979. doi: 10.1016/j.matlet.2016.03.082. URL <http://dx.doi.org/10.1016/j.matlet.2016.03.082>.
- [24] Erno Karjalainen, Dominic J Wales, Deshani H A T Gunasekera, Jairton Dupont, Peter Licence, Ricky D Wildman, and Victor Sans. Tunable Ionic Control of Polymeric Films for Inkjet Based 3D Printing. *ACS Sustainable Chemistry & Engineering*, 6(3):3984–3991, 2018. ISSN 2168-0485. doi: 10.1021/acssuschemeng.7b04279. URL <http://10.0.3.253/acssuschemeng.7b04279><https://dx.doi.org/10.1021/acssuschemeng.7b04279>.
- [25] Yoshihiro Kawahara, Steve Hodges, Benjamin S Cook, and Gregory D Abowd. Instant Inkjet Circuits: Lab-based Inkjet Printing to Support Rapid Prototyping of UbiComp Devices. *UbiComp'13*, pages 363–372, 2013. URL <https://m.alibaba.com/product/60686161637/Thermoplastic-polyurethane-tpu-resin-tpu-pallet.html?s=p&spm=a2706.7843299.1998817009.4.YYDAL>.
- [26] Hiroyuki Kawamoto. Electronic circuit printing, 3D printing and film formation utilizing electrostatic inkjet technology. *International Conference on Digital Printing Technologies*, 1(June):961–964, 2007.

- [27] Seung H Ko, Heng Pan, Costas P Grigoropoulos, Christine K Luscombe, Jean M J Fréchet, and Dimos Poulikakos. All-inkjet-printed flexible electronics fabrication on a polymer substrate by low-temperature high-resolution selective laser sintering of metal nanoparticles. *Nanotechnology*, 18(34):345202, 2007. ISSN 0957-4484. doi: 10.1088/0957-4484/18/34/345202. URL <https://dx.doi.org/10.1088/0957-4484/18/34/345202>.
- [28] Seung Hwan Ko, Jaewon Chung, Nico Hotz, Koo Hyun Nam, and Costas P. Grigoropoulos. Metal nanoparticle direct inkjet printing for low-temperature 3D micro metal structure fabrication. *Journal of Micromechanics and Microengineering*, 20(12), 2010. ISSN 09601317. doi: 10.1088/0960-1317/20/12/125010.
- [29] Daniel W. Koon, Martina Heřmanová, and Josef Náhlík. Electrical conductance sensitivity functions for square and circular cloverleaf van der Pauw geometries. *Measurement Science and Technology*, 26(11), 2015. ISSN 13616501. doi: 10.1088/0957-0233/26/11/115004.
- [30] Gih-Keong Lau and Milan Shrestha. Ink-Jet Printing of Micro-Electro-Mechanical Systems (MEMS). *Micromachines*, 8(6):194, 2017. ISSN 2072-666X. doi: 10.3390/mi8060194. URL <http://10.0.13.62/mi8060194https://dx.doi.org/10.3390/mi8060194>.
- [31] Michael Layani, Xiaofeng Wang, and Shlomo Magdassi. Novel Materials for 3D Printing by Photopolymerization. *Advanced Materials*, 30(41):1706344, 2018. ISSN 0935-9648. doi: 10.1002/adma.201706344. URL <http://10.0.3.234/adma.201706344https://dx.doi.org/10.1002/adma.201706344>.
- [32] H H Lee, K S Chou, and K C Huang. Inkjet printing of nanosized silver colloids. *Nanotechnology*, 16(10):2436–2441, 2005. ISSN 0957-4484 (Print) 0957-4484 (Linking). doi: 10.1088/0957-4484/16/10/074. URL <https://www.ncbi.nlm.nih.gov/pubmed/20818031>.
- [33] Joshua Lessing, Ana C Glavan, S Brett Walker, Christoph Keplinger, Jennifer A Lewis, and George M Whitesides. Inkjet Printing of Conductive Inks with High Lateral Resolution on Omniphobic “RFPaper” for Paper-Based Electronics and MEMS. *Advanced Materials*, 26(27):4677–4682, 2014. ISSN 0935-9648. doi: 10.1002/adma.201401053. URL <http://10.0.3.234/adma.201401053https://dx.doi.org/10.1002/adma.201401053>.
- [34] Vincent Chi-Fung Li, Xiao Kuang, Craig M Hamel, Devin Roach, Yulin Deng, and H Jerry Qi. Cellulose nanocrystals support material for 3D printing complexly shaped structures via multi-materials-multi-methods printing. *Additive Manufacturing*, 28:14–22, 2019. ISSN 2214-8604. doi: 10.1016/j.addma.2019.04.013. URL <http://10.0.3.248/j.addma.2019.04.013https://dx.doi.org/10.1016/j.addma.2019.04.013>.
- [35] Mitsubishi Paper Mills limited. Silver Nano Particle Inks, 2019. URL <http://www.k-mpm.com/agnanoen/agnano-ink.html>. URL: <http://www.k-mpm.com/agnanoen/agnano-ink.html>, Last accessed: April 2021.
- [36] David Mccoul, Samuel Rosset, Samuel Schlatter, and Herbert Shea. Inkjet 3D printing of UV and thermal cure silicone elastomers for dielectric elastomer actuators. *Smart Materials and Structures*, 26(12):125022, 2017. ISSN 0964-1726. doi: 10.1088/1361-665x/aa9695. URL <http://10.0.4.64/1361-665x/aa9695https://dx.doi.org/10.1088/1361-665x/aa9695>.
- [37] Nicholas A. Meisel, Andrew Gaynor, Christopher B. Williams, and James K. Guest. Multiple-material topology optimization of compliant mechanisms created via polyjet 3D printing. *24th International SFF Symposium - An Additive Manufacturing Conference, SFF 2013*, pages 980–997, 2013.
- [38] Hugh Shercliff Michael Ashby. *Materials. Engineering, Science, Processing and Design*. Elsevier Science & Technology, 2013.
- [39] Süss microtech. PiXDRO LP50 Inkjet Printer, 2020. URL <https://www.suss.com/en/products-solutions/inkjet-printing/lp50>. URL: <https://www.suss.com/en/products-solutions/inkjet-printing/lp50>, Last accessed: June 2020.

- [40] Kumar A. Nazir A., Abate K.M. et al. A state-of-the-art review on types, design, optimization, and additive manufacturing of cellular structures. *Int J Adv Manuf Technol* 104, 2019. ISSN 3489–3510. doi: 10.1007/s00170-019-04085-3.
- [41] Rachel Near, Steven Hayden, and Mostafa El-Sayed. Extinction vs absorption: Which is the indicator of plasmonic field strength for silver nanocubes? *Journal of Physical Chemistry C*, 116 (43):23019–23026, 2012. ISSN 19327447. doi: 10.1021/jp309272b.
- [42] Andrea Negro, Thibaud Cherbuin, and Matthias P Lutolf. 3D Inkjet Printing of Complex, Cell-Laden Hydrogel Structures. *Scientific Reports*, 8(1), 2018. ISSN 2045-2322. doi: 10.1038/s41598-018-35504-2. URL <http://10.0.4.14/s41598-018-35504-2><https://dx.doi.org/10.1038/s41598-018-35504-2>.
- [43] K. Noborio. Measurement of soil water content and electrical conductivity by time domain reflectometry: A review. *Computers and Electronics in Agriculture* 31:213–237, 2001.
- [44] Ali Roshanghias, Matic Krivec, and Marcus Baumgart. Sintering strategies for inkjet printed metallic traces in 3D printed electronics. *Flexible and Printed Electronics*, 2(4):45002, 2017. ISSN 2058-8585. doi: 10.1088/2058-8585/aa8ed8. URL <http://10.0.4.64/2058-8585/aa8ed8><https://dx.doi.org/10.1088/2058-8585/aa8ed8>.
- [45] Ehab Saleh, Peter Woolliams, Bob Clarke, Andrew Gregory, Steve Greedy, Chris Smartt, Ricky Wildman, Ian Ashcroft, Richard Hague, Phill Dickens, and Christopher Tuck. 3D inkjet-printed UV-curable inks for multi-functional electromagnetic applications. *Additive Manufacturing*, 13:143–148, 2017. ISSN 2214-8604. doi: 10.1016/j.addma.2016.10.002. URL <http://10.0.3.248/j.addma.2016.10.002><https://dx.doi.org/10.1016/j.addma.2016.10.002>.
- [46] Ehab Saleh, Fan Zhang, Yinfeng He, Jayasheelan Vaithilingam, Javier Ledesma Fernandez, Ricky Wildman, Ian Ashcroft, Richard Hague, Phill Dickens, and Christopher Tuck. 3D Inkjet Printing of Electronics Using UV Conversion. *Advanced Materials Technologies*, 2(10):1700134, 2017. ISSN 2365-709X. doi: 10.1002/admt.201700134. URL <http://10.0.3.234/admt.201700134><https://dx.doi.org/10.1002/admt.201700134>.
- [47] Furlan Schroder, McCool. Broadcast photonic Curing of Metallic Nanoparticle Films. *NovaCentrix*, 2006.
- [48] K.A. Schroder. Mechanisms of photonic curing: Processing high temperature films on low temperature substrates. *NovaCentrix*, 2011.
- [49] Stratasys. Polyjet technology, 2020. URL <https://www.stratasys.com/polyjet-technology>. URL: <https://www.stratasys.com/polyjet-technology>, Last accessed: May 2020.
- [50] Mohammad Vaezi, Hermann Seitz, and Shoufeng Yang. A review on 3D micro-additive manufacturing technologies. *International Journal of Advanced Manufacturing Technology*, 67(5-8): 1721–1754, 2013. ISSN 14333015. doi: 10.1007/s00170-012-4605-2.
- [51] Rafal Walczak, Krzysztof Adamski, and Danylo Lizanets. Inkjet 3D printed check microvalve. *Journal of Micromechanics and Microengineering*, 27(4), 2017. ISSN 13616439. doi: 10.1088/1361-6439/aa6152.
- [52] Rafał Walczak, Krzysztof Adamski, and Wojciech Kubicki. Inkjet 3D printed chip for capillary gel electrophoresis. *Sensors and Actuators, B: Chemical*, 261:474–480, 2018. ISSN 09254005. doi: 10.1016/j.snb.2018.01.174. URL <http://dx.doi.org/10.1016/j.snb.2018.01.174>.
- [53] Herman Wijshoff. The dynamics of the piezo inkjet printhead operation. *Physics Reports*, 491 (4-5):77–177, 2010. ISSN 0370-1573. doi: 10.1016/j.physrep.2010.03.003. URL <https://dx.doi.org/10.1016/j.physrep.2010.03.003>.

- [54] Brandon D Young, Bryan Gamboa, Amar S Bhalla, and Ruyan Guo. Current status of functional and multifunctional materials for 3D microfabrication: An overview. *Ferroelectrics*, 555(1):15–56, 2020. ISSN 0015-0193. doi: 10.1080/00150193.2019.1691382. URL <http://10.0.4.56/00150193.2019.1691382><https://dx.doi.org/10.1080/00150193.2019.1691382>.
- [55] Fan Zhang, Christopher Tuck, Richard Hague, Yinfeng He, Ehab Saleh, You Li, Craig Sturgess, and Ricky Wildman. Inkjet printing of polyimide insulators for the 3D printing of dielectric materials for microelectronic applications. *Journal of Applied Polymer Science*, 133(18):n/a–n/a, 2016. ISSN 0021-8995. doi: 10.1002/app.43361. URL <http://10.0.3.234/app.43361><https://dx.doi.org/10.1002/app.43361>.
- [56] Юкатан. Wikimedia Commons, Photo-polymer scheme, 2015. URL <https://commons.wikimedia.org/wiki/File:Photo-polymer-scheme1.svg>. URL: <https://commons.wikimedia.org/wiki/File:Photo-polymer-scheme1.svg>, Last accessed: June 2021.



Spectrometry experiments

A.1. Design

A design for the spectrometry setup was made using SolidWorks 2019 [13] CAD software. Two custom adapters are designed to be able to connect the two different fiber optic cable to the cuvette sample holder (Thorlabs CVH100). The design is depicted in fig. A.1. In practise, the collimator lens cages were unnecessary and therefore left out.

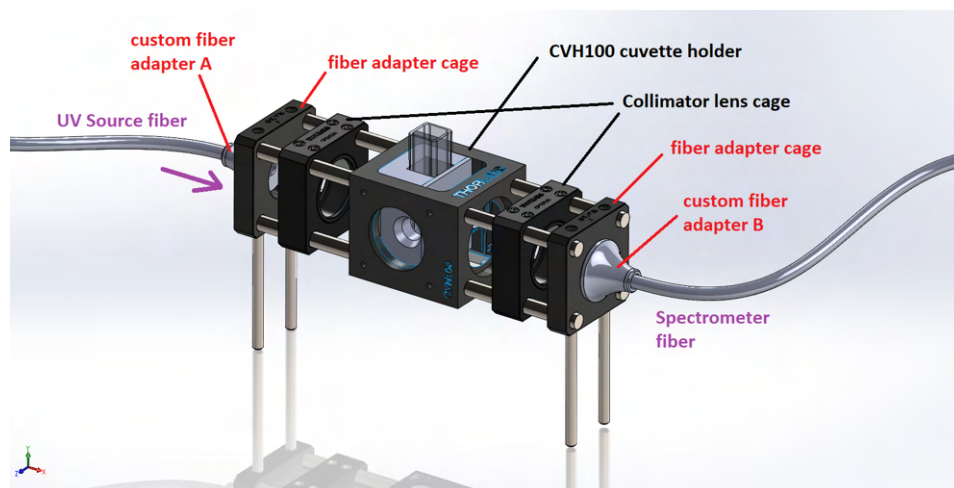
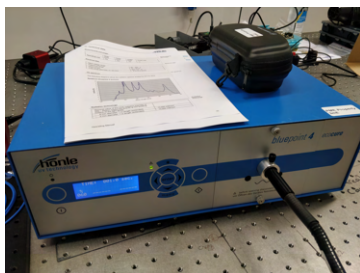


Figure A.1: Spectrometry design in CAD software. The design includes collimator lenses and custom adaptors

A.2. Setup and components

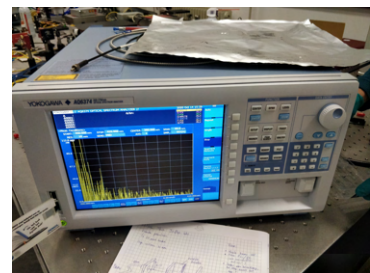
A Honle Bluepoint 4 ecocure Uv spot source is used as received without an optional filter. The fiber optic cable was directly connected to the Thorlabs CVH100 cuvette holder.



(a) Honle UV spot source



(b) Thorlabs CVH100 cuvette holder

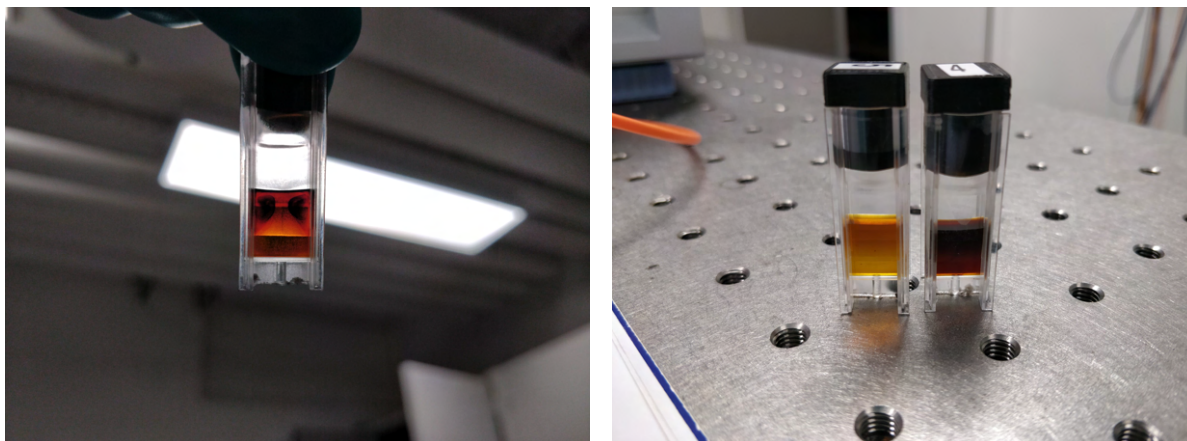


(c) Spectrum analyser Yokogawa, AQ6374

Figure A.2: Main components of experimental setup for spectrometry measurements

A.3. Results

Dark coloration of liquid can be observed after exposing cuvettes with UV light for some time.



(a) Localised dark coloration of cuvette contents after high intensity UV light exposure.

(b) Prepared cuvettes containing diluted AgNP ink before and after exposure to UV light

Figure A.3

A.4. Honle UV source intensity output

The Honle UV source has a non-linear intensity output over a broad range of wavelengths.

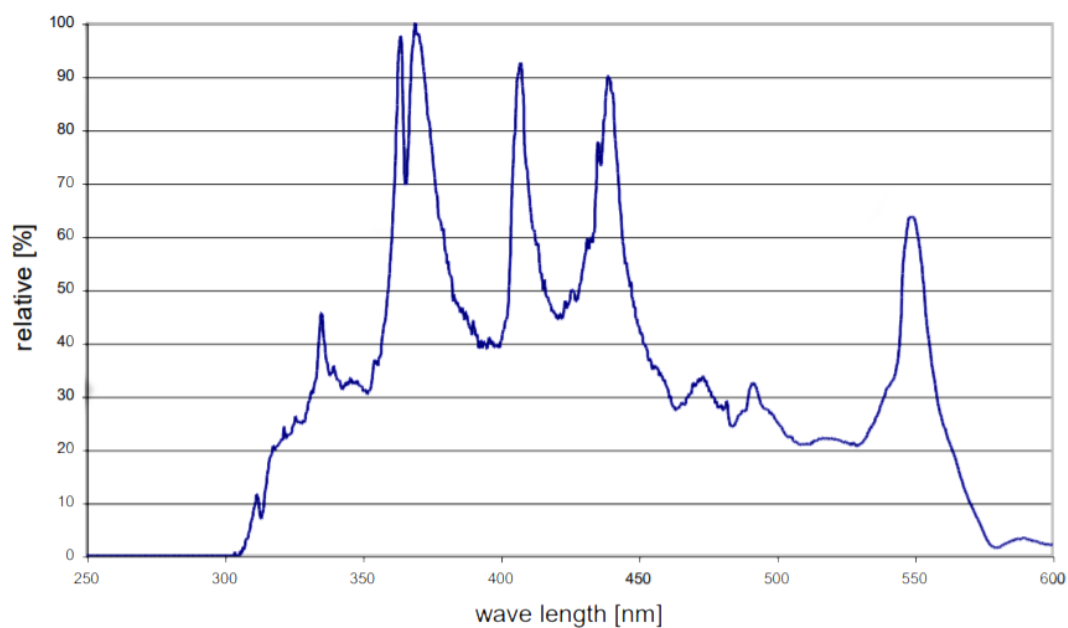


Figure A.4: Radiation spectra emitted by the Honle UV source. Adopted from user manual.

B

AgNP channels in structural material

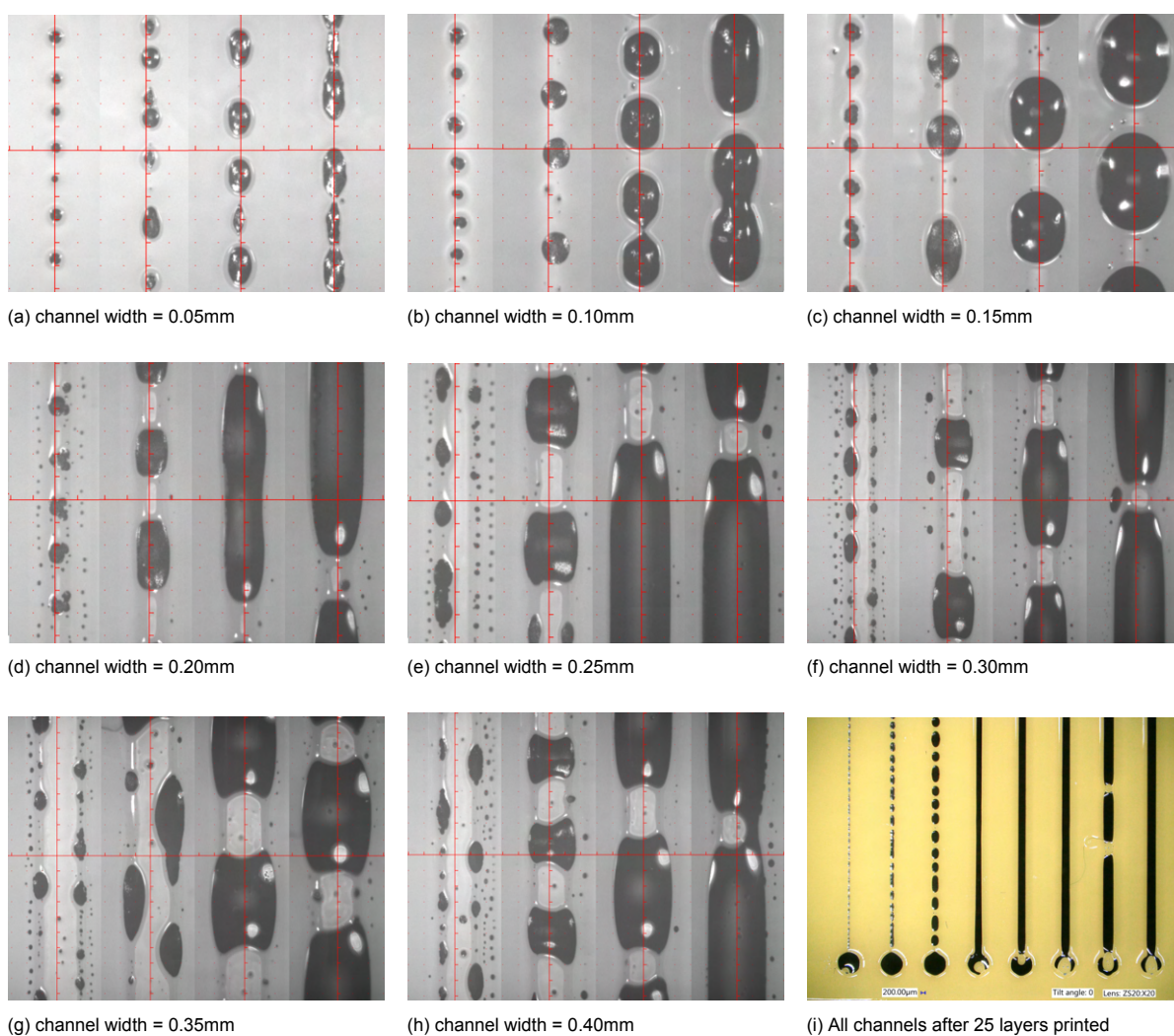


Figure B.1: Varying channel widths and layer heights. All images contain from left to right: 1 layer, 5 layers, 10 layers, 20 layers.

C

Technical drawings

Technical drawings for relevant test structures used throughout the experiments are presented in the following sections.

C.1. 50x50 substrate

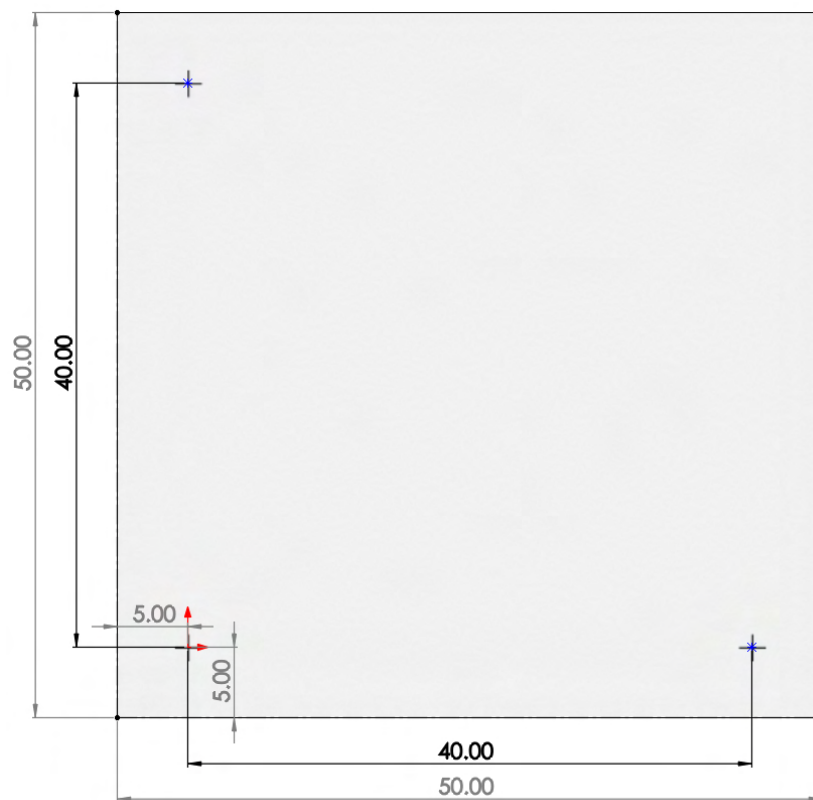


Figure C.1: 50x50mm substrate with markers technical drawing

C.2. Multi-material-bridge

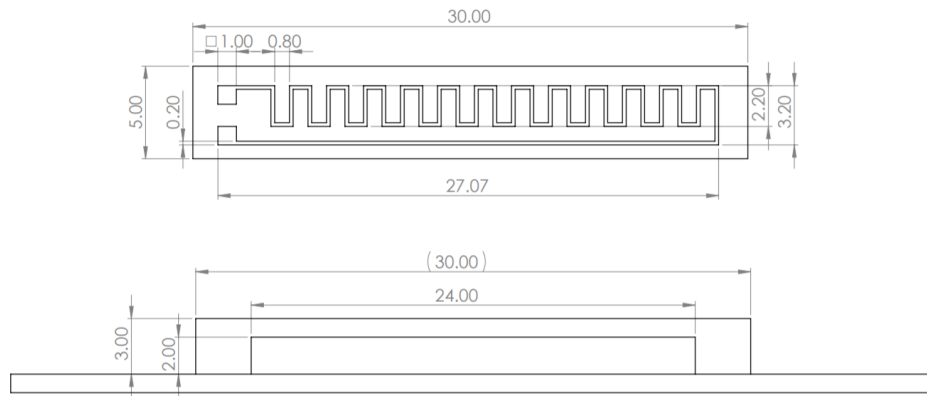


Figure C.2: Multi-material-bridge technical drawing

C.3. AgNP moisture sensor

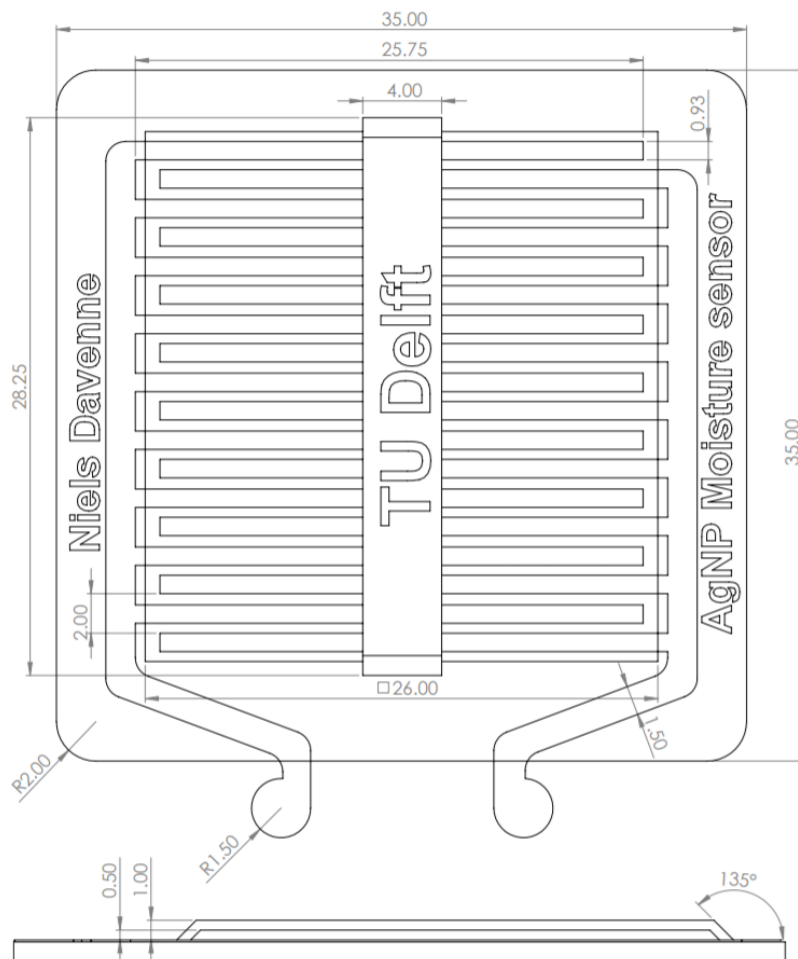
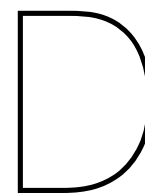


Figure C.3: Ag moisture sensor technical drawing



Support removal solution preparation

To remove the Stratasys SUP706b support material, several methods are recommended. One of these methods is placing the finished model with support material in a sodium hydroxide ($NaOH$) and sodium metasilicate (Na_2SiO_3) solution to dissolve the support material. In this appendix, the method to reproduce this solution is given.

According to the manual, an aqueous solution should be prepared with 2% $NaOH$ and 1% Na_2SiO_3 .

Molar mass of $NaOH$ is $40g/mol$.

Molar mass of Na_2SiO_3 is $122g/mol$.

For a 1L solution, 2% $NaOH$ and 1% Na_2SiO_3 correspond to $20g/L$ and $10g/L$, respectively.

1. Conduct in well-ventilated area or under fume hood and wear appropriate protective clothing.
2. Prepare a suitable container, preferably a plastic bottle with water-tight cap
3. Add 1L of distilled water.
4. Add 20g of $NaOH$ slowly, since an exothermic reaction will take place when the $NaOH$ dissolves. Actively stir the solution and keep the temperature under control. Avoid boiling as water will evaporate quickly. This can take several minutes to dissolve all $NaOH$.
5. Add 10g. of Na_2SiO_3 in a similar way. If using a Na_2SiO_3 solution, calculate the amount of liquid to add based on the mol/L dissolved solids. E.g. if using a 5 molar Na_2SiO_3 solution, 16.39ml corresponds to 10g of dissolved Na_2SiO_3 .

The resulting solution is a ready to use product for support material removal.

Depending on available resources, Na_2SiO_3 can be produced relatively easily in the lab by dissolving silica gel in a solution with $NaOH$. To create a $5mol/L$ sodium metasilicate solution:

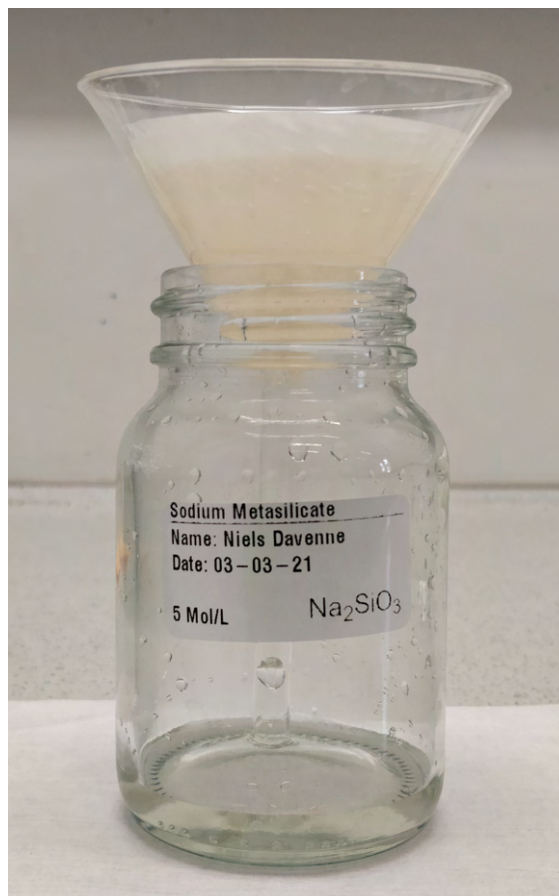
1. Conduct in well-ventilated area or under fume hood and wear appropriate protective clothing.
2. Weigh 60g of silica gel and put in glassware
3. Add 100ml of distilled water
4. Add 80g of $NaOH$ slowly, since an exothermic reaction will take place when the $NaOH$ dissolves. Actively stir the solution and keep the temperature under control. Avoid boiling as water will evaporate quickly. This can take several minutes to dissolve all $NaOH$.
5. Add additional water to create 5 molar solution (in this case, add water to 200ml)



Figure D.1: Overview of required components to make a $\text{NaOH} + \text{Na}_2\text{SiO}_3$ solution with DIY Na_2SiO_3 .

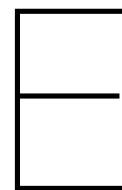


(a) Dissolving silica gel in a NaOH solution to create Na_2SiO_3 .



(b) Filtering the mixture to leave only a pure Na_2SiO_3 solution.

Figure D.2: Dissolving silica gel and filtering of the resulting solution to yield Na_2SiO_3



Preparing a CAD model for 3D printing

To prepare a CAD model for multi-material 3D-printing on the PiXDRO LP50 printers, a few steps are required. This Appendix is divided into several steps:

1. CAD model and support generation
2. Model exporting and slicing
3. Organising images and colour inversion
4. Support material modification (optional, but recommended)
5. Organising images (2)
6. Printing on PiXDRO LP50

In this example, software used is SolidWorks 2019 [13], Chitubox slicer [9] and in-house produced image Color inverter and support modification applications. The described procedure should be similar with other software.

E.1. CAD model and support generation

Try to use a model of your substrate when designing, so you can easily judge scale and alignment on the substrate. Also, this will aid in our process later on when generating support material and aligning it with the structural material. Say you designed a complex 3D model with overhangs and some conductive tracks to be printed on top, fig. E.1. Save it with an easy to distinguish name, such as *DEMO-struct*. Make sure to save all files together in a dedicated folder, called for example *DEMO*.

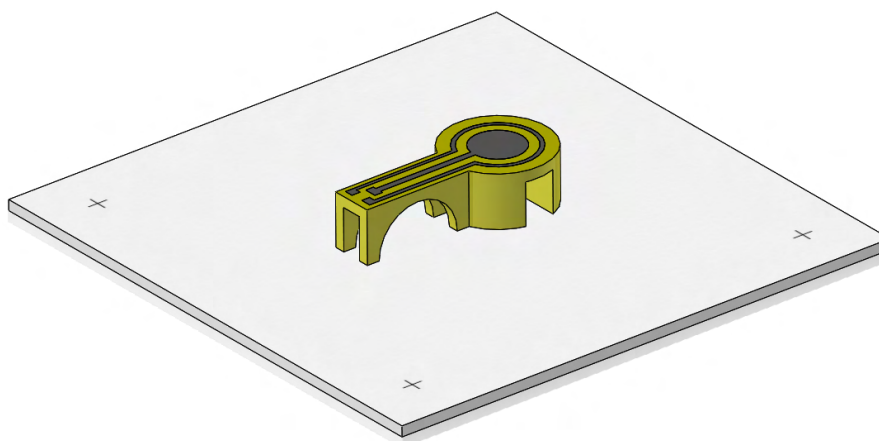


Figure E.1: CAD model of structural part with AgNP tracks on 50x50mm substrate.

Next is to generate appropriate support material. Manually designing a support material structure which perfectly fits the structural material is a cumbersome task. Therefore, the power of Boolean operators

will be used to carve out support material geometry.

First, make an assembly called *DEMO-assy*. Insert the *DEMO-struct* part and fix it in place. Next, an empty file is created to start working on the support material. Open up a new template of your (blank) substrate material and save it as *DEMO-support*. Insert *DEMO-support* into your assembly and align the substrates in place using mates. Constrain all degrees of freedom. The goal is to have both substrates in exactly the same place. When completed, fix both parts and remove the mates again, they are no longer necessary. Now, select the support material part *DEMO-support* (which is still nothing more than a substrate) and start editing the part in place by clicking *Edit Component*, fig. E.2.

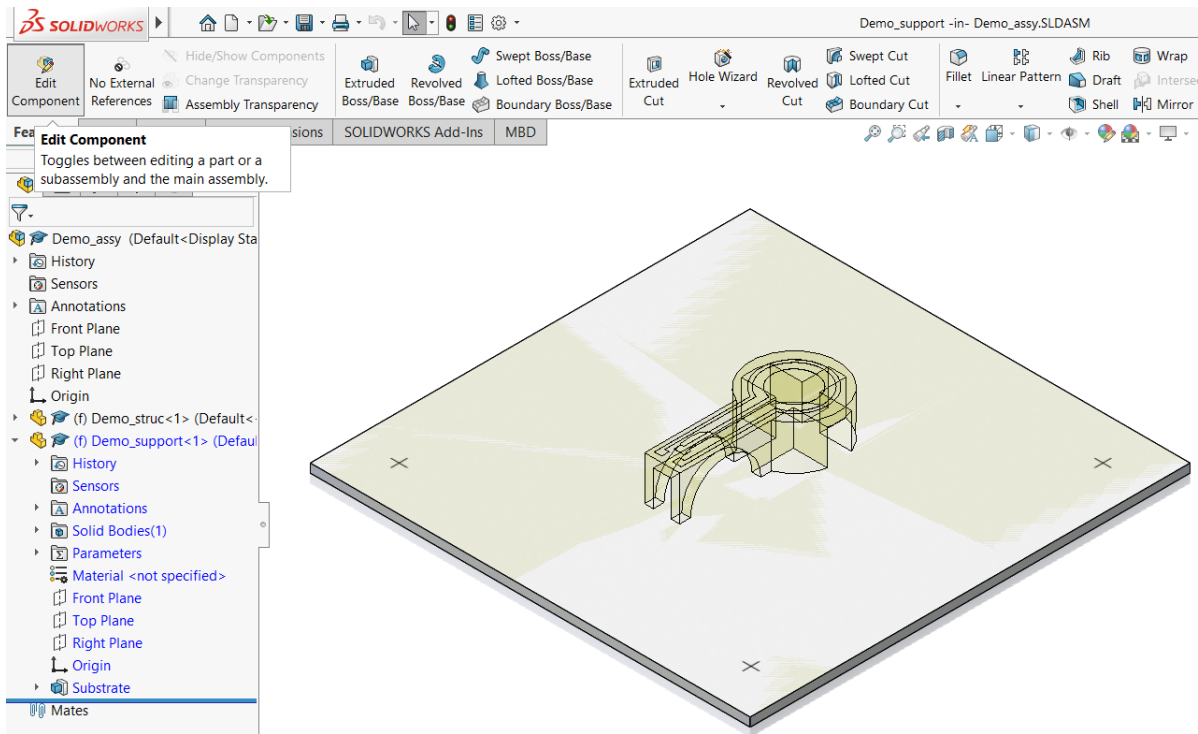
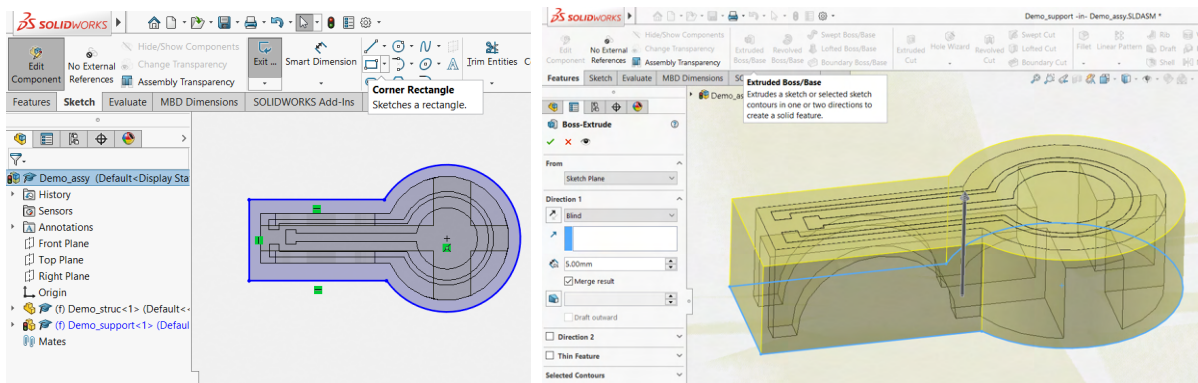


Figure E.2: Edit support material part in Assembly using Edit component.

We're now going to make a rough shape of the support material which surrounds the main part. Head over to *Sketch* in the toolbar and start a new sketch on the substrate. Either follow the geometry as shown in the example (fig. E.3a, or make a simple rectangle which covers the entire main part. Next, exit the sketch and head to *Features* in the toolbar. Make an *Extruded Boss/Base* up to the height of the main part, fig. E.3b.



(a) Sketch a shape of support material around the main part (b) Extrude the material to the same height as the main part

Figure E.3: Sketching and extruding a rough support material shape

Now, let's carve out *DEMO-struct* geometry from the support material so we're only left with what is desired - a part that perfectly supports the structural part everywhere without intersections. Select the *Cavity* function from the main menu bar as shown in fig. E.4.

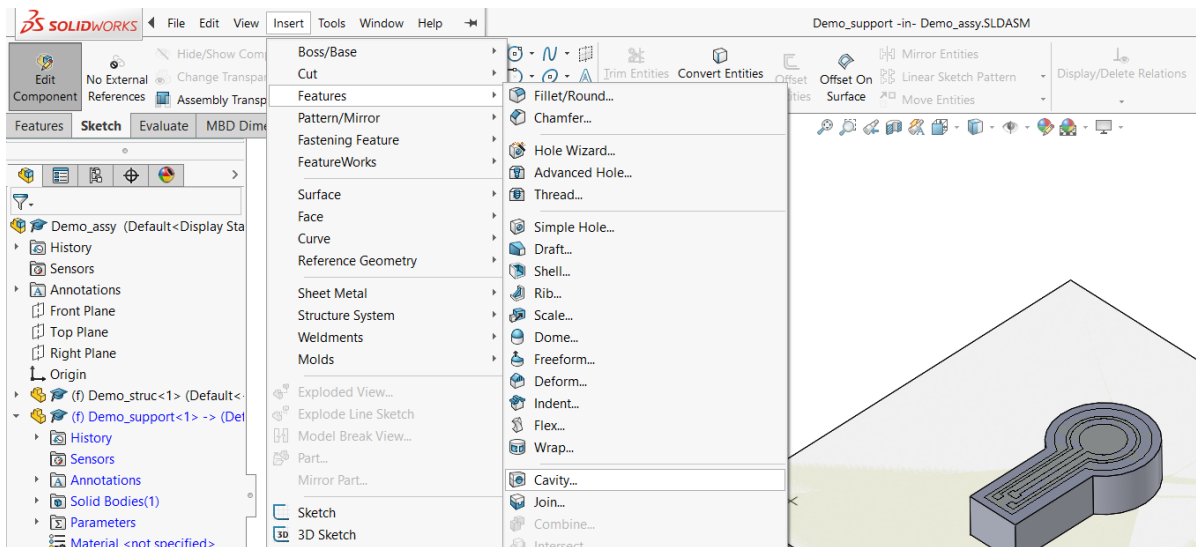


Figure E.4: Use the cavity feature to carve out structural material geometry from the support material

Select the structural material to perform this operation with, by expanding the inspector tree (top left of viewport) and clicking *Demo-struct* part. Make sure it properly shows up in the *Cavity Design Component field*, as shown in fig. E.5. Hit apply. You can now exit from *Edit Component*.

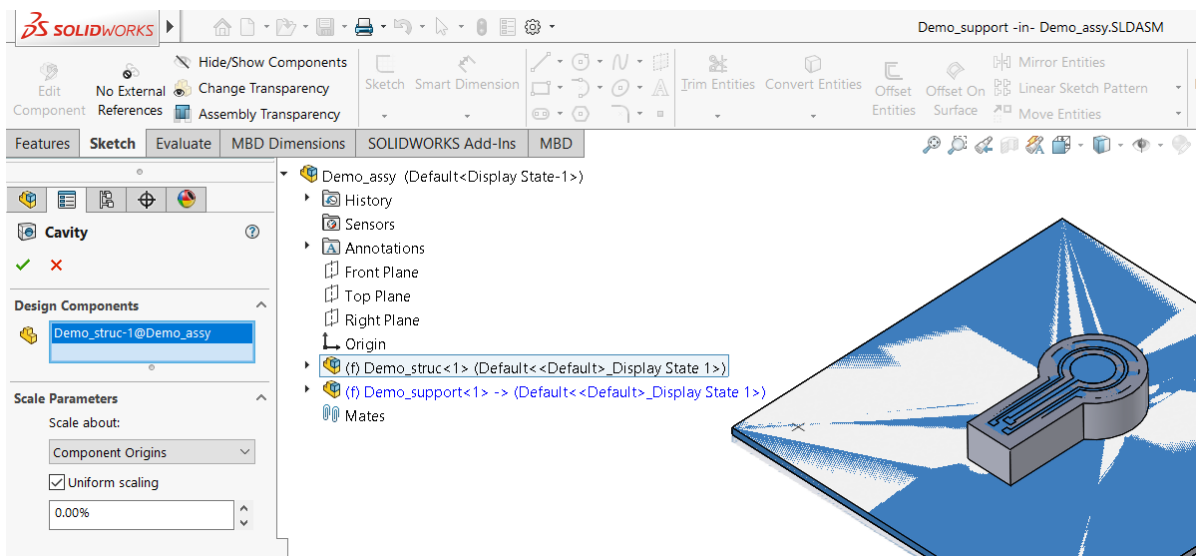


Figure E.5: Select *DEMO-struct* from the inspector tree to perform the operation.

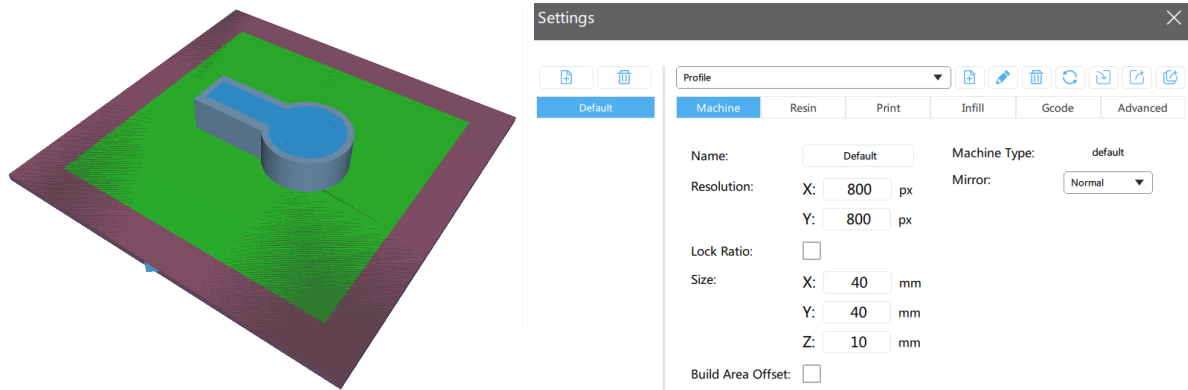
You've now successfully created a structural and support material part ready for export. The support material will no longer have a substrate due to the *Cavity* operation, but that is okay.

E.2. Model exporting and slicing

Export both *DEMO-struct* and *DEMO-support* as STL files by clicking *Save As* (Save as copy and continue). There's no need to export the assembly. Export both STL files to the same folder.

Startup Chitubox slicer and load both STL files. Flatten by face and rotate if necessary. For a 1mm substrate model, also move down the object with the same amount in Chitubox slicer. Perform these operations for both parts until a similar view is obtained as in fig. E.6a.

Apply settings as shown in fig. E.6b. Additionally, layer height should be set according to the ink specification. For VeroYellow structural ink, this is found to be $50\mu\text{m}$, or 0.005mm .



(a) Chitubox view when models are properly aligned and rotated. (b) Chitubox slicer settings.

Figure E.6: Chitubox slicer settings and view

Now, delete one of the parts to only slice images for either one at a time. For example, let's first slice the structural material, *DEMO-struct*. Remove *DEMO-support*. Click *Slice*. Dismiss any warnings about exceeding substrate size, but make sure that your model fits the images. An interactive preview will be shown in which you can scroll through layers to inspect the sliced images. When satisfied, hit *Save*. Save as a .zip file. Default name is sufficient.

Repeat this procedure for the other part.

E.3. Organising images and colour inversion

Up till now, your folder should look something like shown in fig. E.7.

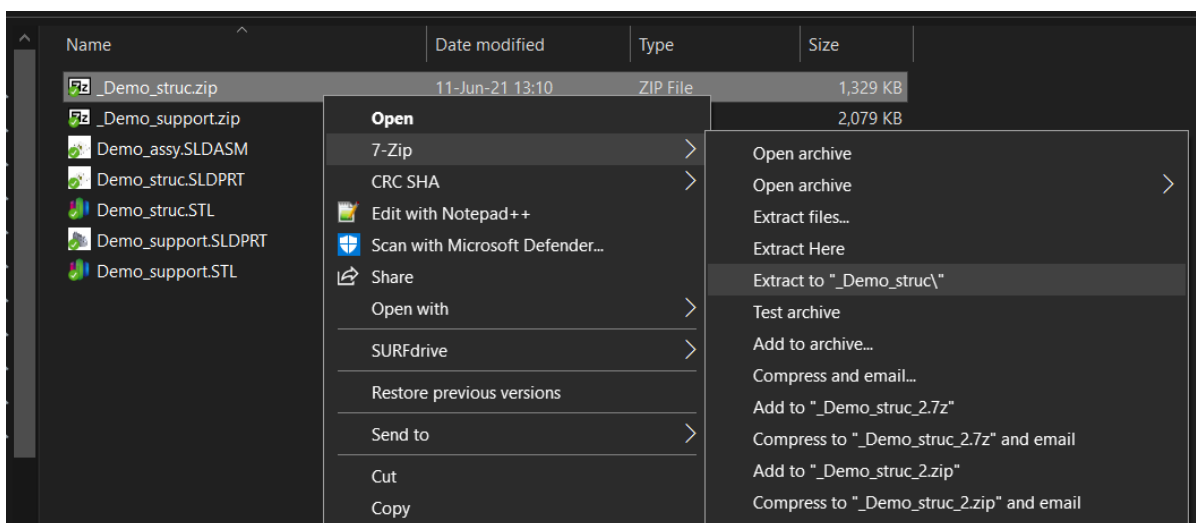


Figure E.7: Folder containing parts and images up till now. Unpack .zip archive into a folder with a program of choice.

Unpack both .zip files into a new folders, so the separate images can be modified. Do not put the files in one folder, but make sure structural material and support material have their own folders.

Copy *ImageColorInverter.exe* into one of the newly created folders with sliced images. Run the application and check that the right prefix is selected, depending on exporting structural or support material. The colours of all images will be inverted (black-white flip). A new folder is created called *inverted*. This folder contains all inverted images with appropriate names.

Repeat this procedure for the other part.

When done, merge the contents of both inverted folders into a new folder, called *DEMO-temp*. This folder will contain all inverted images, ready for processing by the support modification application. Depending on the number of sliced images required for your model, this folder can become quite packed with images. If no support modification is needed, this folder is ready to be loaded onto the PiXDRO LP50 and start printing.

E.4. Support material modification

It is recommended to use modified supports, as the support structure is otherwise often too weak. Especially with a rather high object as the one used in this example.

Copy the support modifier application *SupportModifier.exe* into the *DEMO-temp* folder and launch it. Select a desired matrix density. Default is 20% and should be fine for most applications. Check the extension type is correct for the images and start the conversion. This may take a while. A counter shows progression, though the application might seem to freeze. Wait patiently. When the application finishes, another folder is created inside the *DEMO-temp* folder called *Support-modified*. Inspect the images in this folder - both structural and support images should now have parts of each other included, based on the density matrix. A similar result as shown in fig. E.8 should be noticeable.

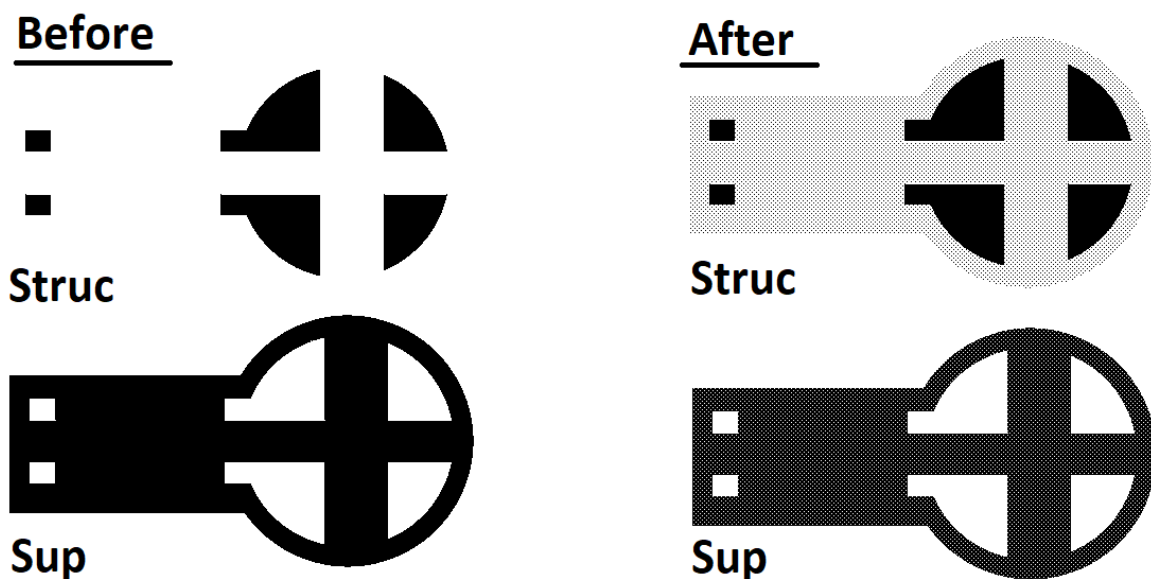


Figure E.8: Support modification images before and after conversion.

No errors should occur when running the application. If they do occur, the cause is most likely a difference in amount of images between structural and support material. This can happen if the structural material is taller than the support material, or vice versa. In that case, the amount of images sliced differ. If the conversion program runs out of images in such case, it throws an error. This is no problem, it just means the conversion stopped. Only remember the number at which the conversion stopped for the next step.

E.5. Organising images (2)

Make a new folder in your root folder called *DEMO-READY*. From *DEMO-temp > support-modified*, copy all images over to *DEMO-READY*. Also, in case of any errors during support modification, copy all (missing) images of struc or sup starting from the number at which conversion stopped from *DEMO-temp*. This process is depicted in fig. E.9.

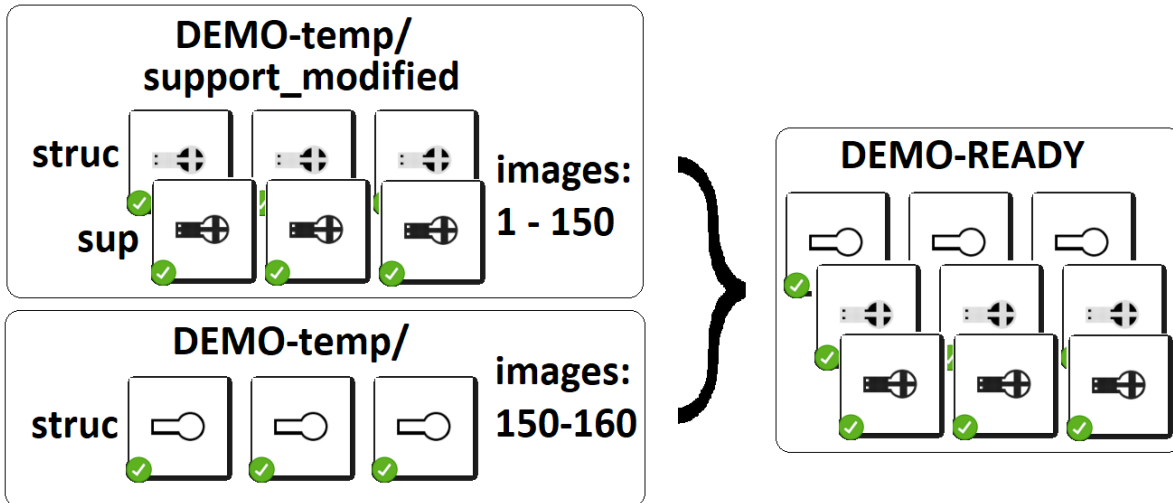


Figure E.9: Copying converted images to final folder. Any images that were not converted can simply be taken from the temporary folder.

E.6. Printing on PiXDRO LP50

The *DEMO-READY* folder can now be copied over to the PiXDRO LP50 machines. It is recommended to use a high speed USB storage device to transfer the folder over the the PiXDRO's main disk. In PiXDRO HMI, make a new recipe using the 3D-DUAL-UV recipe template. This template uses the custom recipe code to enable 3D printing. Select *struc1.png* as first image for the structural material bitmap. Similarly, set *sup1.png* as first image for support material.